
KTH Industrial Engineering
and Management

Towards a Methodology for

# Integrated Design of Mechatronic Servo Systems

FREDRIK ROOS

Doctoral thesis
Department of Machine Design
Royal Institute of Technology
SE-100 44 Stockholm

TRITA – MMK 2007:07
ISSN 1400-1179
ISRN/KTH/MMK/R-07/07-SE

TRITA – MMK 2007:07
ISSN 1400-1179
ISRN/KTH/MMK/R-07/07-SE

Towards a Methodology for Integrated Design of Mechatronic Servo Systems

Fredrik Roos

Doctoral thesis

Academic thesis, which with the approval of Kungliga Tekniska Högskolan, will be presented for public review in fulfilment of the requirements for a Doctorate of Engineering in Machine Design. The public review is held at Kungliga Tekniska Högskolan, Sydvästra Galleriet, KTH Main Library, Osquars backe 31, on September 14, 2007, at 10:00.

**Mechatronics Lab**
**Department of Machine Design**
**Royal Institute of Technology**
**S-100 44 Stockholm**
**SWEDEN**

TRITA - MMK 2007:07
ISSN 1400 -1179
ISRN/KTH/MMK/R-07/07-SE

*Document type*
Doctoral thesis

*Date*
2007-07-06

*Author(s)*

Fredrik Roos
(fredrikr@md.kth.se)

*Supervisor(s)*
Jan Wikander, Hans Johansson

*Sponsor(s)*
Gröna Bilen: Volvo AB, Scania AB, Volvo Cars, SAAB Automobile

*Title:*

# Towards a Methodology for Integrated Design of Mechatronic Servo Systems

*Abstract*

Traditional methods for mechatronics design are often based on a sequential approach, where the mechanical structure is designed first, and then fitted with off-the-shelf electric motors, drive electronics, gearheads and sensors. Finally a control system is designed and optimized for the already existing physical system. Such a design method, that doesn't consider aspects from a control point of view during the design of the physical system, is unlikely to result in a system with optimal control performance. Furthermore, to separately design and optimize each of the physical components will, from a global perspective, generally not result in a system that is optimal from a weight, size or cost perspective.

In order to reach the optimal design of an integrated mechatronic system (mechatronic module) it is necessary to treat the system as a whole, considering aspects from all involved engineering domains concurrently. In this thesis such an approach to integrated design of mechatronic servo systems is presented. A design methodology that considers the simultaneous design of the electric machine, gearhead, machine driver and control system, and therefore enables global optimization, has been developed. The target of the design methodology is conceptual design and evaluation. It is assumed that the load to be driven by the servo system is known and well defined, a load profile describing the wanted load motion and the corresponding torque, is required as input. The methodology can then be used to derive the lightest or smallest possible system that can drive the specified load. Furthermore, the control performance is evaluated and optimized, such that the physical system design and the controller design are integrated.

The methodology is based on modelling and simulation. Two types of component models have been developed, *static* and *dynamic* models. The static models describe relations between the parameters of the physical components, for example a component's torque rating as function of its size. The static models are based on traditional design rules and are used to optimize the physical parts of the system. The dynamic models describe the behaviour of the components and are used for control system design and performance optimization.

The gear ratio is identified to be the most central design variable when designing and optimizing electromechanical servo systems. The gear ratio directly affects the required size of the gearhead, electric machine and the machine driver. But it has also large influences on the system's control performance. It is concluded that high gear ratios generally are better from a control point of view than low ratios. A consequence of this is that it is possible, without compromising the control performance, to use less expensive (less accurate) sensors and microprocessors in high gear ratio servo systems, while low gear ratio systems require more expensive hardware. It is also concluded that it is essential to include all performance limiting phenomena, linear as well as non-linear, in this type of integrated analysis. Using for example a linearized system description for controller design, means that many of the most important couplings between control system and physical system design are overlooked.

*Keywords*
Mechatronics, Servo Systems, Design and Optimization, Integrated Design

*Language*
English

# ACKNOWLEDGEMENTS

When I, back in 2000, graduated from KTH as MSc in mechanical engineering, I thought that I had finished school for good. It was a perfect time to graduate, the industry was screaming for people and I had no intention to apply for a position as PhD student. I started to work for a consultant firm, which turned out to be a challenging and fun job. But after a year or so, the IT-boom was over and I was assigned projects that were not very challenging or fun. I decided that it was time to start looking for a new job. After a while, an advertisement for a PhD-position at my old department at KTH appeared in the paper. The PhD project looked very interesting, so I decided to apply. And suddenly I was back in school again!

I would like to express my gratitude to all the people that have been involved in this project, especially to my supervisor professor *Jan Wikander*, without him this research project would not have existed. Thank you *Jan* for all the support during these years and also for giving me this opportunity. My co-supervisor, associate professor *Hans Johansson*, deserves a big thank you for taking time to answering all of my never ending questions about electric machines and power electronics.

The research presented in this thesis is a result of the 'Auxiliary Systems' part of the Gröna Bilen / FCHEV program, which jointly has been funded by the Swedish government and the Swedish road vehicle manufacturers. Special thanks to the project's advisor board: *Göran Johansson* and *Kent Anderson* at Volvo AB and *Michael Blackenfelt* formerly at Scania CV AB.

I would also like to thank my co-authors: Dr. *Christer Spiegelberg* who has introduced me to the fascinating world of gear design, and *Mats Jonasson* at Volvo Cars, for jointly working with active control of vertical wheel loads, but also for giving me the opportunity to apply my research to a realistic design-case.

During this work I have made many new friends. My old room mates Dr. *Henrik Flemmer* and *Magnus Eriksson*. *Henrik* helped me understand how everything works at the department. He also thought me the art of spending a whole work day surfing the net for chain saws or used cars without getting bored. *Magnus,* who left us for industry but shortly discovered that nothing can compete with the department of Machine Design. Many thanks to Dr. *Johan Ingvast* and *Johan Tegin* for the interesting discussions we have had during all our lunches together. Thanks to all the other colleagues and students at the department for making it a very nice place to work at.

My parents *Agneta* and *Ulf*, my brother *Daniel* and all my friends, thank you for reminding me that there is a world outside KTH and what really is important in life. Finally, but certainly not least, *Cecilia*, thank you for being there, you have brought new dimensions to my life ♡.

Stockholm, June, 2007

# LIST OF APPENDED PUBLICATIONS

**Paper A**

Roos F., Johansson H., Wikander J., "Optimal Design of Motor and Gear Ratio in Mechatronic Systems", In Proceedings of the 3rd IFAC Symposium on Mechatronic Systems, Manley Beach, Sydney, September 2004.

*The work presented in the paper and the writing was made by Fredrik Roos, many of the ideas behind the motor models where provided by Hans Johansson*.

**Paper B**

Roos F., Spiegelberg C., "Relations between Size and Gear Ratio in Spur and Planetary Gear Trains", Technical Report, TRITA-MMK 2005:01, ISSN 1400-1179, ISRN/KTH/MMK/R-05/01-SE, November 2004.

*The work presented in the paper and the writing was performed in close collaboration between the authors.*

**Paper C**

Roos F., Wikander J., "Integrated Design of Servomotor and Gearhead Assemblies", Submitted for publication in Mechatronics-The science of intelligent machines, an international journal, 2007-06-15.

*Fredrik Roos did all the work and writing, Jan Wikander supervised the work.*

**Paper D**

Roos F., Wikander J., "The Influence of Gear Ratio on Performance of Electro-mechanical Servo Systems", In Proceedings of the 4th IFAC Symposium on Mechatronic Systems, Heidelberg, September 2006.

*Fredrik Roos did all the work and writing, Jan Wikander supervised the work.*

**Paper E**

Roos F., Wikander J., "Integrated Control and Mechanism Design of Electromechanical Servo Systems", Submitted to IEEE/ASME Transactions on Mechatronics, 2007-01-08.

*Fredrik Roos did all the work and writing. Jan Wikander supervised and provided input on controller design and analysis.*

*Jan Wikander has made a great work in editing all of the appended papers.*

# ADDITIONAL PUBLICATIONS

1. Roos F., Wikander J., “Mechatronics Design and Optimisation Methodology – A Problem Formulation Focused on Automotive Mechatronic Modules”, Mekatronikmöte -03, Göteborg, August 2003.
2. Roos F., Wikander J., ”Towards a Design and Optimization Methodology for Automotive Mechatronics”, In Proceedings of the 30th FISITA World Automotive Congress, Barcelona May 2004.
3. Roos F., “On Design Methods for Mechatronics – Servomotor and Gearhead”, Licentiate Thesis, TRITA-MMK 2005:02, ISSN 1400-1179, ISRN/KTH/MMK/R-05/02-SE, Jan 2005.
4. Roos F., “Theoretical Evaluation of Electric Power Steering in Heavy Vehicles”, Technical Report, TRITA-MMK 2005:29, ISSN 1400-1179, ISRN/KTH/MMK/R-05/29-SE, 2005.
5. Roos F. Wikander J., “Design and Optimization of Automotive Mechatronic Subsystems”, In Proceedings of OSTT’05, Stockholm, October 2005.
6. Roos F. Wikander J., “Towards a Holistic Design Methodology for Mechatronics”, Mekatronikmöte -05, Halmstad, November 2005.
7. Roos F. Johansson H., Wikander J., “Optimal Selection of Motor and Gearhead in Mechatronic Applications”, Mechatronics, vol. 16, no 1, pp. 63-72, 2006.
8. Jonasson M., Roos F., “Design and Evaluation of an Electromechanical Wheel Suspension”, Submitted for publication in Mechatronics, 2007-06-18.

# CONTENTS

# 1 INTRODUCTION

This chapter gives the background, methods and goal with the research presented in this thesis. First, the area of mechatronics design methods, processes and tool-support is reviewed. Especially the drawbacks with the classical mechatronics development processes and methods are discussed. Then the scope, delimitations and aim of the work is presented. Furthermore, the used mathematical modeling and simulation based approach is described. The research project is partly funded by the automotive industry; the chapter is therefore concluded with a review of the background to the demand of new mechatronics design methods for automotive systems.

## 1.1 THE MECHATRONICS DEVELOPMENT PROCESS

The mechatronics development process differs from conventional development processes in the way that it deals with several engineering domains at the same time. A mechatronic system spans over mechanical engineering, electrical engineering, control engineering and computer science. Separately applying the domain specific design and optimization methods to a mechatronic design problem will not result in an optimal system design. A simple example is the diameter of a shaft, which from a mechanical perspective might be dimensioned to withstand a specific dynamic shear stress load. But the shaft diameter is also directly related to the shaft's stiffness which is a very important parameter for the control engineers. This multi-domain characteristic of mechatronics calls for special design methods and tools that have the potential of finding the global system optimum and not just sub-optima constrained within each discipline.

### 1.1.1 MECHATRONICS PRODUCT DEVELOPMENT

In the traditional methodologies for mechatronics design, system integration is usually handled in the late design stages (Figure 1.1). The structure to be controlled (mechanism) is very often designed first and independently of the controller [1]. Classic control theory supports this approach since it more or less assumes a given and fixed process structure. This sequential approach to mechatronics design has the advantage of dividing a large, complex design problem into several smaller design problems. However, neglecting to include aspects from a dynamics and control point of view into the design of the mechanism will result in a system with non-optimal dynamic performance. This may, in the worst case, require major redesigns of the electromechanical system late in the design process.

It is not just the design processes of the structure and the controller that generally are isolated from each other. The mechanical parts, electromechanical actuators, sensors and control electronics are also often designed independently of each other (Figure 1.1). Typically, the mechanical structure is designed first and then fitted with off-the-shelf electric motors, gears, sensors and control electronics. This approach to mechatronics design results in systems that are non-optimal from a number of aspects, such as weight, size and efficiency. For low

production-volume applications, this might be the most cost effective approach. However, for high-production volume applications, it would be more cost-effective to design application specific components which are optimal from a systems perspective.

Increasing the integration between controller and structure design has potential to shorten the mechatronics design process while increasing the performance of the designed system. Furthermore, increasing the integration between electronics, electro-mechanics and mechanical development, will likely result in systems that are more compact, lighter, more efficient and less costly (at least for high volume products).

The drawbacks with independent development of the mechanical, electrical, electronic, control and software components, and late design integration are recognized in many publications (e.g. [1], [2], [3], [4] and [5] ). Nevertheless, the subject of integrated mechatronics design methods is relatively unexplored. Some work has however been published, especially in the area of integrated structure/control design, which is briefly reviewed in section 2.1.

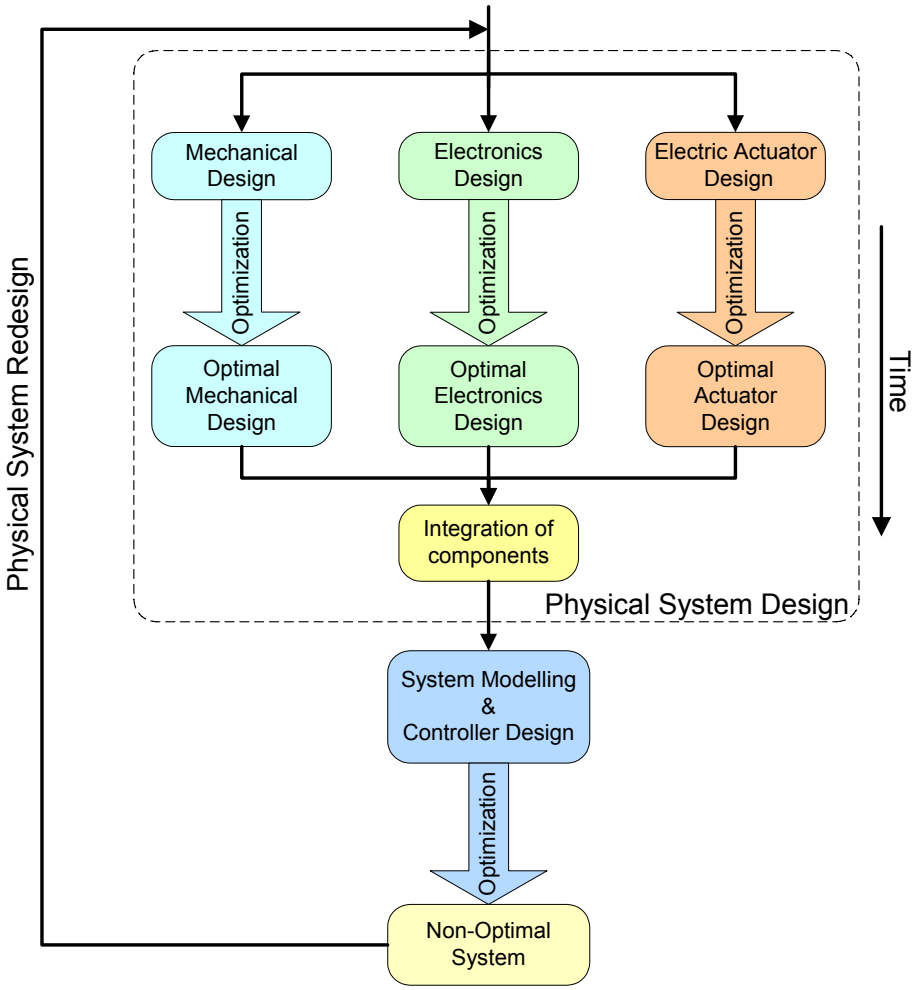


*Figure 1.1. Diagram of a traditional development process for mechatronics, characterized by low integration between the different disciplines.*

The German VDI organization has developed a design process model, *The flexible procedural model,* for the development of mechatronic systems. Its macro-level design process model is shown in Figure 1.2 ([6] and [7]). This model identifies the major phases of a mechatronics development project, and it has been adopted without modifications in this work. It divides a mechatronics development project into three major phases, *system design, domain specific design* and *system integration.* The goal during the system design phase (Figure 1.2) is to define a cross-domain solution concept for the system being developed. In this phase the overall function of the system will be divided into sub functions. It is also here the decision of which sub-functions that should be solved in mechanics, electronics and software is made. This solution concept, will later, in the domain specific design phase, be worked out in more detail [7].

The domain specific design phase, Figure 1.2, can be regarded as several parallel smaller development projects, one for each of the system's main components, e.g. electric machine, gears, controller, electronic hardware and software. It is in this phase geometries, material properties, controller parameters, software design, etcetera, are worked out in detail. Here the total number of design parameters tends to get very large. Also the number of involved design engineers and design tools will be large. The results from the domain specific design are then integrated to the complete mechatronic system in the system integration phase.

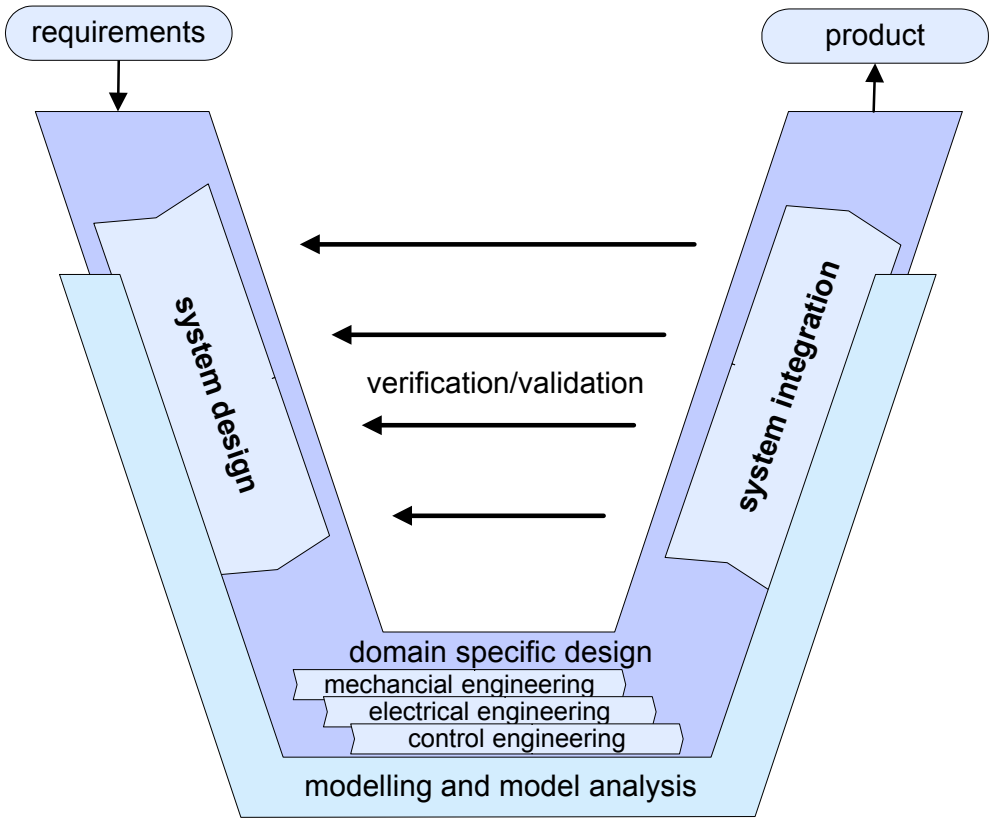


*Figure 1.2. VDI 2206 development model for mechatronic systems [6], [7].*

### 1.1.2 MODELING AND SIMULATION TOOLS

The key to an integrated design and optimization methodology for mechatronics is modeling and simulation. Tool support that enables modeling of phenomena and properties from all involved engineering domains is necessary throughout a mechatronics development project. For mechatronics design, it is essential to integrate the domain specific design tools such that the system can be designed and analyzed across the domain boundaries. This integration can be done in at least two different ways [8]:

i) Creating a multi domain design tool which can be used to model and simulate the entire multidisciplinary system.
ii) Interfacing the domain specific design tools to each other and to a common data base, enabling them to share model data.

The first approach can be very useful during the system design phase (Figure 1.2), where a conceptual design has to be chosen and optimized on the system level. In this phase, design models with a relatively high level of abstraction are used, and the level of detail has to be relatively low in order to facilitate system wide design optimization. Examples of multi-domain modeling and simulation tools are Dymola™ [9], 20-Sim™ [10], and AMEsim™ [11]. Dynamic models of mechatronic systems can generally be built up using just a small number of domain specific elements, such as springs, masses, resistors and capacitors, this is the approach taken by the tools mentioned above. However, these tools are dynamic modeling tools; they do not support static component models which are required to work out component sizes, weights, stiffnesses and other parameters that in turn are required for the dynamic simulation. This is a drawback from the perspective of a holistic mechatronics design methodology. One option is therefore to use a more general math/simulation package like matlab™/ simulink™ [12], stand alone or in combination with a tool as the ones mentioned above. A long term solution would be to add support for component dimensioning (static models) in the multi-domain modeling and simulation tools.

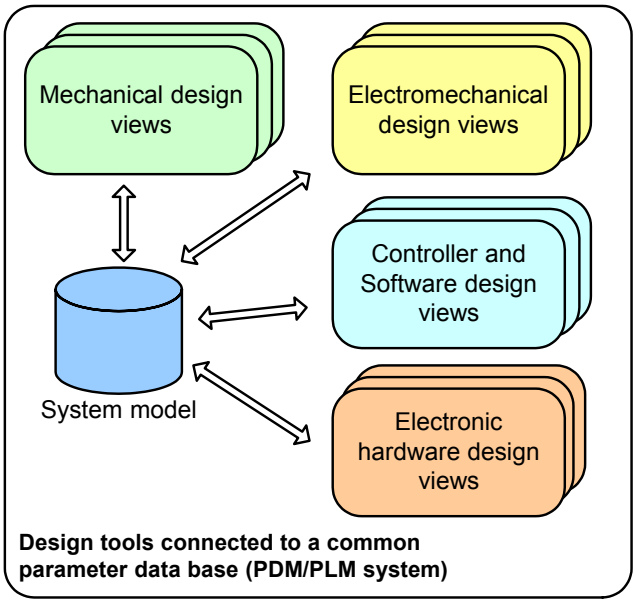


*Figure 1.3. One model, many views.*

During the domain specific design phases the approach with a single, multi-domain design tool is no longer feasible. The number of different aspects that has to be analyzed in a mechatronic system is huge; hence it is not realistic to think that it is possible to create one design tool that covers everything from mechanical and electronic CAD to controller and software design. A much better solution would be to use the second approach, using the existing domain specific design tools that the engineers are used to work with. But it is still important that changes in one domain can be simultaneously evaluated in another. This requires interchangeability of models between design tools from different engineering domains (Figure 1.3).

Tool support, which for instance enables changes made from an assembly point of view to be evaluated in control system simulations, is desirable. This demands a 'core model' or data-base that represents the entire design and that can be viewed from various windows (design tools). It would be a great advantage if changes made in one window were reflected immediately in the other windows [13]. A prototype for such a system has been developed by El-Khoury [14] and is in turn based on a PDM (Product Data Management) system. But it is still a long way to go before all types of tools required during a mechatronics development project are integrated. Problems arise just from the fact that different engineering domains use different models and modeling frameworks during the design work. For example, control engineers are used to models in the form of transfer functions or state space descriptions. Without special precautions, such models generally do not have a direct relation to the physical parameters in a mechatronic system. Furthermore it is necessary to use models with different level of detail during a development project; a complete framework for mechatronic design tools must be able to handle that. An overview of the different design tools required during a mechatronics development project is given in [8].

Another important aspect of tool integration is the ability to simulate the system together with its environment. It is necessary to couple simulation programs and models in real time (so called co-simulation) to simulate the behavior of for example an entire vehicle with powertrain, subsystems and body dynamics. This is getting increasingly important since the trend is that subsystems within a vehicle interact more and more with each other. Different methods for co-simulation are discussed in [15]. One problem with co-simulation is that the time scale of the phenomena analyzed in the different models might differ greatly. Compare for example power electronics simulations with a time scale of nano-seconds, with thermodynamic simulations with timescales up to minutes. This leads to unrealistic simulation times when coupling simulation models with different time resolutions. It may therefore be required, for each component, to develop models with different levels of abstraction and time resolution.

The area of tool and model integration is very important for supporting a holistic cross domain mechatronics development methodology, but it is however not the focus of this thesis and will therefore not be investigated in any further detail.

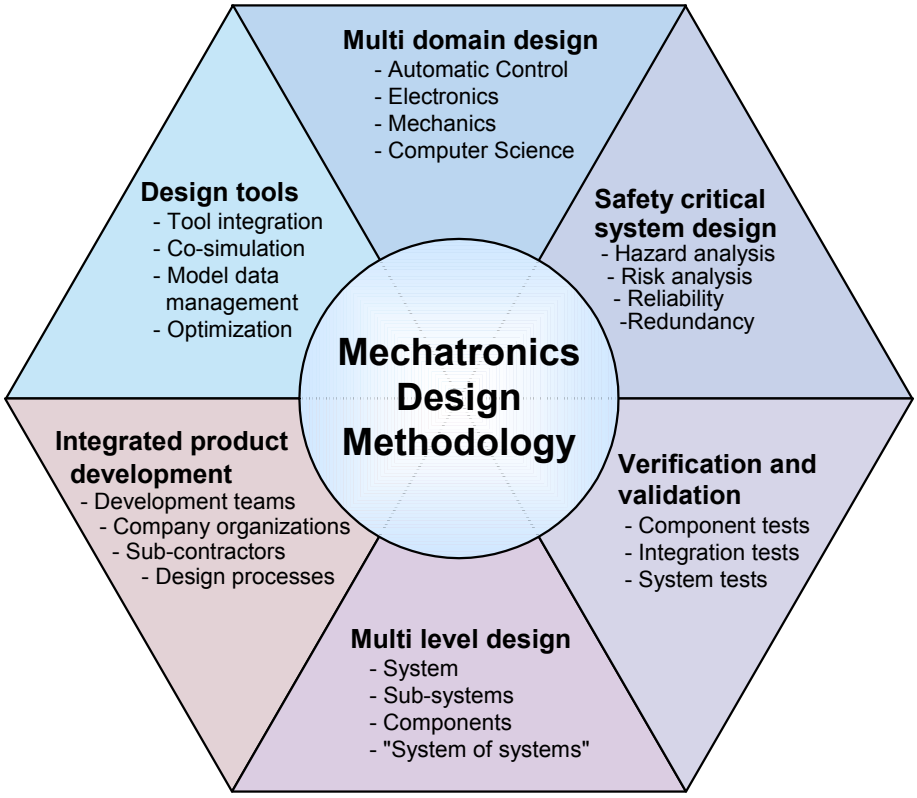


*Figure 1.4. The area of mechatronics design methodologies.*

## 1.2 SCOPE AND GOAL

The area of mechatronics design methodologies is huge, the topic can be approached from a number of different angles. As depicted in Figure 1.4, there are many aspects that have to be included in a complete design methodology for mechatronic systems. Everything from organizational aspects to detailed modeling and design of printed circuit boards may be included in such a methodology. It has therefore been necessary to focus this research project towards one or some of these aspects. As already implied, the chosen focus is multi domain design and optimization methods for mechatronic systems. So, this thesis is delimited to the upper most triangle of Figure 1.4. This triangle alone represents a large and complex research area. The problem that is being approached is hence strongly delimited to a methodology for designing optimal mechatronic modules (Figure 1.5). However, large parts of the methodology are applicable to electromechanical servo systems in general and not limited to the concept of mechatronic modules.

### 1.2.1 MECHATRONIC ACTUATION MODULES

Without claiming to have defined the term mechatronics in general, a mechatronic (sub-) system is here defined as a computer controlled and electrically actuated system which performs some sort of controlled mechanical work.

The level of physical integration between mechanics, electronics, electro-mechanics, and control has generally been low in mechatronic systems. This is mainly a consequence from the use of off-the-shelf components as electric

machines, gearheads and motor drivers, but also from the use of domain specific design methods and traditionally organized development departments. This "low integration" approach, widely employed in mechatronic systems, is space demanding and costly. In the automotive sector, the electronics typically stand for 50% of the total cost of electronically controlled actuators. Within this share, 50% of the cost (i.e. 25 % of the total cost) is related mainly to mechanical parts, as heatsink, housing, PCB, connectors and cables, [4]. Increasing the physical integration of electronic and mechanical parts into mechatronic modules (Figure 1.5) would eliminate the need for many of these parts, and therefore lower the system cost. This, at the same time as the total system size and weight are decreased. The concept of mechatronic modules is not only recognized in the automotive sector, Thramboulidis [5], for example, suggests a modular mechatronic architecture for manufacturing systems.

A mechatronic actuation module is here defined as a self contained physically integrated system that consists of an *electric machine*, a *transmission* (e.g. gears or screw), *sensors*, a low level motion *controller* (hardware and software) and a *motor drive unit* (Figure 1.5). Interfaces to such a module are the *load* interface which mechanically connects the actuator to the load, the *energy* interface to the electric power source and a *communication* interface implemented in electronics and software. The focus of this thesis is design methods for such mechatronic modules. The aim with the work has been

- To develop a *design and optimization methodology* for the simultaneous design and optimization of all constituent components of a mechatronic actuation module.
- The methodology should be as *general* as possible, preferably applicable to all systems that require electrical actuation.

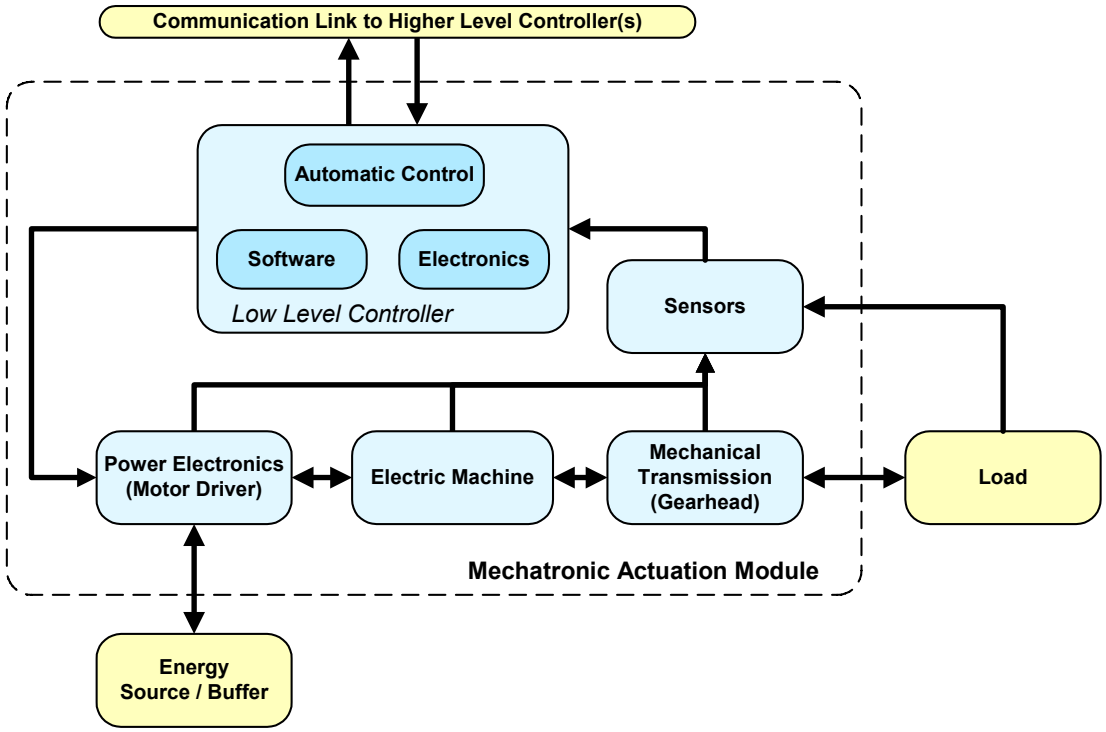


*Figure 1.5. Block diagram of a general mechatronic actuation module.*

*Table 1.1. Component types modeled and analyzed during this research.*

| Component | Type |
|---|---|
| Electric machine | Permanent magnet machines:<br>*DC, Brushless DC*<br>*Synchronous AC* |
| Gearhead | Spur pinion-gear pairs<br>Three-wheel planetary |
| Position sensor | Incremental encoder |
| Controller | PID |
| Motor driver | 3-Phase, passive cooling. |

The components that are analyzed and included in the presented design methodology are: the *electric machine*, *gear reducer, position sensor, position controller* and the *motor driver*. It has been the goal to cover all of these components, therefore, due to time limitations, only one or a couple of variants of each component have been modeled and analyzed. As can be seen in Table 1.1, only components for rotational motion have been included, linear motion components (screws, linear motors, etc.) and other component types are possible to add in future research.

A lot of aspects have to be considered during the design of an electromechanical servo system: cost, vibrations, safety, environmental impact, performance, electro magnetic compatibility etcetera. Here the primary focus is on the *size* and *weight* of the servo system, but also *efficiency, performance* and *cost* are included in the analysis.

### 1.2.2 METHODOLOGY FOR CONCEPTUAL DESIGN

It is important to consider the system as a whole throughout the development process. It is however very difficult to apply any system level optimization method during the domain specific design phase (see Figure 1.2). This is mainly due to the huge number of design parameters, but also due to the large number of involved engineers (with background in different disciplines). It is therefore important that the conceptual design that is being refined and developed further during the domain specific design phase already is optimized on the system level. Hence, the target of the presented methodology is the system design phase, or more precisely, the conceptual design phase of the development process (Figure 1.6). During the conceptual design phase the number of design parameters is relatively small and few people are involved in the development project. It is therefore feasible to systematically analyze, design and optimize the system as a whole, during this stage of the design project.

In addition to presenting the foundation of a complete methodology for integrated design and optimization of electromechanical servo systems, the aim of this thesis is to identify and highlight the most important couplings between parameters originating from the different engineering disciplines.

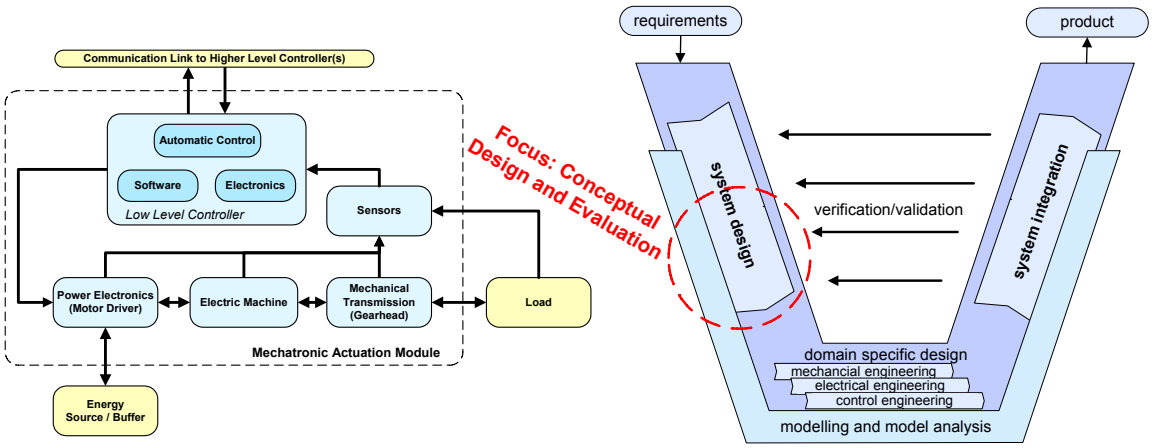


*Figure 1.6. Scope of the methodology: Design and optimization of mechatronic modules in the conceptual design stage.*

## 1.3 RESEARCH APPROACH

This section intends to give the reader an idea of how the results presented later on in this thesis have been reached. An overview of the methods used to derive the integrated design methodology is presented.

The problem has been approached by starting with a thorough analysis of one of the key components of a mechatronic actuation module, the electric machine. The analysis has then been extended component by component, to finally include all of the main components within a mechatronic module. This also corresponds to the order of presentation in this thesis; first the electric machine model is presented and analyzed. Then physical component models of the gearhead and motor driver are presented. Finally the dynamic aspects are investigated and the low level controller and position sensor are integrated into the methodology.

All of the presented research is based on mathematical models of the physical components and their dynamic behavior. No experiments have been performed, but some of the models have been verified against data of commercially available components. Two different types of models are used throughout the thesis: *static* component models that describe relationships between for example a component‘s size and its torque rating and *dynamic* models that describe the dynamic behavior of the components. The static models are used to derive the combined optimal physical parameters of all the constituent components. This optimal parameter set is then used in the dynamic simulation model. This will be described in much more detail later on. Mainly matlab/simulink [12] has been used as modeling environment, but also to a smaller extent Dymola [9].

One of the keys to an integrated design methodology is optimization. The used optimization methods have as far as possible been based on an analytic technique where the optimum either is simply read directly out of a graph or calculated with the help of differential calculus. This approach is very nice since it is simple, and if the design variables are less than three, it gives a graphical representation of how the target function depends on the design variables. This analytical approach has however not been possible to use throughout the project. When non-linear dynamic phenomena and control performance evaluation was included into the analysis it was necessary to introduce a more ‘advanced’

numerical optimization method. The choice fell on a genetic optimization algorithm. The drawback of this method for system optimization is that it is computationally intensive and that there exists no mathematical proof that it actually finds the true optimum. During this research the genetic algorithm in the GEATbx toolbox [16] for matlab has been used.

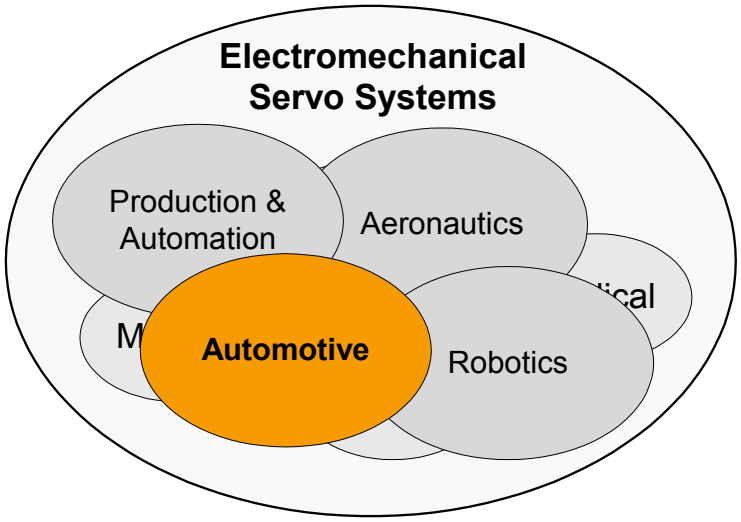


*Figure 1.7. Possible application sectors for the mechatronics design and optimization methodology.*

## 1.4 EXAMPLE OF AN APPLICATION DOMAIN

The developed methodology for design and optimization of electromechanical servo systems is general and applicable to almost any system requiring controlled electric actuation. Industrial sectors that may benefit from using this methodology include *automation*, *aeronautics* and *robotics* (Figure 1.7). However, this research is partly funded by the automotive industry and the models and methods have been developed with automotive applications in mind, therefore this section gives a short introduction to auxiliary electric actuation in road vehicles.

Currently there is a development in the automotive industry towards electrically powered sub-systems. Systems that traditionally have been driven directly by the combustion engine via, for example gears or belts, are being replaced with electrically driven systems. This electrification is lead by the car manufacturers, but the truck and bus manufacturers are likely to follow in their tracks, since, as described below, electrical systems have a number of advantages over the conventional systems.

### 1.4.1 HYBRID AND ELECTRIC VEHICLES

Today the issue of global warming and $CO_2$ emissions is very 'hot'. There is a consensus in the research community that the emissions of $CO_2$ from the burning of fossil fuels have to decrease in order to reduce the foreseen global increase in temperature. In addition to this, the global oil resources are not never-ending and the world's oil dependence may cause further political instability in parts of the

world. In 2003 the transportation sector (including land sea and air transportation) was responsible of 24% of the global emissions of $CO_2$. Cars and other light-duty vehicles represented 10% of the global $CO_2$ emissions alone [17]. This calls for new automotive powertrains that have the potential of reducing the fossil fuel consumption and the $CO_2$ emissions of the road vehicle fleet. Such powertrains can for example be based on alternative fuels as ethanol or hydrogen. Another concept is to improve the total efficiency of the vehicle, which for example can be done with a hybrid-electric powertrain, or to introduce a pure electric powertrain where the emissions are moved from the vehicle itself to an electricity power plant.

Hybrid-electric cars have been available on the market for some years now; well known examples are the Toyota Prius and the Honda Civic Hybrid. In 2006, Hybrid cars represented 1.5% (more than 251 000 units) of the new car market in the US [18]. The hybrid technology is now also spreading to medium- and heavy-duty vehicles. For example, four Japanese commercial vehicle manufacturers (Hino, Isuzu, Nissan Diesel and Mitsubishi Fuso), offer hybrid versions of their light- and medium-duty trucks [19]. In buses, hybrid powertrains have been experimented with for a long time; many hybrid buses have been and are in traffic in cities around the world.

Pure electric vehicles have not yet been introduced on the market in any large scale. But both Nissan Motor and Mitsubishi announce that they have plans to commercialize electric vehicles. Nissan plans to put a lightweight, subcompact electric car, powered by lithium-ion batteries on the market in three years (from November 2006) [20]. Mitsubishi have announced that they plan to sell electric cars in Japan by 2010 [21].

Common for hybrid and electric vehicles is that the auxiliary energy consumers can not depend on the combustion engine for power. Systems such as the air condition and power steering that traditionally have been driven directly by the internal combustion engine (ICE) must now be powered in another way since the ICE (if it exists) might be off during both driving and idling. The logical solution is of course to power these systems with electricity.

### 1.4.2 ELECTROMECHANICAL AUXILIARY SYSTEMS

This research was initially motivated by the need for optimized electro-mechanical auxiliary systems. Examples of such systems include

- Electric power steering and steer-by-wire.
- Electromechanical brakes (brake-by-wire).
- Electromechanical active suspension and leveling systems.
- Electric door opening systems.
- Systems Related to the ICE, electrically powered: Cooling fan, Oil pump, Water pump, Throttle valve (throttle-by-wire)…

Even though hybrid and electric powertrains require electric auxiliary systems, they are not the only reason for the development towards electric auxiliaries. One of the main reasons is the new and improved functionality that is enabled with electric auxiliaries. Electrically powered systems simplify the implementation of advanced functionality as for example automatic cross wind compensation and

automatic parking brake. Furthermore, electric auxiliary systems have the potential of lowering the fuel consumption of conventional vehicles. Electric systems are often more efficient than the conventional ones, mainly due to the possibility to 'on-demand' control. An electric power steering system for example, only consumes energy when you turn the steering wheel, while a conventional hydraulic system is idling and consumes energy when not in use. Furthermore, the efficiency of the conventional power steering is strongly dependent on the speed of the ICE, high engine speeds leads to increased losses in the steering system. The same reasoning is typically also applicable to the engine cooling pump, oil pump and fan. Table 1.2 lists the predicted fuel savings for different technologies related to electric auxiliary systems in a passenger car. The figures presented in the table are valid for the conditions during standardized driving cycles, changing the ambient conditions may influence these figures significantly. For example, the fuel savings with an electric water pump during city driving in cold weather conditions may be as high as 4% [22].

In addition to the advantages of electric auxiliary systems already mentioned, other advantages include: Higher freedom in the placement of the sub-systems in the vehicle and removal of all hydraulic fluids, pneumatic and hydraulic pipes, mechanical linkages, etcetera. All this opens up for new innovative designs of the vehicle.

*Table 1.2. Effect on the fuel consumption of technologies related to electric auxiliary systems of a conventional car during an average of city and highway driving [22].*

| Technology | Estimated Fuel Savings Average of City/ Highway driving |
|---|---|
| Electric Power Steering | 2-3 % |
| Efficient Alternator | ~ 0.5 % |
| Electric Oil Pump | ~ 0.5 % |
| Electric Water Pump | ~ 0.5 % |
| Idle Off[1] | 3-5 % |

*Table 1.3. Estimated peak powers of electric auxiliary systems for cars [23], and peak powers of conventional auxiliary systems in a heavy vehicle [24].*

| | Peak Power(kW) | |
|---|---|---|
| **Auxiliary Load** | **Car** | **Heavy Truck** |
| Active Suspension | 12 | - |
| AC-compressor | 4.0 | 4.5 |
| Electric Power Steering | 1.5 | 4-11 |
| Engine Cooling Fan | 0.8 | 15-30 |
| Water (Coolant) Pump | 0.5 | 2 |
| Oil pump | - | 4.5 |

[1] The internal combustion engine shuts off as soon as it idles, e.g. during red lights or deceleration. Requires electrically powered auxiliary systems.

Table 1.3 presents the peak powers of a number of auxiliary systems for cars and heavy vehicles. The figures for average power have deliberately been left out since they depend very much on the driving conditions (outside temperature, traffic, etc). The table highlights one of the difficulties with electrification of heavy vehicles compared to cars, namely the higher power requirements. High powers equal high currents and therefore large and expensive wiring, assuming the conventional 14/28V electrical system. Furthermore, the conventional electric system is already at its peak capacity, introducing more electric loads require new generators with higher capacity. On the other hand, in hybrid and electric vehicles there exists no such shortage of electric energy and the high voltage system used for the traction motors may be used for the high power auxiliary systems too.

### 1.4.3 THE VEHICLE'S ELECTRICAL SYSTEM

The characteristics of the electric interface are important for the dimensioning of mechatronic actuation modules. This section gives therefore a short presentation of the current and future electric networks in road vehicles.

The conventional electrical system in cars employs a 12 V lead-acid battery for energy storage, creating a power network with a nominal voltage of 14.4 V with the engine on (heavy-duty vehicles generally have an electrical system with a nominal voltage of 28 V, buffered with a 24 V battery). But the actual voltage in a 14.4 V system ranges from about 9 V to 16 V, depending on the alternator's output current, battery age and state of charge [25]. Loads are therefore sized to function properly at the lowest system voltage; thus when the voltage is higher more current than necessary is used.

By 1994 Mercedes Benz realized that they would need a higher voltage to support future electrical systems. The result was a proposal for a 42 V electrical system buffered with a 36 V lead-acid battery [26]. But the 42 V electrical system has not yet been adopted in any major scale by the automotive industry. Vehicles with hybrid and electric power trains already have a high voltage system on board (about 300-600 V) for the traction motors. This high voltage may then also be used for the auxiliary systems. Hence, the 42 V systems might become obsolete even before taken into production. But as identified in [25] and [26], future vehicles will not have one but rather two or more electric networks with different voltages.

The main advantage of a higher voltage system is that it reduces the current and therefore the required copper area of the electrical wires supplying the sub-systems with electrical power. Furthermore it can be difficult to design large electric machines for low voltages. But there are of course also negative aspects with introducing high voltages in vehicles; one of the most important ones is the risk of electric shocks. However, optimization of the system voltage level is outside the scope of this work. The system voltage is therefore considered as a constant design parameter that is required as input to the methodology.

### 1.4.4 AUTOMOTIVE AUXILIARY SYSTEMS AND THE DESIGN METHODOLOGY

The presented methodology for integrated design of mechatronic servo systems is, as already mentioned, more general than just applicable to automotive sub systems. With the exception of this section (1.4), the thesis is written without any special focus on automotive systems. Parts of the methodology have however been applied to two separate automotive sub-systems: An electric power steering system for heavy vehicles and an electromechanical active suspension system for passenger cars. That work is very briefly summarized here; interested readers are recommended to read [27] and [28].

The left part of Figure 1.8 shows the configuration of the electric power steering system that is analyzed in [27]. The design and optimization methodology is used to derive estimations of the required size of the steering assist actuator. The current configuration of the steering linkage is kept and the assist actuator is attached on the steering column side of the steering gear. The required steering torques during standstill are assumed to limit the size of the actuator. Therefore, a model for the required assist torque during static steering on dry asphalt is derived and used as input to the methodology.

In the right part of Figure 1.8, the principles of the electromechanical suspension system analyzed in [28] are shown. The design and optimization methodology is applied to this system to derive the required physical size of the electric damper, but also to optimize the systems performance. In addition, an investigation about the energy requirements of such an active suspension and the possibility of electricity regeneration are presented in the paper.

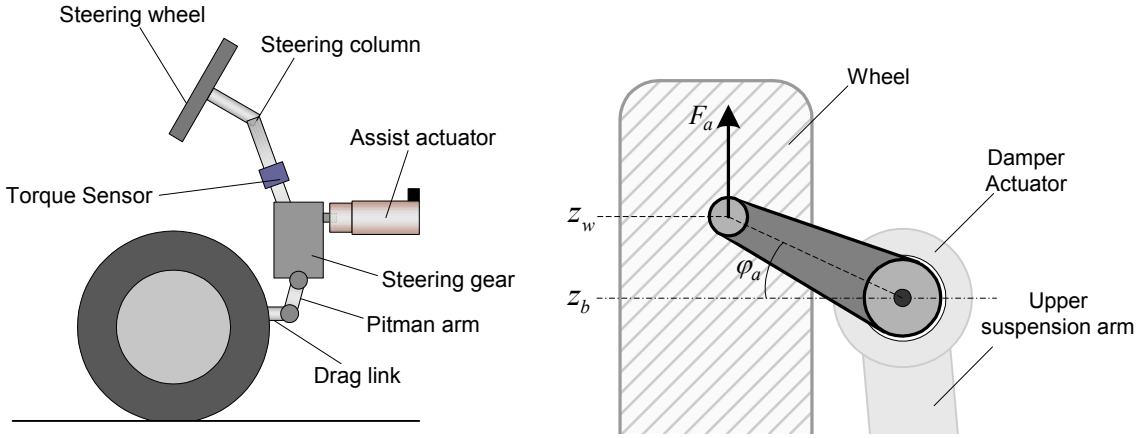


*Figure 1.8. A sketch of the electric power steering system analyzed in [27] to the left. To the right is a sketch of the electromechanical wheel suspension system analyzed in [28].*

## 1.5 SUMMARY OF THE APPENDED PAPERS

### A: OPTIMAL DESIGN OF MOTOR AND GEAR RATIO IN MECHATRONIC SYSTEMS

A method for the optimal design of an electric machine with an ideal gear reducer is presented in this paper. The method, in comparison with many of the previous methods, is applicable to any kind of load, both inertial and constant speed. It approaches the problem in a different way than most of the previous published methods. Instead of finding the best motor from a given set of motors, the method is used to calculate a range of motor dimensions and gear ratios that represent motor/gear ratio combinations which are precisely powerful enough to drive the given load. From this range of motor dimensions the best motor/gear ratio combination with respect to motor weight, size or peak power requirement can be selected

### B: RELATIONS BETWEEN SIZE AND GEAR RATIO IN SPUR AND PLANETARY GEAR TRAINS

Fairly detailed models of the necessary size of spur gear trains required to drive a specified load are derived. The models are based on the Swedish standards for spur gear geometry and spur gear dimensioning. These models can be used to predict the size of a spur or three-wheel planetary gear train as function of gear ratio and output torque. Further on, the equations present the gear inertia, radius and mass as function of output torque, gear ratio and gear width. Even though these models can be used for any kind of application that requires a gear, they have mainly been derived with the intention to be used in design and optimization of electromechanical servo drives.

The derived models confirm what has been well known for a long time in the area: For a given load and gear ratio, three-wheel planetary gears require less volume and mass compared with single spur gear pairs. Also the inertia of a planetary gear train is shown to be much lower than for the corresponding spur gear pair.

### C: INTEGRATED DESIGN OF SERVOMOTOR AND GEARHEAD ASSEMBLIES

A method for the integrated design and optimization of the servomotor and gearhead in mechatronic systems is presented. In contrast to paper A the gearhead is now modeled according to paper B and no longer treated as ideal. The method is intended for applications where it is rational to design application-specific actuators, e.g. high volume applications such as in the automotive sector. From models describing the electric motor and gear size as functions of torque and gear ratio, all the motor - gearhead design combinations that exactly can drive a given load are derived. From this space of combinations, one can then select the best combination with respect to some criterion, such as size or weight. The method is illustrated with two design examples in which the design of the lightest possible motor and gearhead assemblies are derived.

### D: THE INFLUENCE OF GEAR RATIO ON PERFORMANCE OF ELECTRO-MECHANICAL SERVO SYSTEMS

The gear ratio's influence on the dynamic performance of electromechanical servo systems is analyzed. Even though a gear primarily is used to reduce the actuator size and weight it is important to understand how the gear ratio affects the dynamics of the system. A good choice of gear ratio may improve the control performance while reducing the physical size of the system. A physical system is dimensioned with the method presented in paper C, and for each gear ratio the performance is evaluated. It is concluded that for low gear ratios the plant bandwidth is increased with gear ratio. The torque margin of the motor is also shown to increase with gear ratio. Thus, from a control perspective, high gear ratios appear to be better than low.

### E: INTEGRATED CONTROL AND MECHANISM DESIGN OF ELECTROMECHANICAL SERVO SYSTEMS

This paper extends the analysis from paper D with analyzing the effects of gear ratio on control performance but now for a sampled control system and a position sensor with finite resolution. The paper presents an approach to mechatronics design, where design in the physical and control domains are done concurrently. The focus is on the design and optimization of geared electromechanical servo systems. For this kind of system the gear reduction ratio is a very central parameter. Therefore the gear ratio's influence on performance, weight and size of the system is analyzed and discussed. For the example system used in the paper it is shown that the optimal gear ratio from a size and weight perspective also is very good from a control perspective. Generally, a high gear ratio is concluded to result in better control performance than a low. Furthermore, it is concluded that non-linearities as motor current saturation and controller sampling period are important to include in this type of analysis since they are tightly related to control performance as well as to the physical size and cost of the system.

# 2 THE DESIGN AND OPTIMIZATION METHODOLOGY

In this chapter the author's approach to integrated design of electromechanical servo systems is described. The intention is to give an overview of the design and optimization methodology, and to put the models and methods presented in the following chapters in their context. The chapter is introduced with a brief review of previously published research in the area. Then the overview of the design methodology is presented, followed by a section about strategies for design optimization. The chapter is concluded with a presentation of the design example that will be used throughout the thesis.

## 2.1 RELATED WORK

The area of integrated design and optimization methods for mechatronic servo systems is rather unexplored. Obviously, there exist a lot of published methods for design problems constrained to one engineering domain. Expanding the problem so that it includes two components or domains reduces the number of available design methods significantly. Methods that take the entire mechatronic design problem into consideration are extremely rare in the literature. Previously published methods that solve parts of the design problem are referenced and discussed in the subsequent chapters and in the appended papers. Here publications about system level (mechatronic) design and optimization of electromechanical servo systems are reviewed.

Most of the design methods in the area consider only performance optimization of the servo drive, aspects such as weight, size and energy efficiency are not commonly analyzed. However, only considering performance in the integrated optimization of controller and physical system is questionable. In order to obtain optimal performance, parameters such as stiffness, torque capability, sensor resolution and controller sampling frequency should be as high as possible. Hence, if they are not constrained the result from the optimization will in most cases be unrealistic from both a size and cost perspective. On the other hand, the methodology presented in this thesis considers the system performance to be a part of the system specification, and the design task is to design a system that for example is as cheap or light as possible while fulfilling the performance requirements. Furthermore, previously published methods are often based on a selection approach, where the best components are selected from a set of already existing components (off-the-shelf). An approach that may be cost-effective for low production volume applications, but it is less likely to be effective for products produced in large volumes. The target with the presented methodology is to find the optimal design of each component from a system perspective, not to choose components from already existing ones.

It has in several scientific papers been demonstrated that the design of the structure and the design of the controller need to be integrated in order to find the system optimum (e.g. [1] and [2]). However, very few papers present a design methodology for fully coupled mechatronic design problems, where the

individual design of one component depends on the design of the other components and vice versa.

Fathy *et al*. [29] identifies four different strategies for integrated optimization of physical system and controller: *Sequential, Iterative, Nested* and *Simultaneous* (Figure 2.1). The two first represent strategies that only have the potential of finding designs that are optimal within each domain, but sub-optimal on the system level. The other two on the other hand, can, from a system perspective, find the optimal design.

Narrowing the search to integrated design methods for electromechanical servo systems reduces the available methods even further. Reyer *et al*. [30] optimize the physical design of an electric DC-motor together with its control. Their objective is to minimize machine weight, speed response error and the machine voltage. They approach the problem with the nested optimization technique shown in Figure 2.1, which is an interesting approach. However, the system that is optimized is just an electric machine and its controller, a second-order system where the couplings between plant and controller design are somewhat unclear. But they focus on the optimization method and not on modeling and analysis of the electromechanical system.

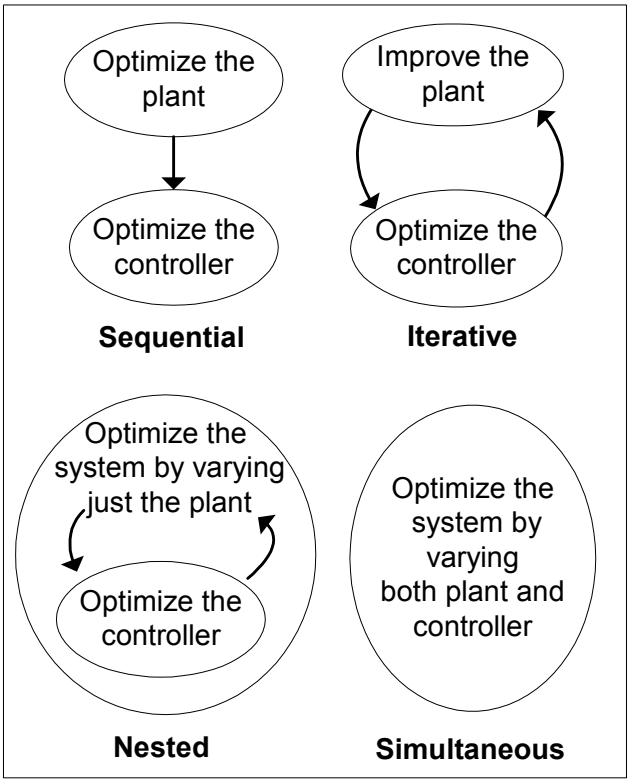


*Figure 2.1. Strategies for integrated plant/controller optimization [29].*

Kim and Chung [31] and [32], present models and a design methodology for ball screw driven servomechanisms. Their focus is performance optimization of the ball screw and controller. The method optimizes parameters of the controller as well as of the ball screw, but the electric machine is selected from a list of already existing machines; it is not truly optimized for the application. It is also unclear why the machine is selected (optimized) with respect to size while the

screw is dimensioned with respect to control performance. Furthermore, the methodology only considers the dynamical aspects of the servo drive; it is not obvious if for example mechanical stresses in the screw are considered. Design variables such as controller sampling frequency and sensor resolutions are not considered, but that may be natural from a performance optimization perspective, since those variables would end up to be as high as possible. The methodology looks very nice for performance optimization of linear motion servos, but since it does not consider the size, weight or cost of the components it does not compare directly to the design methodology presented here.

## 2.2 OVERVIEW OF THE METHODOLOGY

Figure 2.2 shows a block diagram of the proposed methodology for integrated design of electromechanical servo systems. The target is electromechanical actuation systems in general, but so far only models of components for rotational motion servo systems have been derived and included into the methodology (see Table 1.1). It is intended to be applied during the conceptual level of the design process and primarily be used for concept evaluation and selection. The idea is that the methodology should be used to optimize a number of proposed conceptual design solutions with respect to the same criterion, which then enables a fair comparison of the solution concepts. The retrieved system parameters of the selected concept may then be transferred to the detailed design phase as design requirements or design objectives.

In the top of Figure 2.2 the input to the methodology is presented, namely the system requirements and the servo configuration (conceptual design). The methodology is then used to derive a design (set of parameters) that exactly fulfills the requirements while being optimal with respect to some criterion. The current implementation of the methodology is most powerful for *size* and/or *weight* optimization, but *performance* and *efficiency* are also analyzed.

The methodology is based on two types of models, or design views (see also section 1.1.2): *static* and *dynamic* models. The *static* component models describe relations between the design parameters of the individual components. For example models relating the physical dimensions of a gear to its torque rating. The static component models are mainly used to optimize the physical components. But also to derive parameters and constraints required for the dynamic simulation model. The *dynamic* models describe the components' behavior as function of time, which is necessary for control system design and performance optimization.

As depicted in Figure 2.2, the physical system is first optimized for a specific load profile, by the use of the static component models. This design method for the physical parts of the system is a very powerful tool in itself. From estimations, simulations or measurements of the load, the method quickly gives an estimate of the final size and weight of the servo actuator. One of the nice things about this part of the methodology is that it does not require a mathematical model of the load. However, in order to find the true system optimum it is necessary to include the control system design into the methodology.

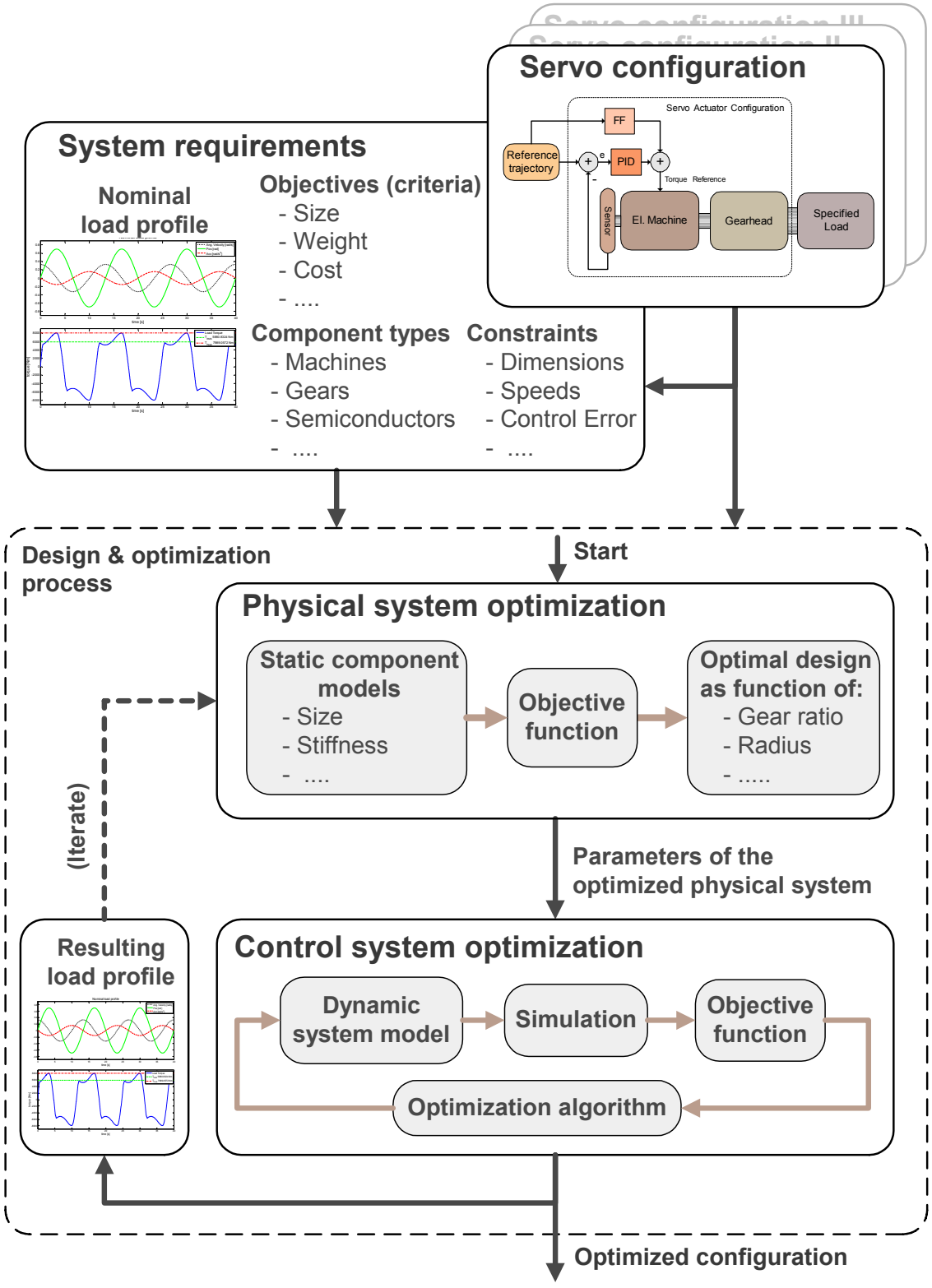


*Figure 2.2. Overview of the presented design and optimization methodology for mechatronic servo systems: Based on the system configuration and performance requirements the physical system is optimized. The parameters of the optimized physical system are then used in the dynamic simulation model used for control system optimization.*

Consequently, from the static component models, parameters such as stiffness and inertias are transferred into the dynamic simulation model. In this second optimization loop the control system parameters are optimized for the already optimized physical system. Since the parameters of the control system affect the physical system design and vice versa it is necessary to iterate between physical system optimization and control system optimization in order to reach the exact system optimum. However, in many cases the accuracy of the input data, the component models and maybe also the requirements are rather low so this iteration may be omitted.

In this research the methodology has been implemented in matlab/simulink. The static component models are implemented in matlab script-files while the dynamic system model is implemented in simulink. It would of course be possible to implement the dynamic model part in a multi-domain modeling tool as the once mentioned in section 1.1.2. However, the natural coupling between matlab and simulink is the main reason why the choice fell on them.

## 2.3 INPUTS AND DESIGN REQUIREMENTS

In the upper part of Figure 2.2 the required inputs to the design and optimization methodology are illustrated. First of all, a solution concept specifying the configuration of components and component types is required (the current implementation only supports a few component types, see Table 1.1). In addition, constraints on for example the maximum allowed control error need to be specified. The most important input to the methodology is however the nominal load profile. The load profile describes the required torque and angle of the outgoing shaft of the servo actuator as function of time. The load profile is not only describing the design load for the physical system, if applicable, it also specifies the reference signal for the control system. As an example, the nominal load profile of an electromechanical power steering system is shown in Figure 2.3 below.

The nominal load profile is defined to be cyclic, which means that the system is designed and optimized to drive this profile repetitively without breaks. However, if the cycle time is longer than the thermal time constant of the electric machine, the most demanding part of it has to be selected. Methods for identifying the dimensioning part of long load profiles are not included in the methodology. Such a method may be rather complex, since different parts of the load profile might be dimensioning for each of the components. One part of the profile might for example limit the size of the gearhead while a different part limits the size of the electric machine. This is however left for future research to investigate.

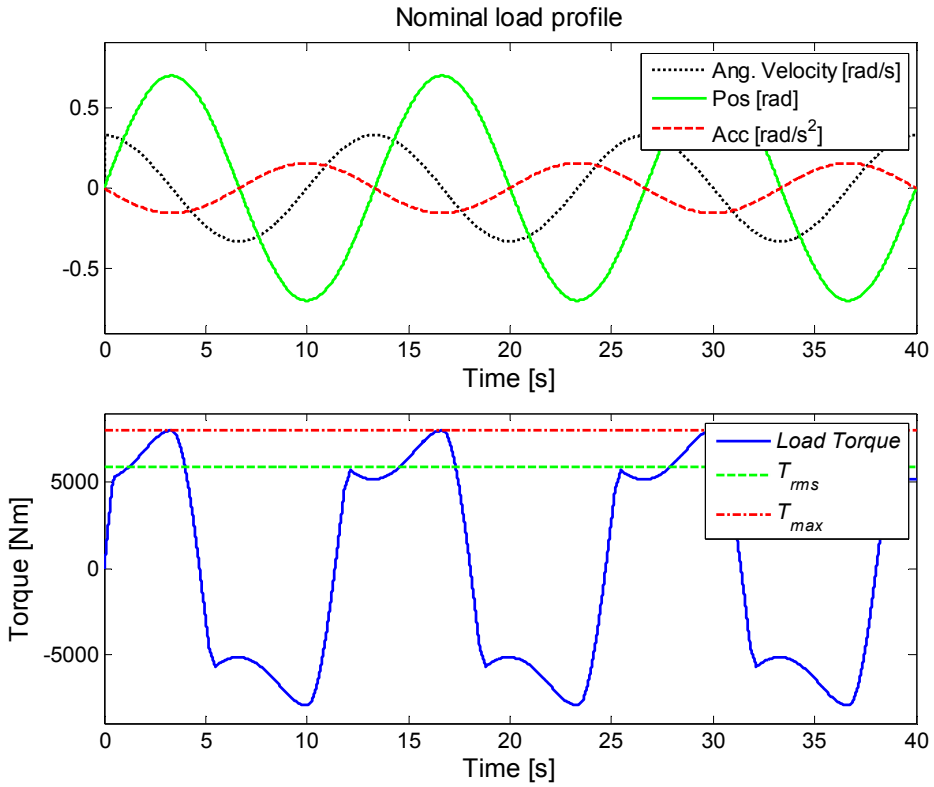


*Figure 2.3. Example of a load profile specification, angle and torque of the servo's outgoing shaft as function of time. This specific load profile describes the load in a heavy vehicle's power steering system during a sinusoidal steering pattern at standstill.*

Hence, in this work it is assumed that the nominal load profile is known and can be used as input to the design and optimization process. However, in applications where the requirements are of the type: *move a specific load from point a, to point b, in a limited time*, the shape of the velocity/position profile is up to the system designers. For a pure inertial load, it has been shown that a parabolic velocity profile minimizes the energy dissipation in the electric machine [33]. The energy dissipation (losses) are often vital to minimize, since reducing the losses means that a smaller machine may be used to accomplish the same task; alternatively the system's performance (cycle time) may be improved. For a more realistic load with viscous friction, an exponential shaped velocity profile is optimal, according to [33]. However, in many design cases it is impossible for the system designers to shape the velocity profile, in an electric power steering system for example, it is the driver who decides the profile. Even though the topic of velocity profile optimization is interesting and important, it has not been included in this research. To some extent the iterations in the design and optimization process shown in Figure 2.2 represent optimization of the load profile. For example, if the controller is optimized such that it minimizes the machine torque (with a constraint on control error), it will result in lower torque requirements than specified by the nominal load profile. The physical system may then be re-optimized for these lower torque requirements. But this is far from a complete method for load profile shaping, since the controller reference is assumed to be the one specified by the nominal load profile. A natural extension of the methodology would be to include full optimization of the shape of the velocity/position profile.

In order to specify and evaluate the system performance, it is necessary to quantify the control performance with some sort of index. Examples of such indices are: the maximum absolute error (*MAE*), the integral absolute error (*IAE*) and the integral square error (*ISE*)

$$MAE = \max | r(t) - y(t) | \tag{2.1}$$

$$IAE = \int_0^\tau | r(t) - y(t) | \, dt \tag{2.2}$$

$$ISE = \int_0^\tau (r(t) - y(t))^2 \, dt \tag{2.3}$$

where *r(t)* is the controller reference signal and *y(t)* the system output. One or several of these indices may be used to specify the constraint on maximum allowed control error. Or if performance is the objective with the optimization, one of these or a combination may be used as objective function.

## 2.4 DESIGN OPTIMIZATION

The intention of this section is to describe the optimization strategies, objectives and criteria used for the integrated system optimization.

### 2.4.1 OPTIMIZATION STRATEGIES

As seen in Figure 2.2, the optimization of the physical system is separated from the optimization of the control system. This approach to system optimization would therefore be classified as nested (Figure 2.1). The separation of physical system design and control system design is mainly done because the two design problems are very different in nature. As discussed above the methodology is based on two types of component models, *dynamic* and *static* models. The static component models are algebraic expressions which make it possible to derive the optimal design in an analytic way, without having to simulate the system. In contrast, the dynamic system model is based on differential equations and needs to be simulated. The complexity of solving (simulating) the differential equations makes it unrealistic to simulate the system for all possible combinations of design variables. It is therefore necessary to apply a more advanced optimization method for the controller design.

Thus, for the design and optimization of the physical system, the optimal design may either be read directly from a 2D or 3D graph, or if the number of design variables are larger than two, be derived with the help of differential calculus.

For the control system optimization a non-gradient based optimization technique is preferable, since it is difficult to calculate the derivatives of an objective function resulting from a numeric simulation model. In this work a genetic optimization algorithm has been used, but other non-gradient based optimization algorithms would probably be as good. The basic idea of genetic algorithms (GAs) is the mechanics of natural selection. Each optimization parameter (design variable) is coded into a gene, in this case as a real number. The corresponding genes for all parameters form a chromosome which describes each individual, for example:

$$Chromosome = [P \quad I \quad D]$$

where $P$, $I$ and $D$ represents the controller gains.

Each individual represents a possible solution, and a set of individuals are called a population. For each individual in the population the objective function value is calculated (simulated). The best individuals are selected for mating, which is performed by combining genes from different parents to produce a child. Random mutations may also occur. Finally the offspring are inserted into the population and the process starts over again until the maximum number of generations has been reached.

### 2.4.2 OPTIMIZATION CRITERIA AND DESIGN VARIABLES

A complete design methodology for mechatronics should cover several optimization criteria. Depending on application the primary objective of the optimization process might be: cost, weight, performance, energy efficiency, etcetera. The primary optimization criteria targeted in this research is *size* and *weight*. The methodology is very powerful when it comes to finding the smallest possible system design that fulfills the requirements on performance. This approach is also closely related to finding the design solution that represents the lowest component *cost*. Other targeted optimization criteria are *performance* and *energy efficiency*. However, optimization with respect to these two criteria is not as straight-forward as the previous two. In its current implementation the methodology only supports *weight* and *size* optimization, but system efficiency and performance are evaluated.

Even though the modeling detail is kept low for each of the constituent components the total number of design variables tends to get large in this type of cross-component, cross-domain analysis. A large number of design variables makes not only the optimization problem very computation intensive, it also makes it impossible to graphically display the design objective as function of the design variables. Even though not required to find the design optimum, such graphs are very useful in order for the design engineers to get an understanding of how the design variables affect the system design. Hence, one of the main objectives during the modeling phase has been to reduce the number of free design variables as far as possible. This has been achieved in part by considering many of the more peripheral design variables as constant parameters. But the number of variables still gets large; therefore the number of free design variables has been reduced further by deriving relations between them. These relations are mainly based on traditional dimensioning rules from each domain. For example, the gears in a gearhead are dimensioned with respect to mechanical fatigue, eliminating all gears that are too small to drive the load but also all gears that are over-dimensioned with respect to mechanical fatigue. By doing this it is possible to express the gear radius as function of its width and torque rating. In other words, the dimensions of the gearhead have been forced to exactly fulfill the constraints set by mechanical fatigue. The torque constraint becomes a design rule that has to be fulfilled. The same idea is used for the electric machine, where only dimensions of machines that exactly can drive the given load with respect to torque are derived. This approach reduces the number of free design variables to a minimum.

The approach described above is indirectly based on that the design objective is to obtain the smallest possible components for the application. However, this approach is not guaranteed to yield in an optimal design if performance or efficiency is evaluated in the objective function. Consider for example efficiency optimization of an electric machine, adding more copper to the winding reduces the resistive losses, but increases the machine size, weight and cost. You end up with a machine that from a traditional mechanical design point of view would be unnecessarily large for the application. The approach taken throughout this thesis is focused on that each of the physical components is dimensioned to be as small as possible without braking, a very common approach to machine design in general. However, in order to reach the true system optimum with respect to performance or efficiency (given constraints on for example system size), it is necessary to let all design variables free. Unfortunately this results in a much more computation intensive methodology which also has the disadvantage that it is not possible to graphically show the objective function. The primary focus in the subsequent chapters and in the appended papers is however size and weight optimization. Performance and efficiency, even though not optimized, are analyzed and discussed.

## 2.5 ASSUMPTIONS AND LIMITATIONS

The goal has throughout this research been to develop a methodology that is as general as possible. However, it is difficult to be general and accurate at the same time, especially if it also is important to keep the complexity relatively low. Many assumptions have been made, most of them only have marginal effects of the end results, but some may influence the result significantly. There is not room to list and discuss all assumptions here; they are instead mentioned in their context in the following chapters and in the appended papers. The possible implications of the assumptions are generally discussed in short where they are introduced, but a longer discussion about the effects of some of the assumptions is presented in section 6.2.

The design and optimization methodology has many advantages, but in its present implementation also some limitations. For example, as mentioned before, only one or a few component types are modeled, which limits the applicability of the current implementation of the methodology. The machine models are valid for permanent magnet machines in general, while the models of the motor driver only cover drivers for three-phase AC synchronous machines. This means that the implementation of the complete methodology only is applicable to permanent magnet synchronous machines (PMSM) and not brushless-DC and DC-machines. Another limitation is that the methodology does not consider the geometrical integration of the components. Even though the volumes of the individual components are optimized, the components' shapes and geometries are not optimized. This may lead to that the shapes of the components are badly matched and therefore to a low volumetric utilization of the integrated system. These limitations and others are discussed in more detail in section 6.2.

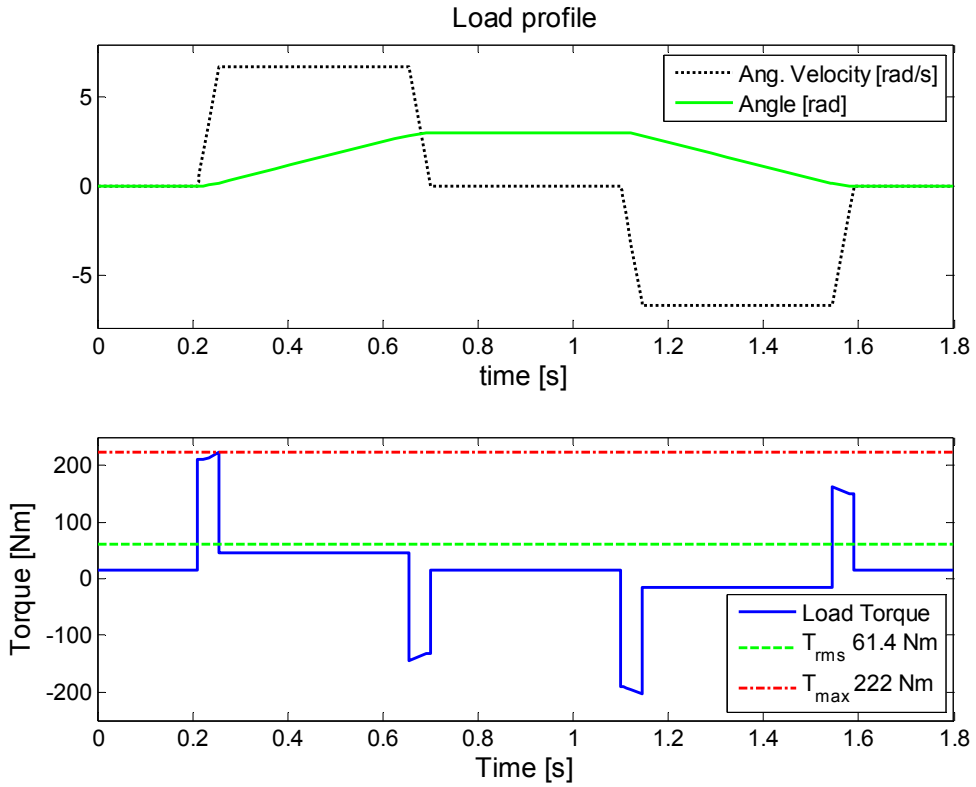


*Figure 2.4. The nominal load profile used as design example in the thesis.*

## 2.6 DESIGN EXAMPLE

A design example will be used throughout the thesis in order to illustrate the methodology. The example load is presented in Figure 2.4, it is intended to resemble a joint load in an industrial robot. It is however constructed with a very simple mathematical model and may miss some characteristics of a typical robotic joint load. The mathematical interpretation of this load profile is

$$T_l = J_l(1+0.5\sin\varphi_l)\ddot{\varphi}_l + T_{fric}\,\mathrm{sgn}(\dot{\varphi}_l) + T_{static} \tag{2.4}$$

Where $J_l$ represents the load inertia, $T_{fric}$ a coulomb friction torque and $T_{static}$ a static load torque, Table 2.1 lists the values of these parameters. $\varphi_l$ represents the load angle according to Figure 2.4. For the parts of the methodology that deal with the design and optimization of the physical system, the mathematical model of the load is unnecessary. However, for the other part, dynamic analysis and control system optimization, a mathematical simulation model of both the servo system and the load is required.

*Table 2.1. Parameters used in the model of the example load (2.4).*

| **Load inertia** $J_l$ | **Friction torque** $T_{fric}$ | **Static torque** $T_{static}$ |
|---|---|---|
| 1.1 kgm$^2$ | 30 Nm | 15 Nm |

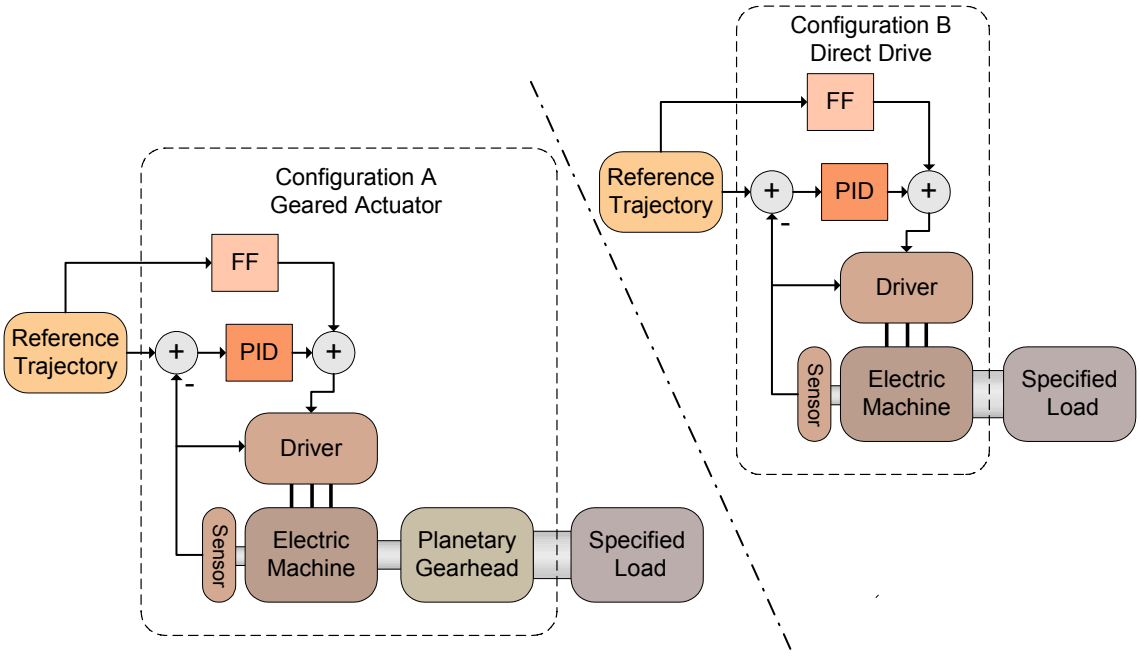


*Figure 2.5. Example configurations.*

Two different design concepts or configurations will be designed and optimized to drive this load, one direct drive configuration and one with a gearhead between the load and the machine. A conceptual drawing of the two configurations is shown in Figure 2.5. The focus will be on the geared solution throughout the thesis, but the direct drive will be used for comparison. For the direct drive solution, a commercially available direct drive machine from Alxion [34] has been selected, Table 2.3. This machine fits the load almost perfectly; its rated torque is only slightly higher than the torque required by the load (63 Nm compared to 61 Nm).

It is also of interest to compare the results of the presented methodology with the more conventional approach of selecting the best set of existing components for the application. Here the conventional approach is illustrated by selecting the smallest motor that can drive the load from a list of existing motors (Table 2.2). By calculating the required torque as function of gear ratio for all the machines in Table 2.2, and then eliminating combinations that result in too high speed or torque, result in the graph presented in Figure 2.6. The method used for this selection is presented in detail in [35].

The volume of the direct drive machine is also shown in the figure. As seen, the gear ratio has a great influence on the required machine size; the direct drive machine is about 10 times larger than the smallest possible geared solution. It should however be mentioned that the gearhead have here been treated as ideal, and its size must be added to the machine size for a fair comparison. These results are only valid for the example load profile in Figure 2.4, the difference in size between the direct drive and geared solution might be much smaller for other loads. The direct drive configuration also has advantages when it comes to controllability, which is evaluated in section 4.3.3.

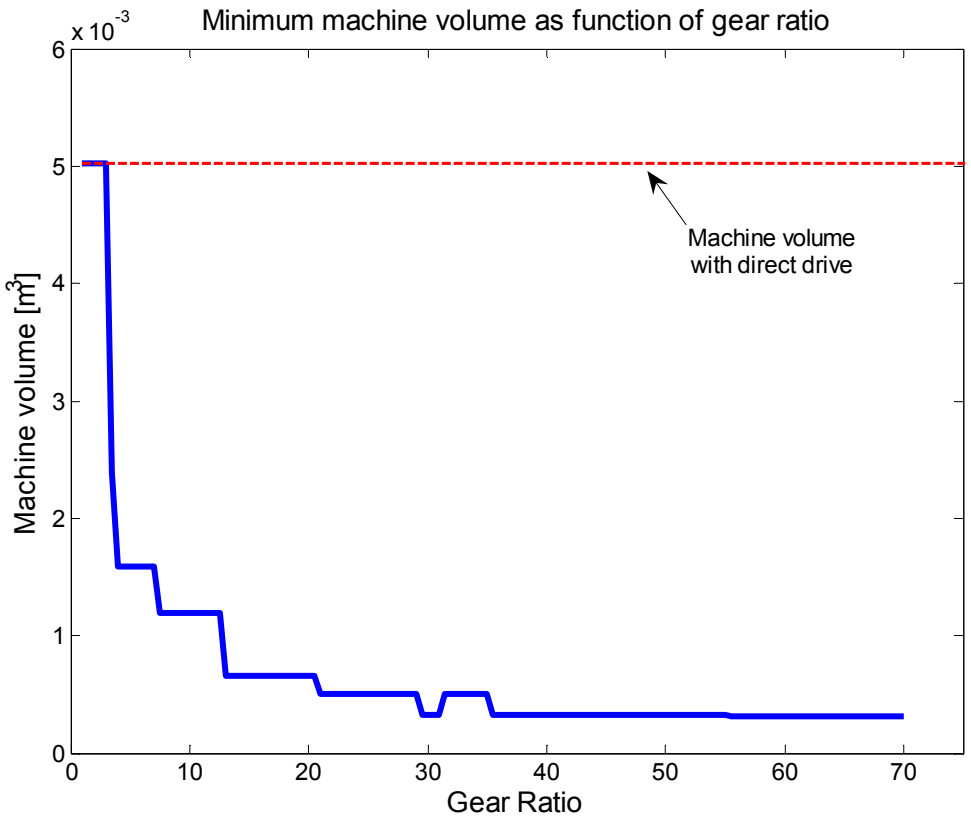


*Figure 2.6. Required machine volume as function of gear ratio (gear assumed ideal).*

*Table 2.2. Data on motor candidates to drive the example load, Elmo [36]. $T_{rated}$ is the rated rms- torque, $J_m$ the machine inertia, see page 105 for the others.*

| Machine | $T_{rated}$ [Nm] | $\omega_{rated}$ [rpm] | $J_m$ [kgm$^2$] | $r_m$ [m] | $l_m$ [m] | $R_p$ [Ω] | $L_p$ [mH] | $K_e$ [Vs] |
|---|---|---|---|---|---|---|---|---|
| PSA60/4-50A | 0.63 | 6000 | 0.79e-4 | 0.03 | 0.05 | 2.45 | 5.2 | 0.12 |
| PSA60/4-75A | 1.00 | 6000 | 0.98e-4 | 0.03 | 0.075 | 1.9 | 3.5 | 0.12 |
| PSA60/4-112A | 1.50 | 4500 | 1.30e-4 | 0.03 | 0.112 | 1.9 | 3.5 | 0.15 |
| PSA90/6-52A | 2.60 | 2000 | 2.90e-4 | 0.045 | 0.052 | 4.0 | 7.7 | 0.23 |
| PSA90/6-52B | 2.10 | 4500 | 2.90e-4 | 0.045 | 0.052 | 1.75 | 2.5 | 0.14 |
| PSA90/6-52C | 2.30 | 3000 | 2.90e-4 | 0.045 | 0.052 | 2.0 | 4.0 | 0.18 |
| PSA90/6-79A | 3.50 | 3000 | 3.80e-4 | 0.045 | 0.079 | 0.75 | 2.8 | 0.20 |
| PSA90/6-105A | 4.50 | 3000 | 4.70e-4 | 0.045 | 0.105 | 0.55 | 2.1 | 0.20 |
| PSA90/6-79B | 3.10 | 4500 | 3.80e-4 | 0.045 | 0.079 | 0.42 | 1.7 | 0.15 |
| PSA90/6-105B | 5.00 | 2000 | 4.70e-4 | 0.045 | 0.105 | 1.2 | 4.7 | 0.30 |
| PSA130/6-50A | 5.90 | 4000 | 12.2e-4 | 0.065 | 0.05 | 0.24 | 1.9 | 0.18 |
| PSA130/6-90A | 9.20 | 4000 | 16.7e-4 | 0.065 | 0.09 | 0.12 | 1.1 | 0.19 |
| PSA130/6-120A | 16.3 | 1200 | 21.2e-4 | 0.065 | 0.120 | 0.55 | 5.8 | 0.52 |
| PSA130/6-150A | 17.5 | 1200 | 25.7e-4 | 0.065 | 0.150 | 0.40 | 4.5 | 0.52 |
| PSA130/6-180A | 19.0 | 2000 | 30.1e-4 | 0.065 | 0.180 | 0.23 | 2.5 | 0.36 |

*Table 2.3. Data on a suitable direct drive motor from Alxion [34] (190STK4M).*

| Rated torque | Peak torque | Rated speed | Inertia | Shaft diameter | Weight | Volume |
|---|---|---|---|---|---|---|
| 63 Nm | 238 Nm | 500 rpm | 75 kgcm$^2$ | 72 mm | 22 kg | 5.0 L |

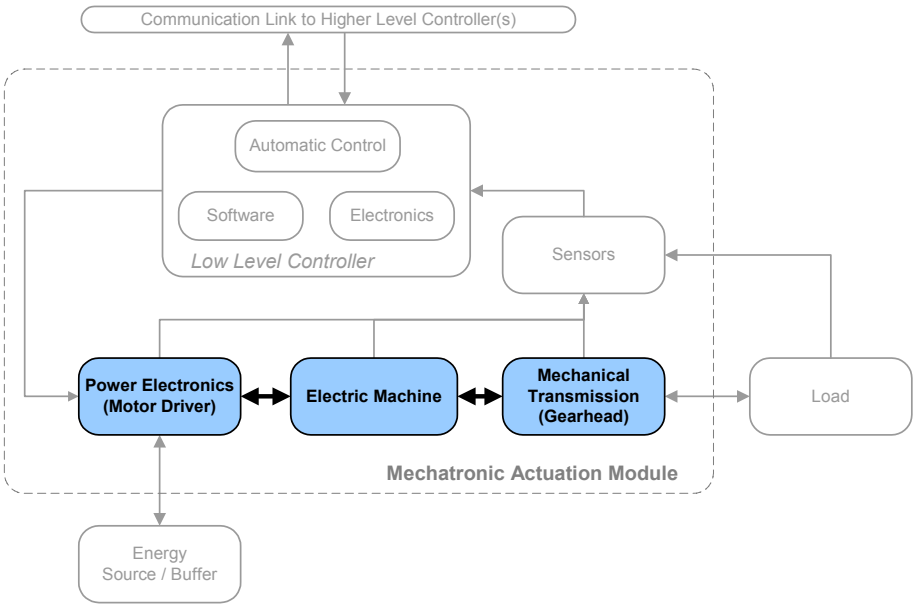


# 3 PHYSICAL SYSTEM DESIGN AND OPTIMIZATION

This chapter focuses on the design and optimization of the powertrain of a mechatronic servo system. Parts of the contents are described in more detail in the appended papers A-C. Other parts, as for example the section about the motor driver, are new and have not been published before.

The components included in the powertrain are the motor driver, the electric machine and the planetary gearhead. The focus is on integrated servo systems where all components are integrated into one physical module as in Figure 3.1. However, the methodology is also applicable to conventional, less integrated, servo drives, where for example the motor driver is placed in a separate box.

First, the models of the electric machine are presented. Then the physical models of the gearhead are introduced followed by the modeling of the motor driver. In order to visualize the methodology all models and methods are applied to the design example presented in the previous chapter. The chapter is concluded with a discussion about the results of the design and optimization method.

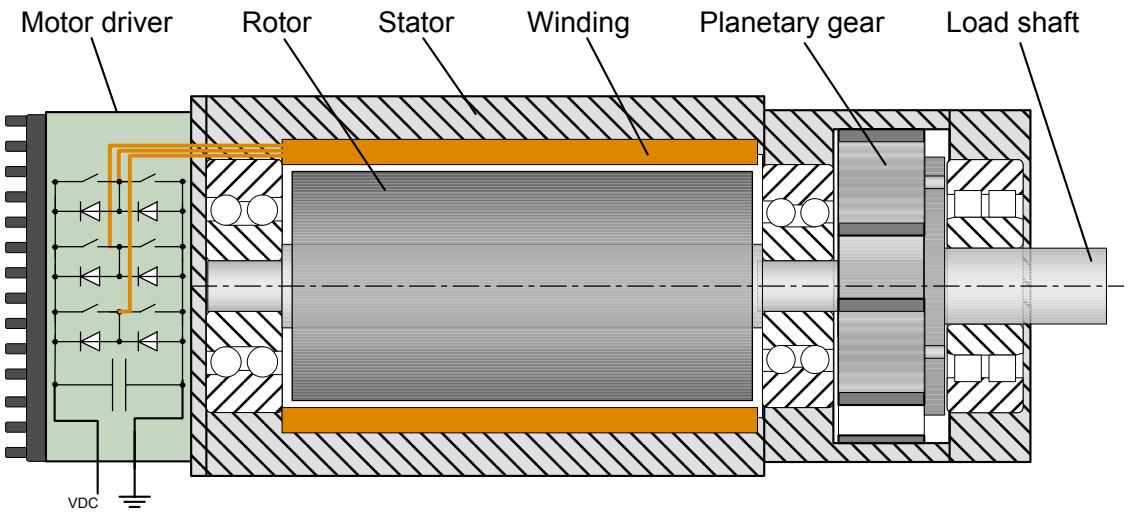


*Figure 3.1. Possible configuration of a physically integrated servo actuator.*

## 3.1 RELATED WORK

This section gives an overview of the previously published research in the area of integrated design of the physical parts of a servo system. A nice overview of the design and optimization issues in servo systems is given by Cetinkunt [37]. He does however not present any design or optimization method, but identifies that the optimal design of servo systems includes much more than just the optimal sizing of servo motors.

The problem of finding the optimal servo design is often divided into sub-problems concerning one or two of the constituent components. The author does not have knowledge about any previously published holistic design method for the complete servo system. A few publications about integrated design of drive electronics and electric machine does however exist. Harris *et al.* [38] present the design of an integrated motor and driver for an automotive water pump, where the pump, motor and electronics are integrated into one physical module. They do not present any general design method for such systems, but concludes that the motor driver not only stands for a significant part of the cost, but also a significant part of the system's size. In particular the DC-link capacitor is identified as a bulky and expensive component, but also the electronic components associated with the EMI filter contributes significantly to the total system size.

The problem with finding the optimal machine and gearhead combination is in the literature generally reduced to the problem of selecting the optimal gear ratio for a given electric machine. Usually the objective is to optimize the system performance (cycle time). Pash and Seering [39], derive the gear ratio, $n_{opt}$ that optimizes the actuator's output torque for the special case with a pure inertial load

$$n_{opt} = \sqrt{J_l / J_m} \tag{3.1}$$

where $J_l$ is the inertia of the load and $J_m$ the machine inertia. They also conclude that the optimal gear ratio will be close to the one given by (3.1) also when friction and other dissipative forces are present. Van de Straete *et al.* [40] and [41] propose a general method for servo drive selection and optimization. Their method is applicable for all rotational load types (friction, inertial, etc.), and valid for many types of electric machines. It does however, as most methods, assume an ideal gearhead. Roos *et al.* [35] present a method for the optimal selection of electric machine and gearhead that also considerers the physical aspects of the gearhead. However, all of the mentioned methods are only applicable for the problem of selecting the optimal components from a discrete set of already existing components. In contrast, the methodology presented here aims at solving the problem of finding the optimal weight, size and other physical properties of the constituent components, without being limited to already existing components.

Ottoson & Sekkinen [42] present a method for optimal design of electric machine and gearhead in machine tools for screw tightening. Their approach is partly

based on the methodology presented here, but it is heavily focused on the particular aspects of electromechanical screw tightening tools.

The main differences of this work in contrast to the majority of the previously published works are: *1*.) The holistic approach, very few (if any) of the previously published methods include all constituent components in the same analysis. *2*.) The majority of the previously published work focuses on selection of the best components from a discrete set of already existing components, the focus of this methodology is the design of new application optimized components.

## 3.2 REQUIRED TORQUES

In order to dimension the components of the drive train it is necessary to analyze the torques acting on the gear and on the electric machine. Throughout this chapter the system is, for the sake of simplicity, modeled as stiff (stiff gears and shafts). However, even though these components are stiff, they are not infinitely stiff. In addition, backlash is often present in the gearhead. How the flexibilities and backlash influence the required machine torque is analyzed in the next chapter (4). Assuming a stiff system, the torque, $T_m$ required by the machine to follow a given load profile is

$$T_m = \left(J_m + J_g + J_0\right)\ddot{\varphi}_m + \frac{T_l}{n\eta_g} \tag{3.2}$$

where $J_m$ represents the inertia of the machine's rotor, $J_g$ is the gearhead inertia at the machine side of the gears and $J_0$, represents all other inertias in the system (shafts, bearings, etc.). $\varphi_m$ is the rotor angle, $T_l$ the load torque as specified by the nominal load profile (e.g. Figure 2.4), $\eta_g$ is the gearhead efficiency and $n$ is the total gear ratio, which is defined as

$$n = \frac{\varphi_m}{\varphi_l} = \frac{\dot{\varphi}_m}{\dot{\varphi}_l} = \frac{\ddot{\varphi}_m}{\ddot{\varphi}_l} \tag{3.3}$$

where $\varphi_l$ represents the load angle according to the nominal load profile. Inserting (3.3) into (3.2) gives the machine torque

$$T_m = \left(J_m + J_g + J_0\right)\ddot{\varphi}_l n + \frac{T_l}{n\eta_g} \tag{3.4}$$

As seen in equation (3.4), the required machine torque depends on the load, but also on the machine's rotor inertia $J_m$. This makes it relatively complex to design or select a machine for an application that requires high accelerations. It is impossible to judge if the machine can drive the load by just comparing the machine's rated torque with the load torque, an analysis of the influence of the rotor inertia is needed.

The output shaft of the gearhead is assumed to be directly connected to the load. Assuming a stiff coupling between load and gearhead, gives that the gear output torque, $T_g$ equals the load torque $T_l$.

$$T_g = T_l \tag{3.5}$$

## 3.3 ELECTRIC MACHINE SIZING AND OPTIMIZATION

This section deals with the modeling and dimensioning of the electric machine only. The gearhead and all other system components are assumed to be ideal. This section is an extended summary of paper A, but also parts from paper C are included.

As already depicted in Table 1.1 the methodology focuses on permanent magnet (PM) electric machines (e.g. DC, Brushless DC and Synchronous AC); which are commonly used in mechatronic servo systems. PM machines are known for their high torque density, high efficiency and good controllability. Most of the models presented in this section are valid for all of the mentioned machine types. However, only complete models for synchronous permanent magnet AC machines are presented.

As mentioned before, it is important to keep the level of complexity down in the models, therefore a number of assumptions have been introduced. The most important once are: The power losses in the machine are assumed to be dominated by the copper losses, iron and friction losses are hence ignored. The copper losses are generally known to be the largest heat source in a servo motor. However, for very high speed load profiles, it is possible that the other losses will dominate. This is one of the largest simplifications in this work and it is strongly recommended to investigate how the speed dependent magnetic losses can be included into the methodology (this is further discussed in chapter 6). Another simplification is that only radial heat transfer is considered (see also Figure 3.2), which is ok for long machines, but the modeling error gets larger for short machines with large diameters. However, as shown in paper A, the model accuracy is rather good anyway. Further assumptions are mentioned in the appended papers.

### 3.3.1 CONSTRAINTS ON THE MACHINE TORQUE AND SPEED

In order for a machine to be able to drive a given load, mainly three criteria have to be fulfilled. First: in order to avoid overheating the continuous torque rating of the machine has to be higher than the root mean square (rms) of the machine torque. Secondly, the maximum torque of the load profile has to be lower or equal to the machine's peak torque rating. And finally, the speed limit of the machine has to be higher or equal to the top speed required by the load profile. These limits are summarized in Table 3.1.

*Table 3.1. Physical constraints on permanent magnet synchronous machines.*

| Continuous torque limit | Peak torque limit | Speed limit |
|---|---|---|
| Overheating of the winding insulation | Demagnetization of the permanent magnets | Mechanical |
| $T_{m,rated} \geq T_{m,rms}$ | $T_{m,peak} \geq T_{m,\max}$ | $\omega_{m,peak} \geq \dot{\varphi}_{\max}$ |

Starting with analyzing the constraint on continuous machine torque: the root mean square of the required machine torque is given by

$$T_{m,rms} = \sqrt{\frac{1}{\tau}\int_0^{\tau} T_m^2 dt} \tag{3.6}$$

where $\tau$ represents the cycle time of one load cycle ($\tau$ has to be shorter than the thermal time constant of the machine, as discussed in section 2.3). First, by combining equation (3.4) with equation (3.6), the following constraint for the rated torque of the machine $T_{m,rated}$, is obtained.

$$T_{m,rated} \geq \sqrt{\frac{1}{\tau}\int_0^{\tau}\left(\left(J_m + J_g + J_0\right)\ddot{\varphi}_l n + \frac{T_l}{n\eta_g}\right)^2 dt} \tag{3.7}$$

By separating the load parameters from the machine and gear parameters in equation (3.7) the number of calculations during the machine sizing procedure can be reduced significantly. How this is done is shown in paper A.

The second constraint that has to be fulfilled is that the maximum torque of the application has to be lower than or equal to the rated peak torque of the machine, $T_{m,peak}$

$$T_{m,peak} \geq \max\left|\left(J_m + J_g + J_0\right)\ddot{\varphi}_l n + \frac{T_l}{n\eta_g}\right| \tag{3.8}$$

And finally the maximum allowed speed of the machine, $\omega_{m,peak}$ has to be higher than or equal to the speed requirements of the load.

$$\omega_{m,peak} \geq \max\left|\dot{\varphi}_l\right| n \tag{3.9}$$

If all these conditions (equations (3.7)-(3.9)) are fulfilled the machine is assumed to be able to drive the given load. The last constraint (3.9) may be reformulated as shown in (3.10), expressing the maximum allowed gear ratio (considering the electric machine).

$$n \leq \frac{\omega_{m,peak}}{\max\left|\dot{\varphi}_l\right|} \tag{3.10}$$

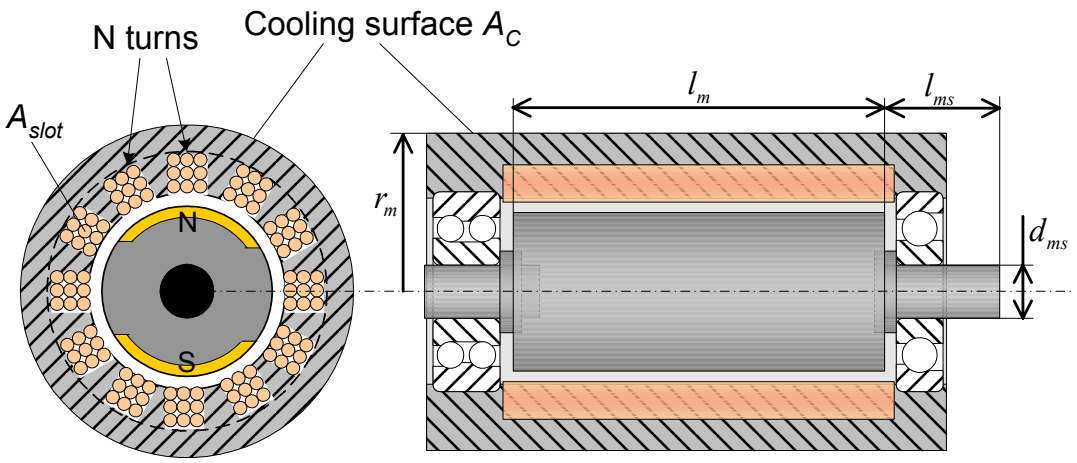


*Figure 3.2. Cross section of a 2-pole PM machine.*

### 3.3.2 MECHANICAL MODELING OF THE MACHINE

This section presents models expressing the parameters of an electric machine as function of its size. The presented models are based on a scaling approach, where data of an existing machine are scaled to retrieve data of fictive machines of the same type, but with different sizes. In paper A, a model for the machine's rated torque as function of its rotor radius and rotor length is derived. That model is then further developed in paper C, to express the rated torque as function of the stator radius, $r_m$ according to equation (3.11) (see also Figure 3.2).

$$T_{m,rated} = C_m l_m r_m^{2.5} \tag{3.11}$$

where $C_m$ is constant for a specific machine type and for the same cooling conditions (e.g. natural convection at an ambient temperature of 25° C). Results from this model are compared to data of existing machines in section 3.3.4. In order to avoid unrealistic shapes of the machines a constraint according to equation (3.12) is introduced, the values used here are just examples and may be different depending on the design case.

$$5 \geq \frac{l_m}{r_m} \geq 0.5 \tag{3.12}$$

In most mechatronic applications it is the constraint on the rated (continuous) torque, equation (3.7), that is active and determines the size of the machine. It is therefore the focus of the methodology; however in extreme intermittent duty applications it is the peak torque that limits the design. In many machine data sheets the peak torque rating is given as a multiplier of the rated torque, an approach that has been adopted in this work. Here is however room for future improvement by developing a model for the peak torque rating based on electromagnetics. But for now, the machine's peak torque rating is approximated to be linear with the rated continuous torque according to

$$T_{m,peak} = C_{pt} T_{m,rated} \tag{3.13}$$

where $C_{pt}$ usually lies between 3-6 for permanent magnet machines, assuming passive cooling, using active cooling results in a lower value.

The limit of the machine's peak velocity due to mechanical stress is proportional to the peripheral velocity of the rotor, which is directly proportional to the machine radius. The maximum allowed gear ratio, equation (3.10), should therefore be higher for a machine with a small radius than for a machine with a larger radius. This is however related to the discussion about speed dependent (magnetic) losses, a high peak speed implies higher losses and the other way around. Since no speed dependent losses are included in the machine model, the rated peak velocity of the machine is in the current implementation of the methodology set to be constant, and independent of machine radius.

$$\omega_{m,peak} = C_{\omega} \tag{3.14}$$

Further, as seen in equation (3.7) an expression of the machine inertia, $J_m$ , as function of the machine radius and length is needed. Equation (3.15) presents such a model which is derived in paper C (assuming a cylindrical, solid rotor).

$$J_m = C_{mj} l_m r_m^4 + J_0 \tag{3.15}$$

Where $C_{mj}$ is, in the same way as descried above, constant for a specific machine type, and is preferably calculated from a machine with known data (the same machine as the one used to calculate $C_m$ and $C_{pt}$). $J_0$ represents the inertia of shafts and bearings and is simplified to be independent of the machine size. Applying equation (3.15) on the machines presented in Table 2.2 on page 30, results in Figure 3.3 below. As seen, the agreement is quite good. Here, machine no 5 (PSA90/6-105) is used as reference for $C_{mj.}$ $J_0$ is set to 10% of the original machine inertia.

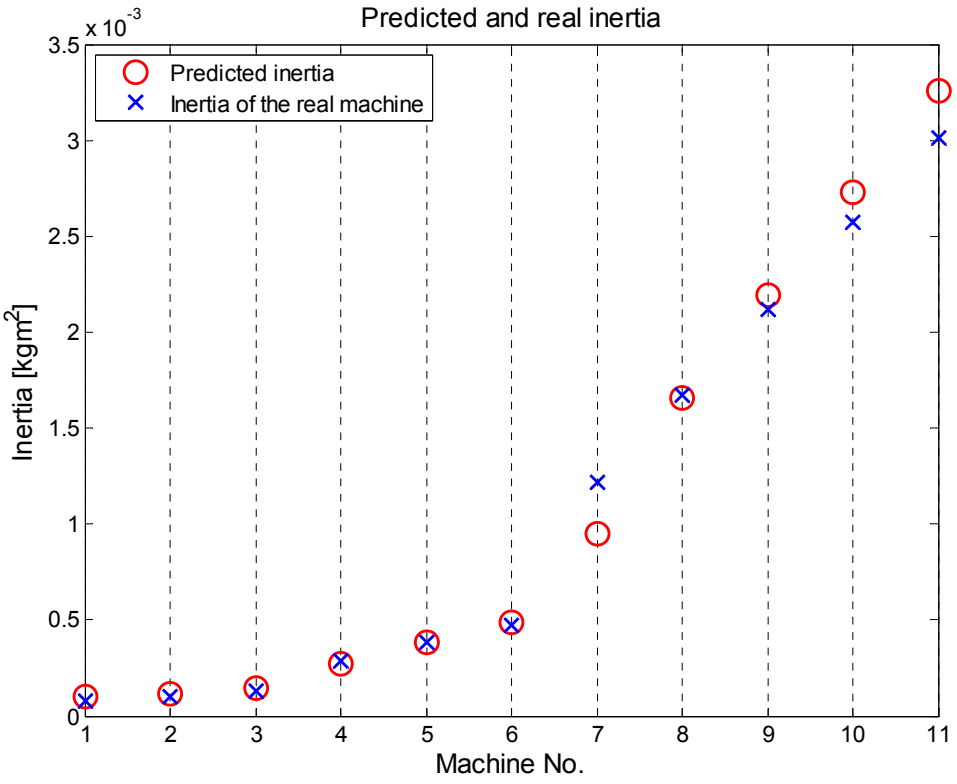


*Figure 3.3. Predicted inertia compared to the inertia specified by the manufacturer of the machines presented in Table 2.2.*

The total stiffness of the servo actuator is very important for the system's dynamic performance. Even though not considered in this chapter, a model predicting the stiffness of the machine shaft is required for the dynamic analysis presented in the next chapter. The shaft is assumed to be a solid cylinder with the length $l_{ms}$ and diameter $d_{ms}$ (Figure 3.2). The machine shaft stiffness, $k_{ms}$ is then given by (paper D)

$$k_{ms} = \frac{\pi E}{64(1+\nu)} \frac{d_{ms}^4}{l_{ms}} = \{steel\} = 7.9 \cdot 10^9 \frac{d_{ms}^4}{l_{ms}} \tag{3.16}$$

where $E$ is the module of elasticity and $\upsilon$ represents Poisson's number.

In order to reduce the number of design variables, the scaling approach may be used on equation (3.16) too. Assuming that the shaft is dimensioned in such way that its peak shear stress load is constant, regardless of machine size, the following expression is valid

$$\sigma_{\tau,\max} = \frac{16}{\pi} \frac{T_{m,peak}}{d_{ms}^3} \Rightarrow d_{ms} = C_{ms} \sqrt[3]{T_{m,peak}} \tag{3.17}$$

where $\sigma_{\tau,\max}$ is the maximum allowed shear stress, and $C_{ms}$ is constant for cylindrical shafts made of the same material. However, if the objective is to optimize the servo's dynamic performance, it might be required to dimension the shaft with respect to stiffness and not shear stress. This is discussed further in the next chapter, treating dynamic analysis of the system.

Finally, the weight of the machine, $m_m$ is approximated to

$$m_m = \pi r_m^2 l_m \rho_m \tag{3.18}$$

Where $\rho_m$ is the average mass density of the stator, air gap, winding and rotor, a realistic value may be 6000-7000 kg/m$^3$.

### 3.3.3 MODELING OF THE MACHINE WINDING

The size and torque rating of a machine is ideally independent of its voltage and current rating. The relation between phase voltage and current depends on the number of turns of copper wire in the machine winding. But the resistive losses for a given output torque, are independent of the number of winding turns and thus of the supply voltage (assuming that the copper fill factor is independent of the number of turns). This means that it is possible to optimize the size of an electric machine without considering its electric properties. However, when designing and optimizing the motor driver, the electric properties of the machine are very important. Hence, this section presents models for the phase resistance, inductance and voltage constant of three-phase permanent magnet synchronous machines. Also here, the models are based on a scaling approach where parameters of an existing machine are used to derive parameters of non-existing machines with different physical dimensions and voltage ratings than the existing machine. All of the presented equations below assume a permanent magnet synchronous machine, where the phase currents and voltages are sinusoidal shaped. This part of the current implementation of the methodology is therefore only applicable to synchronous AC machines.

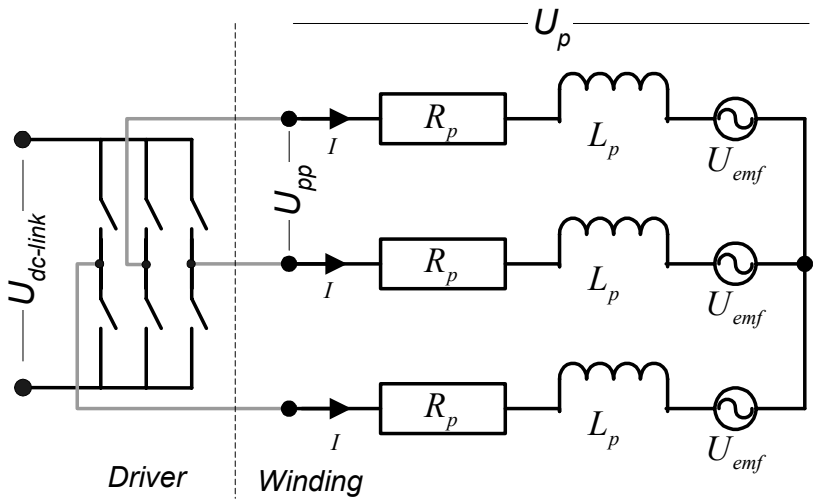


*Figure 3.4. Model of the winding of a synchronous AC machine.*

The induced voltage (emf), $U_{emf}$ in one phase of the machine winding equals (derived from [43])

$$U_{emf} = \frac{p}{2\pi}\omega_m N_p \phi \tag{3.19}$$

Where $p$ is the number of poles, $N_p$ is the number of winding turns per phase and $\omega_m$ the machine speed. The magnetic flux per pole $\phi$, equals

$$\phi = \frac{4\pi}{p} r_r l_r B_{ag} \tag{3.20}$$

Where $r_r$ and $l_r$ is the rotor radius and length respectively, $B_{ag}$ is the magnetic flux density in the air gap which is constant for a specific machine design (property of the permanent magnet). Combining (3.19) and (3.20) gives

$$U_{emf} = 2B_{ag} N_p r_r l_r \omega_m = K_e \omega_m \tag{3.21}$$

For a three phase PM machine the ideal relation between voltage constant, $K_e$ and torque constant, $K_t$ is

$$T_m = K_t I = 3K_e I \tag{3.22}$$

where $K_e$, is (from equation (3.21))

$$K_e = 2B_{ag} N_p r_r l_r = C_K N_p r_r l_r \tag{3.23}$$

where $C_K$ is constant for a specific machine design.

The phase resistance, $R_p$ is given by [44]

$$R_p = \rho \frac{l_w}{A_w} = \frac{2 l_r N_p}{A_w} = \frac{2 l_r N_p^2}{A_{slot}} \Rightarrow \left\{ A_{slot} \sim r_r^2 \right\} \Rightarrow R_p = C_R \frac{l_r N_p^2}{r_r^2} \tag{3.24}$$

where, $l_w$ is the total length of the phase winding, $A_{w,}$ the cross sectional area of the wire, $\rho$ is the resistivity and $A_{slot}$ the copper area in one slot (constant fill factor assumed). Also here a constant, $C_R$ replaces those parameters that are constant for a specific machine type.

Finally a model for the phase inductance, $L_p$ is given by [43]

$$L_p = \frac{\pi r_r l_r N_p^2 \mu_0}{\delta} = \{\delta \propto r_r\} = C_L l_r N_p^2 \tag{3.25}$$

where $\delta$ is the gap (air gap + radial thickness of magnets) and $\mu_0$ is the permeability of air.

As these models are supposed to be used to scale a machine with known data, the following relations are introduced

$$\varepsilon_r = \frac{r_r}{r_{r0}} = \frac{r_m}{r_{m0}} \quad \varepsilon_l = \frac{l_r}{l_{r0}} = \frac{l_m}{l_{m0}} \quad \varepsilon_N = \frac{N_p}{N_{p0}} \tag{3.26}$$

where index 0 refers to the corresponding parameter of a real machine with know data (the original machine). From equation (3.23), the following expression for the voltage constant $K_e$ can be derived.

$$\frac{K_{e0}}{N_{p0} r_{r0} l_{r0}} = C_K = \frac{K_e}{N_p r_r l_r} \Rightarrow K_e = K_{e0} \varepsilon_N \varepsilon_r \varepsilon_l \tag{3.27}$$

Similarly, from equations (3.24) and (3.25), the following expressions for the phase resistance and phase inductance are retrieved.

$$\frac{R_{p0} r_{r0}^2}{l_{r0} N_{p0}^2} = C_R = \frac{R_p r_r^2}{l_r N_p^2} \Rightarrow R_p = R_{p0} \frac{\varepsilon_l \varepsilon_N^2}{\varepsilon_r^2} \tag{3.28}$$

$$\frac{L_{p0}}{r_{r0} l_{r0} N_{p0}^2} = C_L = \frac{L_p}{r_r l_r N_p^2} \Rightarrow L_p = L_{p0} \varepsilon_l \varepsilon_N^2 \tag{3.29}$$

Assuming a sinus shaped voltage and current, the phase voltage $U_p$, is given by

$$\boldsymbol{U_p} = R_p \boldsymbol{I} + \boldsymbol{U_{emf}} + j\omega_m \frac{p}{2} L_p \boldsymbol{I} \tag{3.30}$$

where $j$, is the imaginary number ($-1^{1/2}$) and variables in bold indicate that they are complex numbers. Assuming that the machine current $\boldsymbol{I}$ is controlled such that it is in phase with the induced voltage ($\boldsymbol{U_{emf}}$) and defining them as real yields

$$\boldsymbol{U_p} = R_p I + U_{emf} + j\omega_m \frac{p}{2} L_p I \tag{3.31}$$

The absolute value of the phase voltage is then given by

$$U_p = \sqrt{\left(R_p I + U_{emf}\right)^2 + \left(\frac{p}{2} \omega_m L_p I\right)^2} \tag{3.32}$$

Combining (3.32) with equations (3.22), (3.27), (3.28) and (3.29), yields:

$$U_p = \sqrt{\left(\frac{R_0 \varepsilon_N}{K_0 3 \varepsilon_r} T_m + K_0 \varepsilon_r \varepsilon_l \varepsilon_N \omega_m\right)^2 + \frac{L_0^2 \varepsilon_N^2 p^2}{36 K_0^2} \omega_m{}^2 T_m{}^2} \tag{3.33}$$

The maximum phase voltage is required when the peak torque is delivered at the peak velocity which gives the following constraint.

$$U_{p,\max} \geq \sqrt{\left(\frac{R_0\varepsilon_N}{K_0 3\varepsilon_r}T_{peak} + K_0\varepsilon_r\varepsilon_l\varepsilon_N\omega_{peak}\right)^2 + \frac{L_0^2 N_\Delta^2 \varepsilon_N^2 p^2}{K_0^2}\omega_{peak}^2 T_{peak}^2} \quad (3.34)$$

Solving equation (3.33) with respect to $\varepsilon_N$, gives

$$\varepsilon_N \leq \frac{6\varepsilon_r^3 K_0 U_{p,\max}}{\sqrt{4R_0^2T_{peak}^2 + 24R_0K_0^2\varepsilon_r^4\varepsilon_l T_{peak}\omega_{m,peak} + 36K_0^4\varepsilon_r^8\varepsilon_l^2\omega_{m,peak}^2 + p^2L_0^2\varepsilon_r^4T_{peak}^2\omega_{m,peak}^2}} \quad (3.35)$$

The maximum allowed phase voltage $U_{p,max}$, does of course depend on the supply voltage in the system. The power converter in the motor driver can not control the phase voltage directly, but it controls it through the phase-to-phase voltage, $U_{pp,}$ between two terminals of the machine (Figure 3.4). The relation between phase voltage and phase-to-phase voltage is

$$U_p = \frac{U_{pp}}{\sqrt{3}} \quad (3.36)$$

In order for the driver to be able to deliver the required phase-to-phase voltage, its peak value may never be higher than the dc-link voltage, $U_{dc\text{-}link}$ (Figure 3.4). This gives that the maximum phase voltage $U_{p,max}$ (rms) is given by (again assuming sinus shaped voltage and current)

$$U_{p,\max} = \frac{U_{pp,\max}}{\sqrt{3}} = \frac{U_{dc-link}}{\sqrt{3}\sqrt{2}} \quad (3.37)$$

The copper losses are assumed to be equal regardless of the number of turns in the winding, but it is generally favorable for the converter to utilize the full range of the supply voltage in order to keep the current in the semiconductors as low as possible. Hence, by replacing the '≤', in equation (3.35) with an '=', and inserting the maximum allowed phase voltage from (3.37) it is possible to derive the relative number of turns, $\varepsilon_N$ that maximizes the utilization of the supply voltage. Equations: (3.27), (3.28) and (3.29) may then be used to derive an estimation of the voltage constant, phase resistance and phase inductance respectively. Applying the models on the voltage constant of the machines in Table 2.2 (page 30), results in Figure 3.5 below. As seen, the agreement is ok, but not excellent. One possible source of error is that some of the machines in the table might not utilize the entire range of the supply voltage. They are rated at even speeds (3000, 3500, 4000, etc) and it is likely that it is possible to drive some of the machines a bit faster than the rated speed.

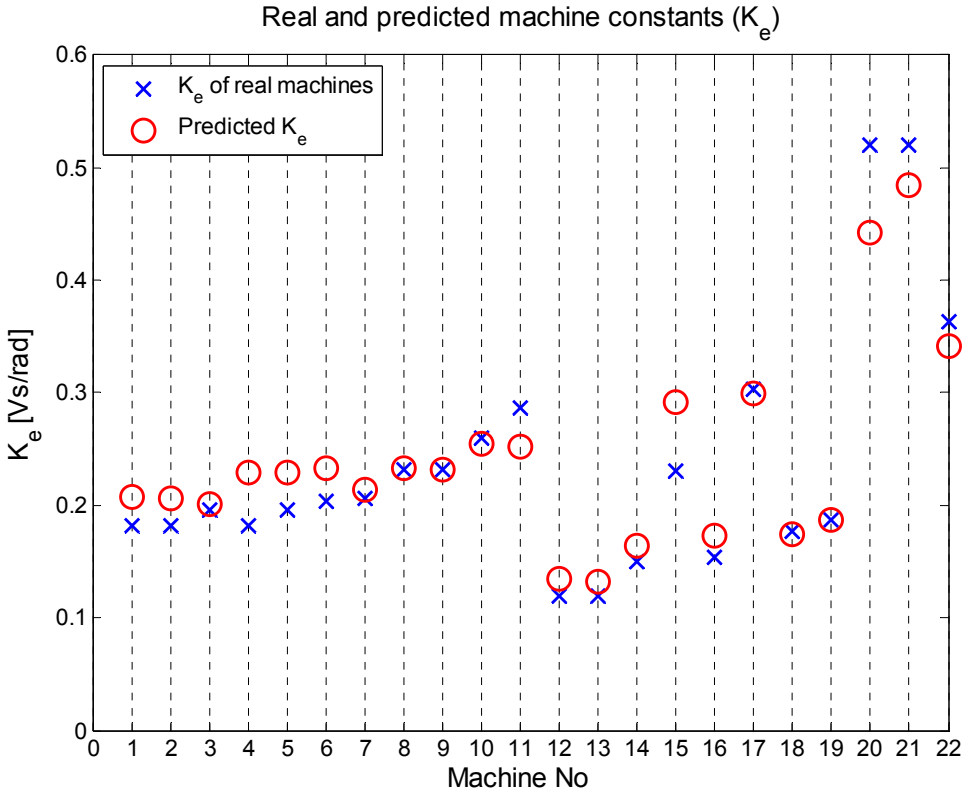


*Figure 3.5. Predicted and real machine constants.*

### 3.3.4 OPTIMIZATION OF ELECTRIC MACHINE AND GEAR RATIO

Here the method for machine/gear ratio optimization is applied to the design case presented in chapter 2.6. By combining equations (3.7), (3.11) and (3.15), the following relation is obtained

$$\left(C_m r_m^{2.5} l_m\right)^2 = \frac{1}{\tau}\int_0^{\tau}\left(\left(C_{mj} r_m^4 l_m + J_0\right)\ddot{\varphi}_l n + \frac{T_l}{n}\right)^2 dt \tag{3.38}$$

For now, the gearhead is assumed to be ideal, its efficiency is therefore set to one, and its inertia to zero. Solving equation (3.38) with respect to the length of the machine, $l_m$ yields in an expression for the smallest possible motor length given a radius and gear ratio (see paper A for details).

In this case, the machine designated PSA90/6-79B in Table 2.2 is used to retrieve the values of $C_m$, and $C_{mj}$. $J_0$ is assumed to be 10% of the inertia of the original machine (Table 3.2). The results from (3.38) when applied to the load profile presented in Figure 2.4, are shown in Figure 3.6 - Figure 3.8. The darker part of the surfaces represents the data points that are within the constraints given by (3.12). The increase of volume seen at high gear ratios with high motor radii is a consequence of the high torques required to accelerate the rotor inertia of the machines.

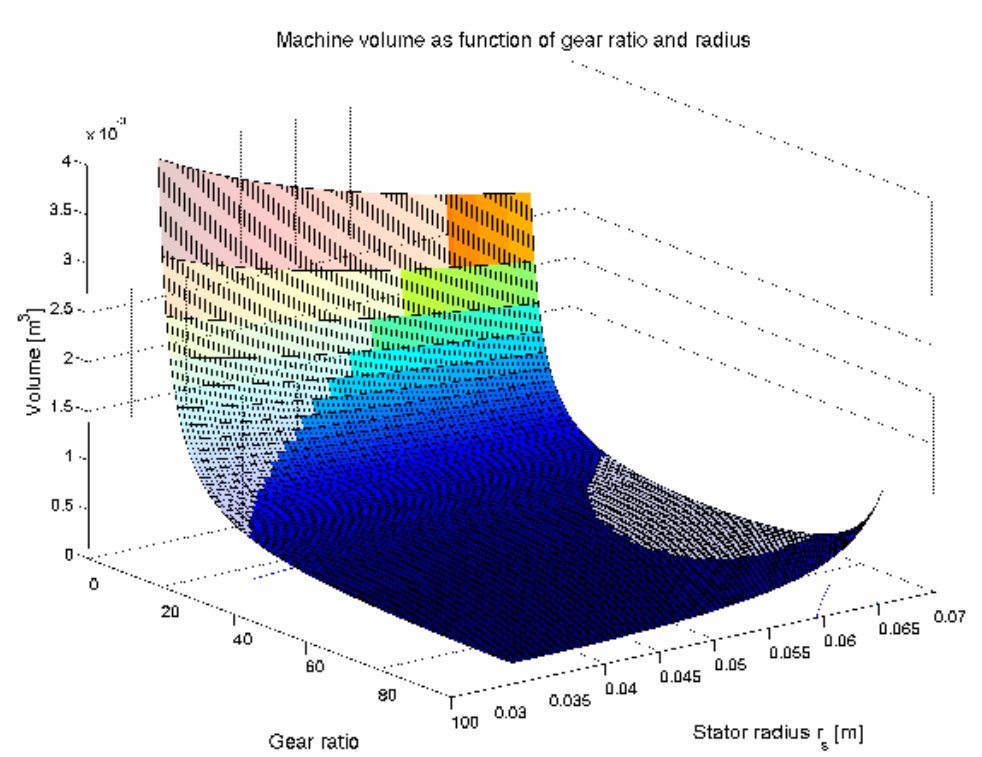


*Figure 3.6. Minimum machine volume as function of gear ratio and radius.*

In Figure 3.7, a magnification of the gear ratios above 20, is shown. In this case it is seen that the machine volume is minimized at a gear ratio of 100 and smallest possible radius. The effect of the machine rotor inertia is here clearly seen, increasing the radius means an increase of the machine inertia proportional with the radius to the power of 4 (see equation (3.15)).

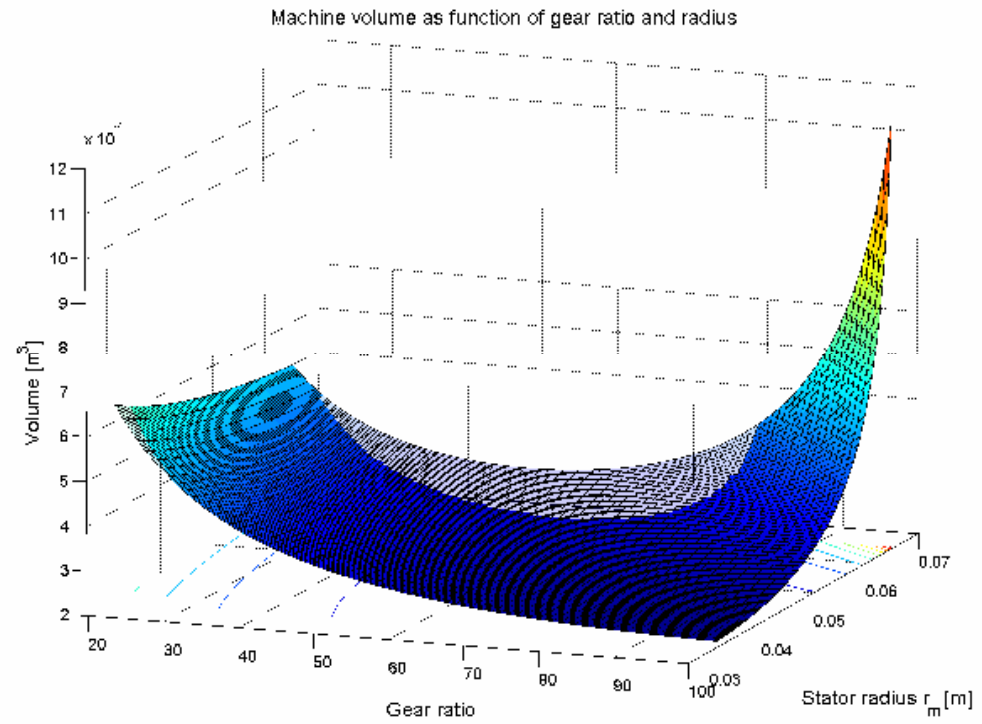


*Figure 3.7. Minimum motor volume as function of gear ratio, magnification of gear ratios 20-100.*

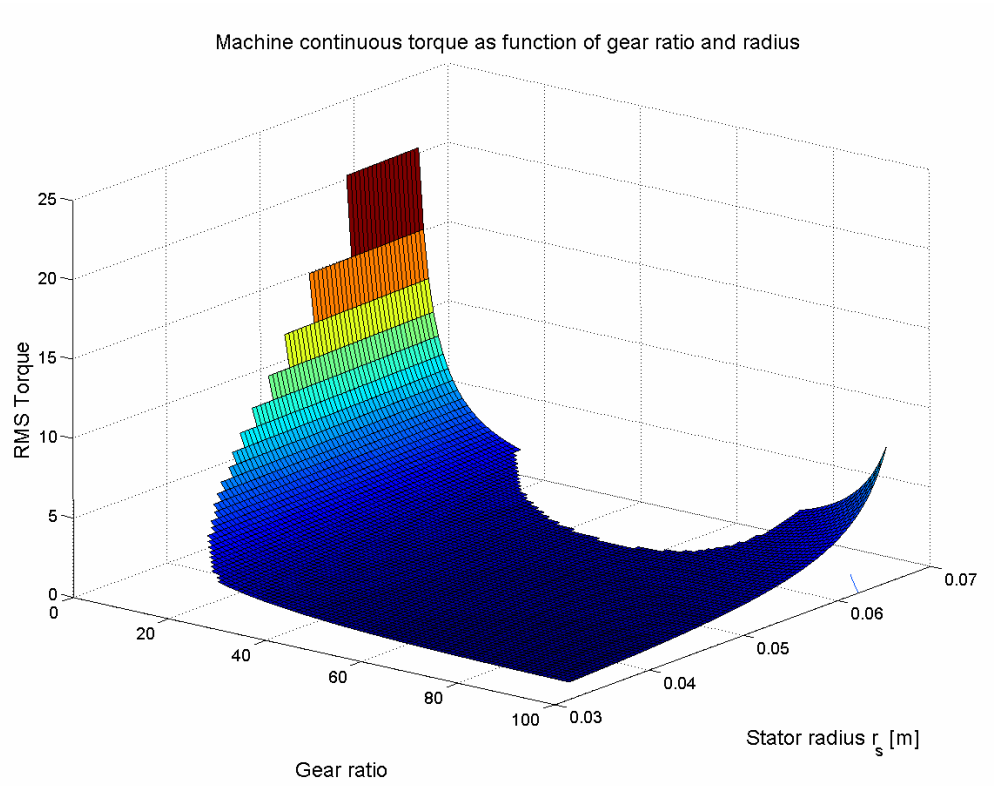


*Figure 3.8. Machine rated torque as function of gear ratio and radius. The rated torque is equal to rms-torque required to drive the load.*

In Figure 3.8, the machine's rated torque is presented. The machine is dimensioned such that it precisely can drive the load; therefore the rated torque is equal to the required torque. Also here the increase in required torque at high ratios and large radii is visible.

If the machine volume is minimized for each gear ratio (by selecting the smallest possible machines from Figure 3.6), the volumes represented by the dotted line in Figure 3.9 are obtained. Also the curve representing the optimal selection of existing machines (Table 2.2) is shown in the figure. As seen, the difference between the two curves is small. This verifies that the simplifications made during the modeling of the machine are reasonable, at least for this load example. The advantage of this method is, as seen in the figure, that the motor is optimized for each gear ratio, as opposed to the discrete method where each machine is optimal or close to optimal for just one single gear ratio. None of the existing machines with a higher rated speed than 4500 rpm can drive this load. This leads to that the maximum possible gear ratio with the existing machines, is 70. With the design method, on the other hand, it is possible to design machines that can drive the load with rated speeds up to $\omega_{m,peak}$, which in this case means a maximum gear ratio of 100.

*Table 3.2. Machine constants (derived from PSA90/6-79B Table 2.2).*

| $C_m$ [N/m$^{2.5}$] | $C_{mj}$ [kg/m$^3$] | $J_0$ [kgm$^2$] | $C_{pt}$ [1] | $\omega_{m,peak}$ [rad/s] |
|---|---|---|---|---|
| 91350 | 1056 | 3.8e-5 | 5 | 650 |

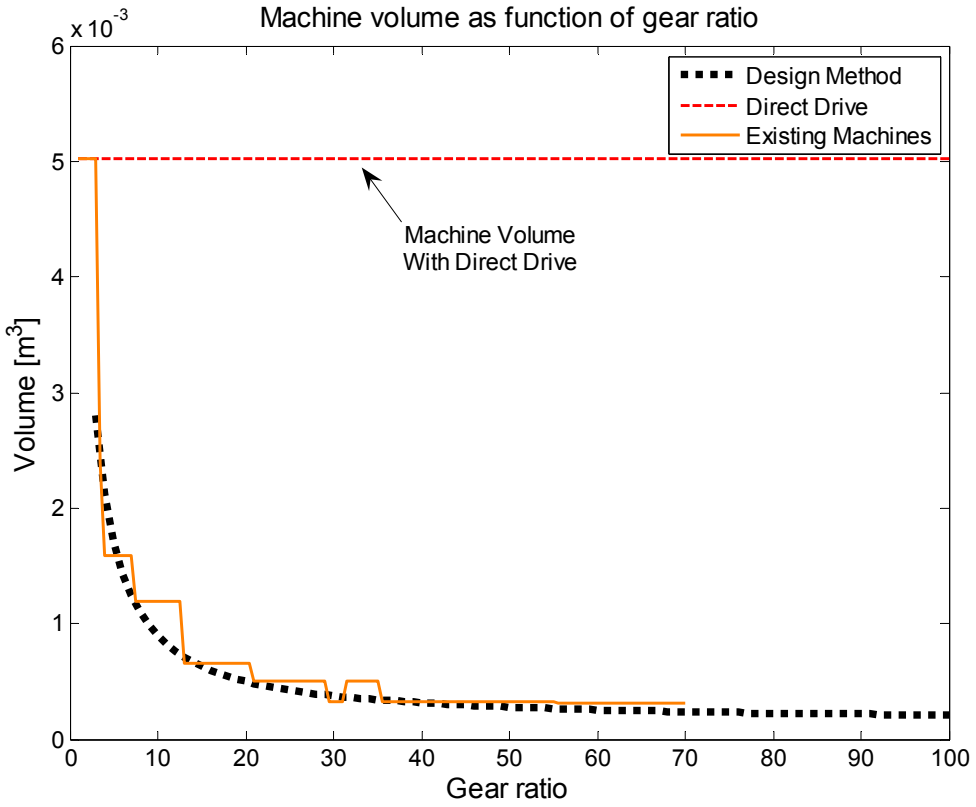


*Figure 3.9. Minimum machine volume as function of gear ratio, compared with the volume of the existing machines. The small difference between the two curves verifies that the simplifications made in the machine models are acceptable (at least for this load profile).*

Referring to Figure 3.9 again, the machine volume decreases drastically with gear ratio, the direct drive machine is more than 14 times larger than the machine volume required at gear ratios above 70. As seen, the optimal gear ratio with respect to volume is equal to the maximum gear ratio of 100. Remember however that this volume only represents the machine, for a fair comparison with a direct drive solution the gear volume needs to be added to the machine volume.

## 3.4 GEARHEAD DIMENSIONING AND OPTIMIZATION

In the previous section the gearhead was assumed to be ideal, a simplification often made in methods for design or selection of electric machines. However, the gearhead may constitute a significant part of the servo system's size and weight, which makes it important to include models of the required gearhead size in an integrated design methodology. Furthermore, gearhead efficiency, backlash and stiffness affect the global design optimum and needs to be included in the analysis.

Three types of speed reducers are commonly used in mechatronic servo systems: conventional spur and helical gear pairs, three-wheel planetary gears and harmonic/cycloidal drives. Harmonic and cycloidal reduction gears are common in applications that require high gear ratios (up to ~200 in a single stage). They also have lower backlash than planetary gearheads, but are on the other hand not as stiff. Another drawback is that it is difficult to efficiently achieve low gear ratios (under ~50) with harmonic and cycloidal drives [45]. Moreover, harmonic and cycloidal gearings generally have lower efficiency than planetary gearings. During this work only spur gear pairs and three-wheel planetary spur gears have been analyzed (Figure 3.10), but models of the other gear types may be added in the future.

Large parts of this section are based on the contents of paper B and paper C. In paper B it is concluded that spur gear pairs require significantly larger volume, weight and inertia to transmit the same torque than three-wheel planetary gearheads (see Figure 3.11). Therefore only models of planetary gearheads are presented here, but the models representing spur gear pairs are presented in paper B.

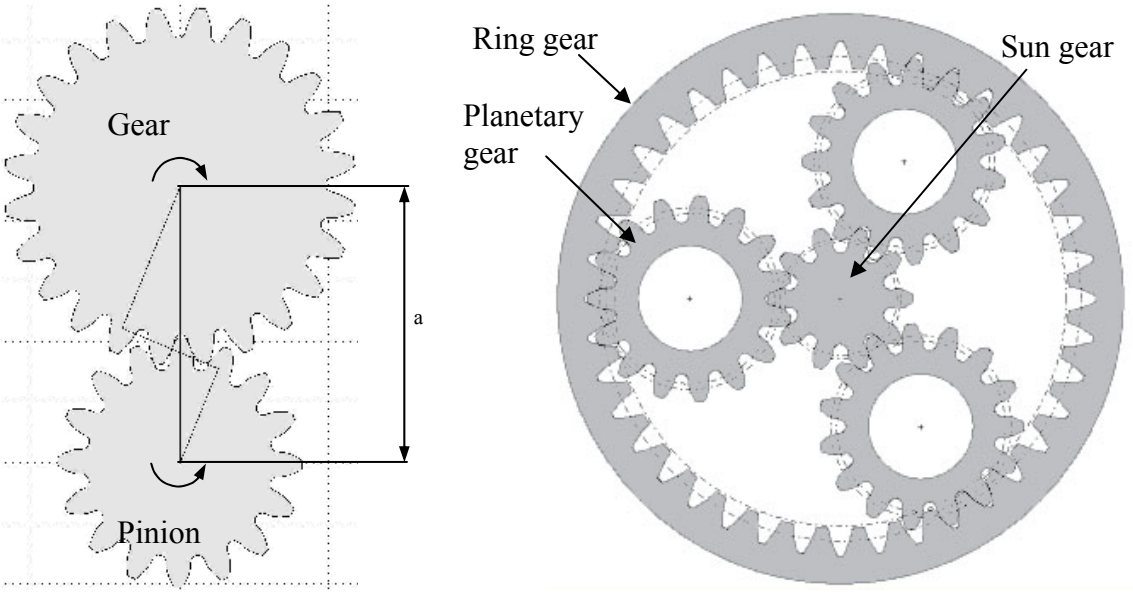


*Figure 3.10. Spur pinion-gear pair to the left and three-wheel planetary gear to the right.*

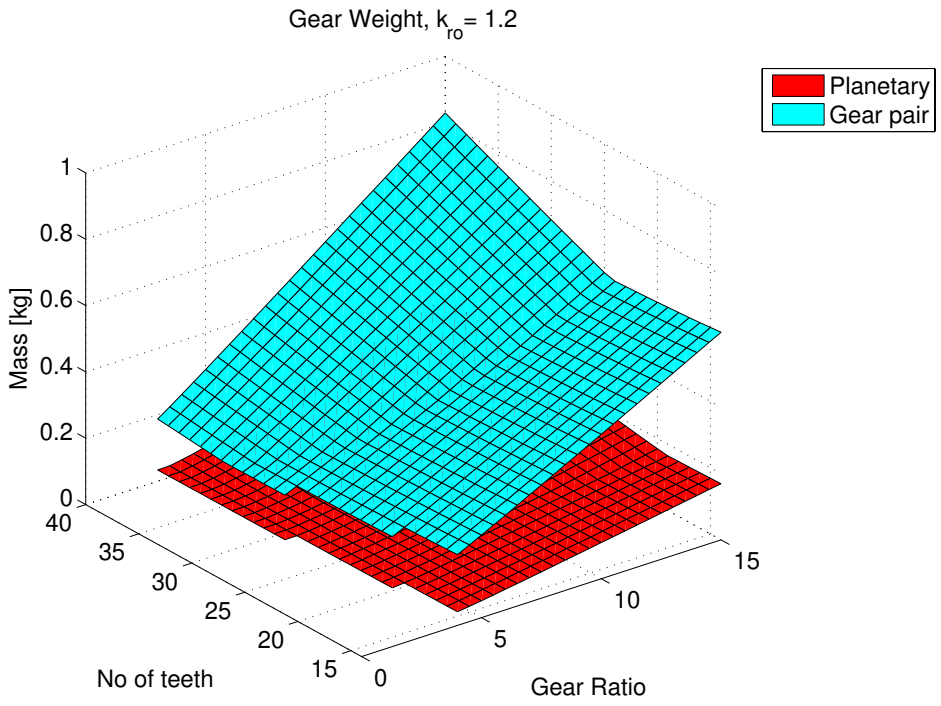


*Figure 3.11. Required weight of a pinion-gear pair compared to the weight of a three-wheel planetary gearhead. In this comparison solid gearwheels are assumed and the weight of the planet carrier is not included. It is therefore likely that the planetary weight is a bit underestimated.*

### 3.4.1 CONSTRAINTS ON THE GEARHEAD TORQUE AND SPEED

A gearhead is traditionally dimensioned with respect to mechanical fatigue. Either the bending stress in the root of a gear teeth or the contact pressure on the gear surface limits the minimum gear size for a given load. The gear models derived during this research are based on the Swedish standard for spur gear dimensioning, SS1863 [46] and SS1871 [47].

One problem with the standardized method for spur gear dimensioning is that the method more or less assumes a constant torque load on the output shaft of the gear train. In a typical mechatronic system, on the other hand, the load torque varies with time. Hence, the non-constant load torque needs to be replaced with some sort of equivalent continuous torque. For the sizing of the electric machine the rms-norm of the load torque is used as equivalent continuous torque. It is however not as straight forward to derive a similar norm for the equivalent gear torque. In this work, the maximum torque of the load profile is used as equivalent constant torque for gear dimensioning. The motivation for this approach is that if a gear is to withstand a huge number of load cycles, the total time it has to transmit the peak torque will be very long, hence it must be dimensioned to withstand this torque. This approach and others are discussed in more detail in paper B. There is however a risk that this approach results in over-dimensioned gearheads. For example, a large Swedish manufacturer of mechatronic equipment uses the same approach to gear dimensioning, and they now have gears in production with safety factors of about 0.3, which indicate that it is possible that the use of the peak torque as design torque results in oversized gears.

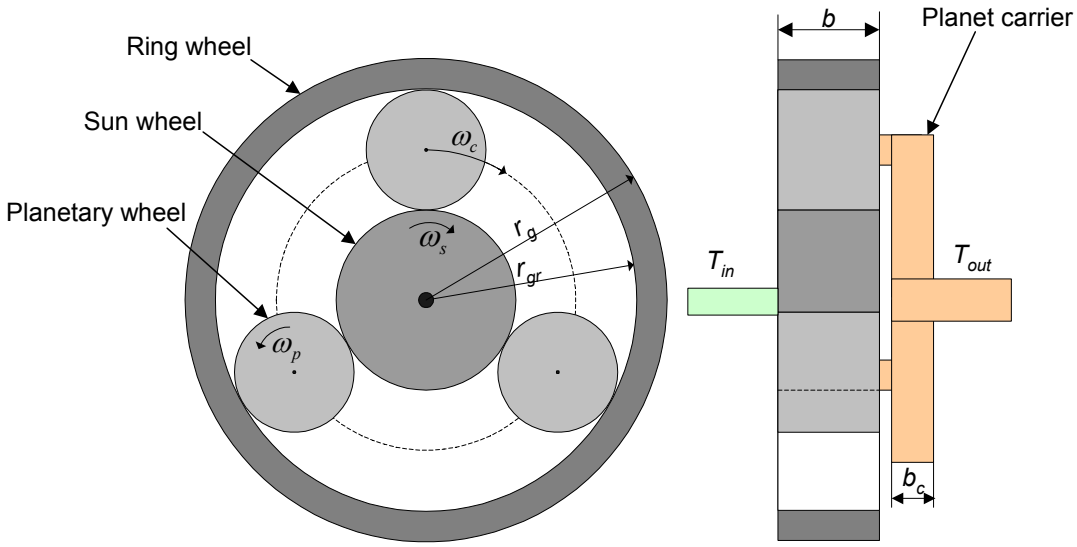


*Figure 3.12. Schematics of a three-wheel planetary gearhead.*

The constraint on the gearhead torque $T_g$ becomes

$$T_{g,rated} \geq \max \left| T_l \right| \tag{3.39}$$

Only the mechanical limits of the gear teeth are considered here, but even though they limit the size of the actual gear wheels, other parts as bearings and planet carriers may in some cases limit the torque rating of a gearhead.

### 3.4.2 GEAR MODELING

As mentioned above, it is the teeth root bending stress or the hertzian pressure at the teeth contact surfaces that is assumed to limit the gear design. As seen in Figure 3.12, a planetary gearhead consists of three types of gears: the sun gear, ring gear and planetary gears. This means that the root stress and the Hertzian pressure need to be checked in both the sun/planet mesh and planet/ring mesh. Furthermore, the root bending stress is not the same in both gearwheels in one mesh, so it has to be checked twice for each mesh. This means that there are six constraints on the gear size that have to be checked in order to evaluate if a planetary gear design can drive a given load. However, in paper B it is concluded that the Hertzian pressure always is higher in the sun/planet mesh than in the planet/ring mesh, hence the constraints can be reduced to five. Furthermore it is concluded that the root stress always is larger in the smaller wheel of the two in mesh, hence the root stress in the ring gear may be omitted, since its diameter has to be larger than the diameter of the planet wheels. Left are four constraints. To be on the safe side all these four constraints have to be checked. These constraints are derived and presented in paper B. However, to keep this section relatively short and the number of design variables as low as possible a simplified approach is presented here.

If the number of sun gear teeth is kept relatively low, and assuming that the gears are made of a steel that is not extremely hard, the Hertzian pressure will limit the required gear size. This has not only the advantage of reducing the number of constraints from 4 to 1, it also makes the gear size independent of the number of gear teeth, which eliminates a design variable. However, even though the

Hertzian pressure is likely to limit the gear size, it is of course vital to check that the bending stress is within limits before proceeding with a design. In order to keep within the limit of maximum Hertzian pressure in the sun/planet mesh, the following constraint on the gear size has to be fulfilled (given steel as gear material and most parameters set to their respective standard values, see paper C for details),

$$r_g^2 b \geq 4 \cdot 10^{10} C_{gr}^2 \frac{T_{eq}(n_s - 1)^2}{(n_s - 2)\sigma_{H\max}^2} \tag{3.40}$$

where, $r_g$ is the outer radius of the ring gear according to Figure 3.12, $b$ is the gear width and $n_s$ the gear ratio of the particular stage. $\sigma_{Hmax}$ is the maximum allowed flank pressure and is given by

$$\sigma_{H\max} = \frac{\sigma_{H\lim}}{SF} \tag{3.41}$$

where $\sigma_{Hlim}$ is the maximum allowed Hertzian pressure for the particular gear material and $SF$ is the safety factor. Depending on the shape of the load profile, the safety factor may be set to 1 (or even lower) since the gears are dimensioned with respect to the maximum torque of the load profile. $C_{gr}$ is the relation between the outer radius of the ring gear and the reference radius $r_{gr}$ (Figure 3.12) according to

$$C_{gr} = \frac{r_g}{r_{gr}} \tag{3.42}$$

$T_{eq}$ is the equivalent continuous torque to be transmitted by the gear stage and is according to the discussion above given by

$$T_{eq} = \max\left|T_{gs}\right| \tag{3.43}$$

where $T_{gs}$ is the required torque to be transmitted by gear stage $s$ (see section 3.4.3).

In Figure 3.13 the simplified model (dark/red surface) of the gear size is compared to the original one (light transparent surface). As seen, the agreement is good for a low number of sun-gear teeth, but gets worse for a higher number of teeth. That is because the bending stress in the teeth roots limits the size for a high number of teeth. The steel used here is however very hard (SS2511) and for softer steels the agreement is good independently of the number of teeth. The agreement shown in Figure 3.13 is generally good enough, since there is no point in using more teeth than required to avoid so called under cut gears (over 14 teeth is usually enough). So for the mechatronics design methodology it is good-enough to use the model presented here, but since the author already has the full model presented in paper B implemented in numeric software, it will be used in the presented examples. In the presented examples the number of teeth is therefore selected such that it minimizes the gear volume.

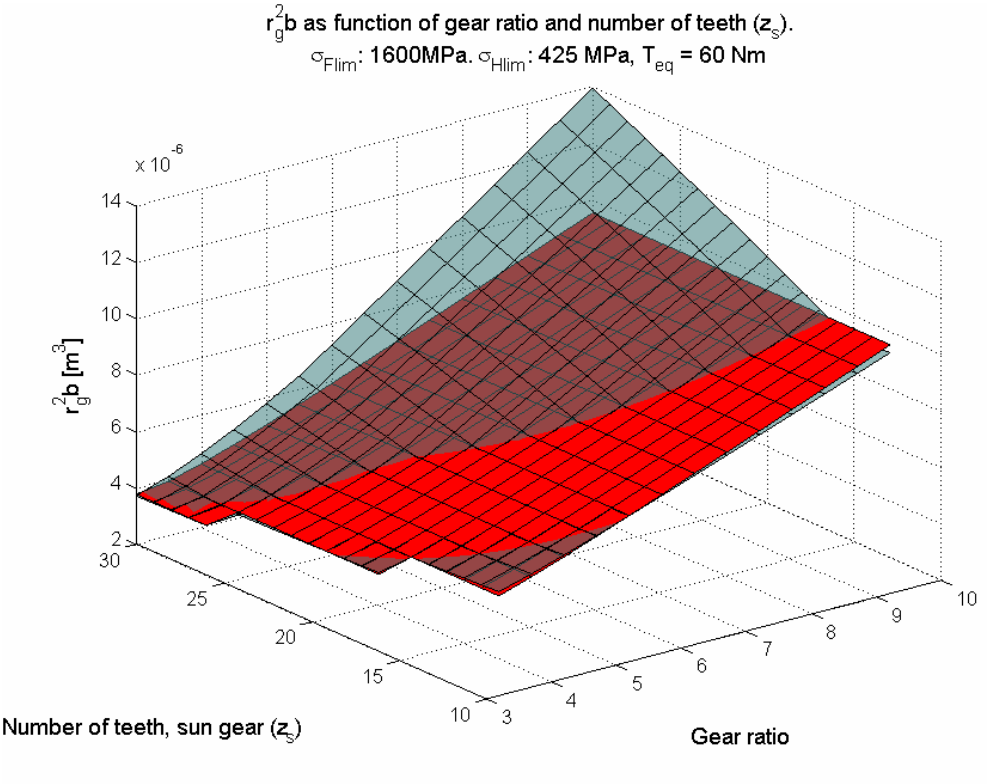


*Figure 3.13. Required gear size as function of the number of sun gear teeth and gear ratio. The lighter transparent surface represents the full model derived in paper B while the darker (red) surface represents the simplified model presented above (equation (3.40)).*

The weight of the gears and carrier in a planetary gear stage is given by (paper B)

$$m_{gs} = \frac{r_g^2}{C_{gr}^2} b\pi\rho_g \left( \frac{1}{(n_s-1)^2} + \frac{3}{4}\frac{(n_s-2)^2}{(n_s-1)^2} + (C_{gr}-1) + \frac{b_c}{b}\frac{n_s^2}{4(n_s-1)^2} \right) \quad (3.44)$$

where $b_c$ is the width of the carrier (assuming cylindrical shaped carrier as in Figure 3.12) and $\rho_g$ is the mass density of the gears and carrier.

The inertia of a planetary gear stage is defined at the input (machine) side and is given by (paper B)

$$J_{gs} = \frac{\rho_g \pi r_g^4}{32 C_{gr}^4} \frac{(9bn_s^2 + b_c n_s^2 - 36bn_s + 52b)}{(n_s-1)^4} \quad (3.45)$$

It is important to have a model of the losses in the gearhead in order to predict the torque required by the electric machine, but also for system efficiency optimization and evaluation. The losses in a gearhead are mainly due to mechanical friction between teeth but also oil churning losses and windage losses contribute to the heating of a gearhead. For the sake of simplicity only a coulomb friction model is used here, which is implemented as a constant efficiency, $\eta_{gs}$ for each gear stage. A realistic value for the stage efficiency is about 96-97 %. The choice of using a speed independent friction model is mainly based on the lack of published papers about speed dependent efficiency models but also the fact that gear manufacturers generally only give a single figure of the efficiency of a gearhead. This simplification might however be one of the largest in this thesis

and it is possible that a more realistic friction model in combination with a model of the speed dependent losses in the electric machine would affect the results from the optimization significantly. It is thus recommended for future research to investigate the effects of speed dependent losses.

For performance optimization and controller design, the gearhead flexibility and backlash are of great importance. It is however difficult to derive a model that expresses the gear stiffness as function of gear ratio and load, since the stiffness depends largely on the bearings which are not modeled here. The backlash of a gearhead is possibly even harder to express as function of gear ratio and torque load, since the backlash mainly depends on other factors such as the tolerances in the production equipment. Therefore, these two properties are not modeled during this work, instead realistic values are retrieved from data sheets of commercially available gearheads.

Many simplifications and assumptions have been made in the presented gear models, in addition to those already mentioned the main ones are: The number of gear teeth on each wheel is in reality discrete, which in combination with standardization in gear modulus gives a discrete number of possible gear ratios. Furthermore, bearings come in standard widths which constrain the gear width of the planet wheels to those standard dimensions. Finally, it is here assumed that the planetary gear has three planetary wheels, adding extra planet wheels may increase the torque capability of the gearhead.

### 3.4.3 GEAR STAGES

It is difficult to manufacture and design a planetary gear with a gear ratio above 10, it is therefore necessary to connect several planetary gear stages in series to achieve higher ratios. Here, the problem with finding the optimal gear stage combination is limited to finding the best gear ratio of two stages in combination. Two stages are enough to reach all ratios between 3 and 100, the total weight and size of the gearhead may however in some cases benefit from adding additional stages even though the total ratio is below 100. The method for gearhead optimization presented here is applicable for gearheads with three or more stages too, but the results are not as easy to visualize as they are with only 2-stages.

The total efficiency of the gearhead, $\eta_g$ is given by

$$\eta_g = \eta_{gs}^s \tag{3.46}$$

where $s$ is the number of gear stages and $\eta_{gs}$ the efficiency per stage.

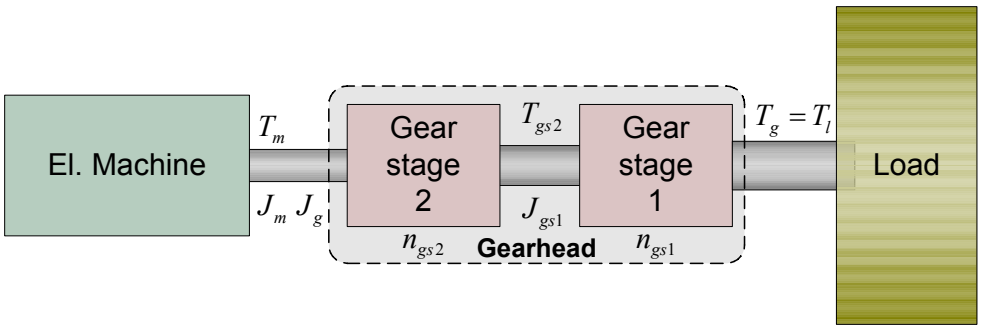


*Figure 3.14. Block diagram of a two-stage gearhead.*

The torque acting on stage 1 equals the load torque (Figure 3.14). The torque load on the second stage is however a function of the gear ratio of the first stage. The torques are defined at the load side of the gear and are given by

$$T_{gs1} = T_g = T_l$$
$$T_{gs2} = \frac{T_l}{n_{s1}\eta_{gs}} \tag{3.47}$$

The total gear ratio $n$ equals

$$n = n_{s1}n_{s2} \tag{3.48}$$

Finally the gearhead inertia $J_g$ is given by (defined at the machine side)

$$J_g = J_{gs2} + \frac{J_{gs1}}{n_{s2}^2} \tag{3.49}$$

Applying the gear sizing models on both stages in a two-stage gearhead for a given load, and plotting the sum of the volume ($r_g^2 b$) of stage 1 and 2, results in Figure 3.15. As seen, the required size increases faster with the gear ratio of stage 1 than of stage 2. Compare for example the required volume for a gear ratio of 10 in stage 1, and 3 of stage 2 with the opposite, (stage 2=10 and stage 1=3). Both these combinations result in a total gear ratio of 30, but the required gear size is much larger for the first combination. It is apparent that it generally is most favorable from a size perspective to keep the ratio of stage 1 lower than the ratio of stage 2.

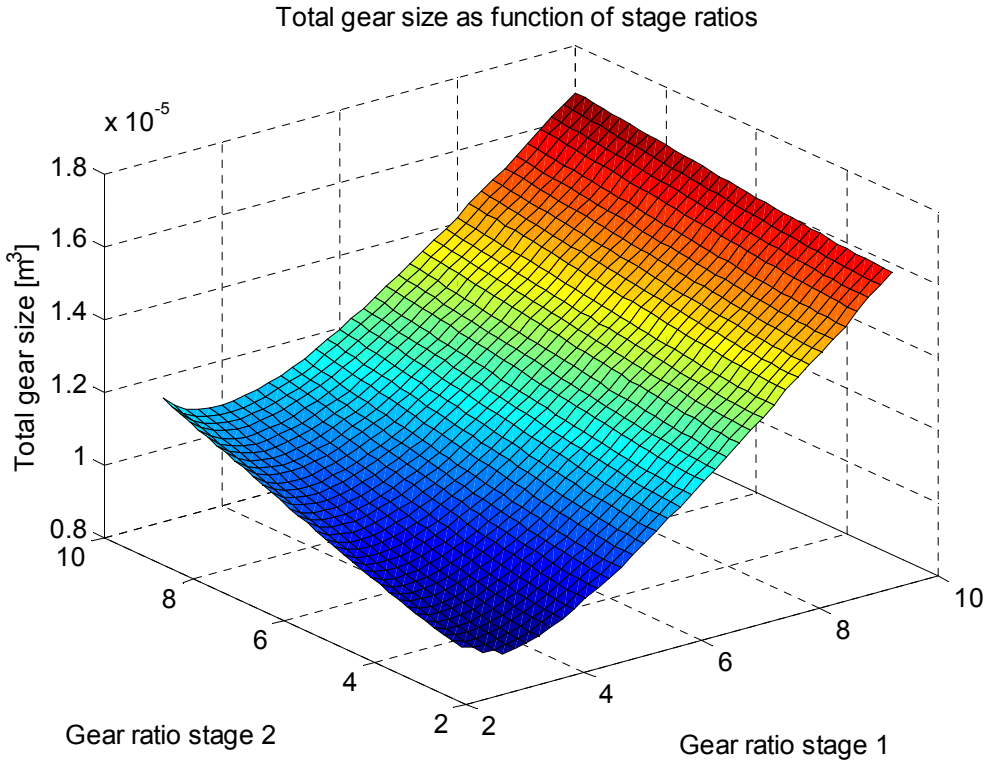


*Figure 3.15. Minimum active gearhead size as function of stage ratios, $(r_g^2 b)_1 + (r_g^2 b)_2$, equation(3.40), i.e. the size of the carriers and other parts are not included.*

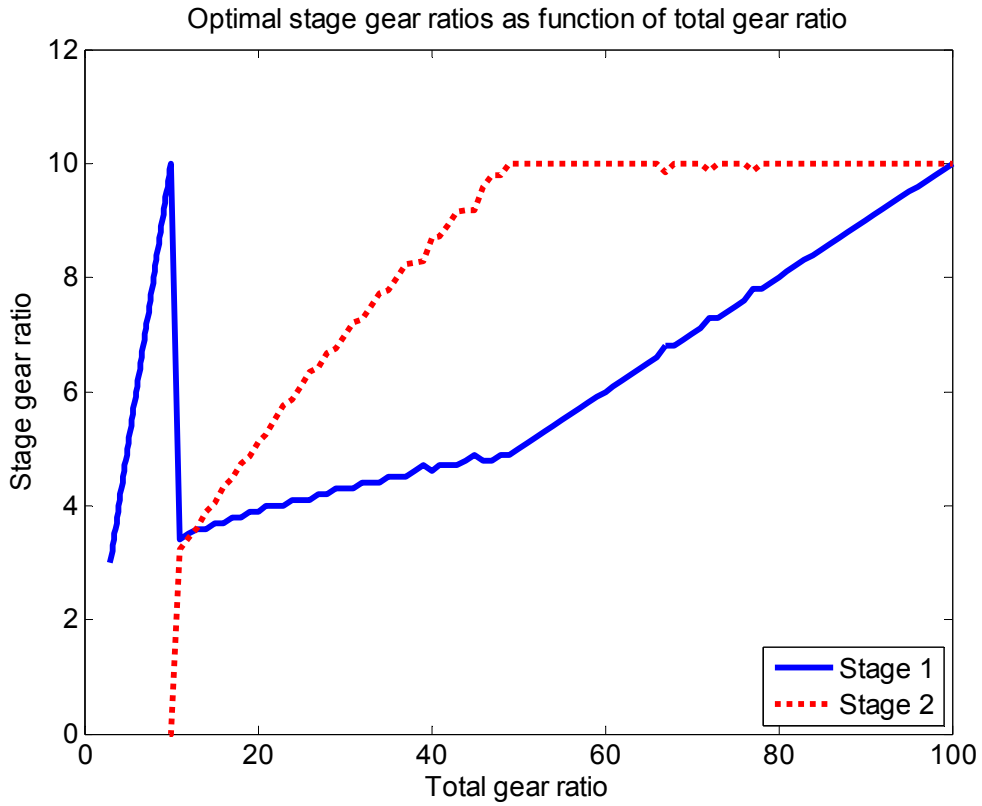


*Figure 3.16. Optimal stage gear ratios ($n_{s1}$ and $n_{s2}$) as function of total gear ratio.*

In Figure 3.16, the stage gear ratios that minimize the total size of the gearhead are plotted as function of total gear ratio (equation (3.48)). As seen, for gear ratios above 10, the gear ratio of stage 2 is always larger than the one of stage 1. Calculating the gear weight, by applying equation (3.44) on both stages, results in the gearhead weight shown in Figure 3.17. As seen, the weight decreases significantly in the transition from one to two gear stages. Adding a third stage would probably decrease the weight further for gear ratios above ~50. But there is off course a trade-off between the increased number of components and the decrease in size and weight when adding a gear stage. Furthermore, since this design method only considers the weight of the gears and carrier, but neglects the weight of other parts, it is possible that some of the gain in size and weight by adding stages is eaten up by the weight of the parts not considered here (shafts, casing, etc…).

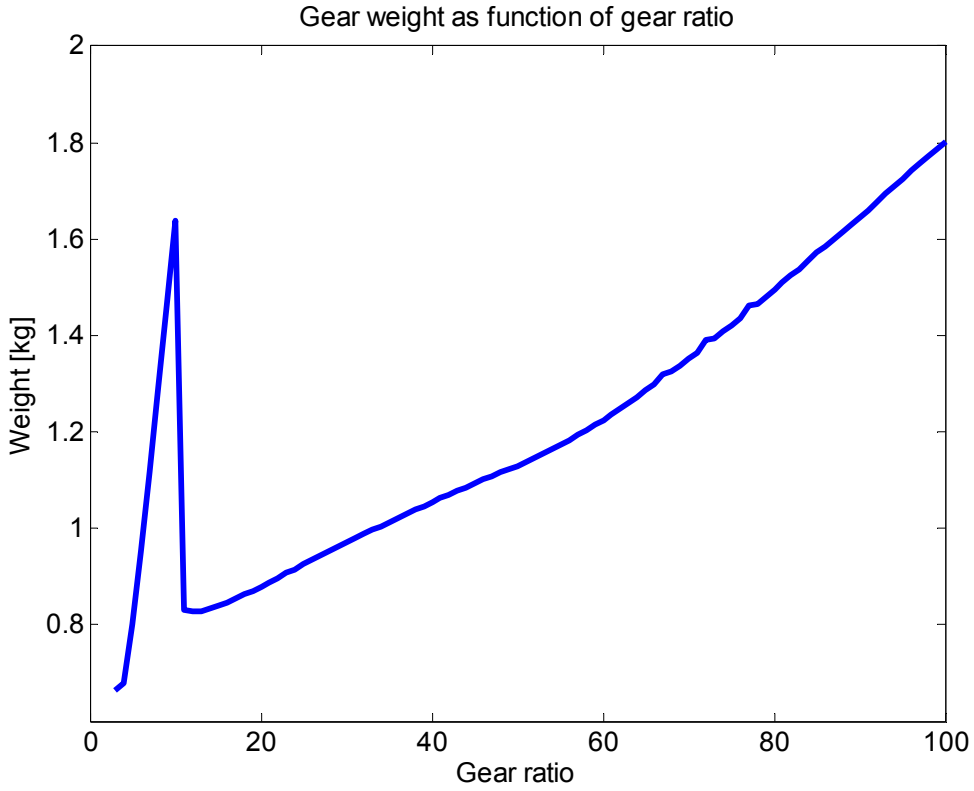


*Figure 3.17. Minimum gear weight as function of total gear ratio. Carrier width is assumed to be half the width of the gearwheels.*

### 3.4.4 INTEGRATED DESIGN OF ELECTRIC MACHINE AND GEARHEAD

With the models presented above it is possible to calculate the required size of the gearhead that can drive the example load presented in Figure 2.4. However, in order to compare the volume of the gearhead with the volume of the electric machine one additional equation is required. The total volume enclosed by the gearhead, $V_g$ is calculated as

$$V_g = \pi r_g^2 (b_1 + b_{c1} + b_2 + b_{c2}) \tag{3.50}$$

where it is assumed that both stages have the same outer radius (the same ring wheel). As inputs to the gear sizing models the design parameters presented in Table 3.3 (below) are used. Calculating the required gear sizes as presented above, and for each gear ratio selecting the radius that gives the smallest possible gear volume results in the gearhead volumes presented in Figure 3.18.

As seen in equation (3.2), two properties of the gearhead affect the machine torque and therefore the machine volume, its inertia $J_g$ and efficiency $\eta_g$. The gearhead inertia is shown to generally be much smaller than the inertia of the electric machine (paper C). Therefore, the gear inertia may be approximated to zero. This conclusion assumes that the gear and machine have been dimensioned properly for the load; the inertia of an oversized gear may of course be of the same magnitude as the motor. The assumption of low gear inertia is verified below for the design example.

Executing the optimization algorithms for the electric machine once again, but now with a gear efficiency of 0.965 per stage (see equation (3.49)), results in the dashed line in Figure 3.18. Comparing this to the machine size obtained in the previous section (Figure 3.9), which assumes an ideal gear, shows that the difference in machine size with this more realistic model is small.

Nevertheless, adding the gear volume to the machine volume (solid line in Figure 3.18) shows that the system optimum with respect to volume now has moved from a gear ratio of 100 to a gear ratio of about 55. However, the curve is rather flat for gear ratios higher than 20. So the total volume does not appear to be so dependent on gear ratio as long as it is higher than 20. Another conclusion is that the combined volume for the machine and gear still is much smaller than the required volume of the direct drive machine ( ~5 liters, see Figure 3.9).

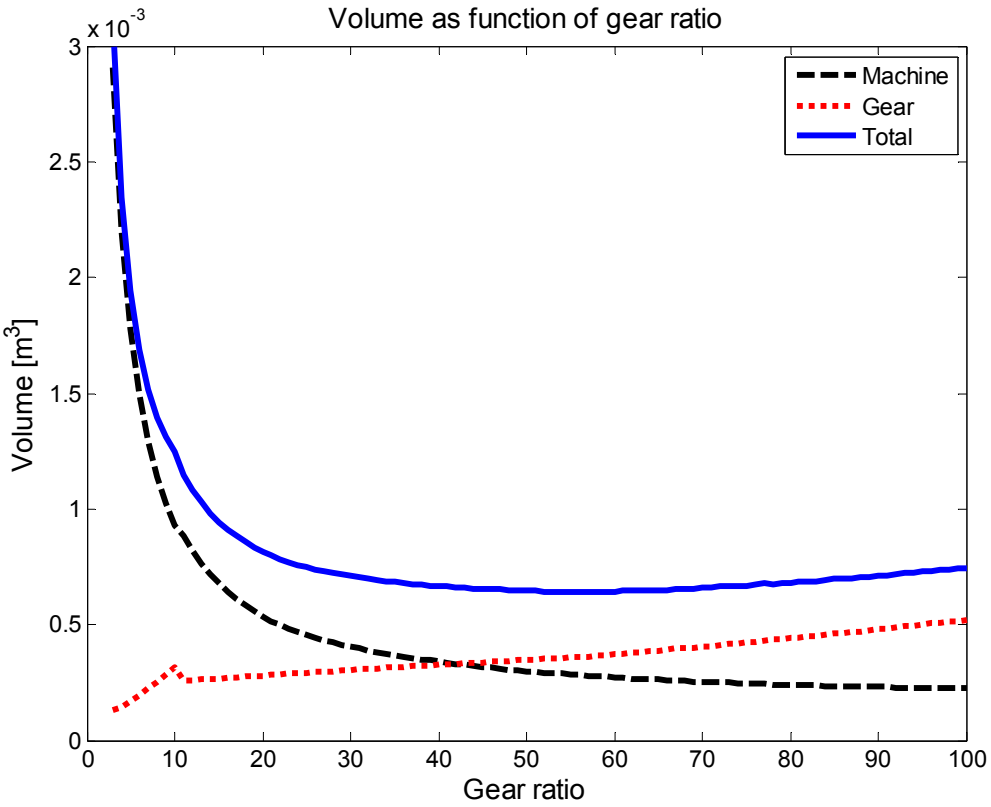


*Figure 3.18. Gearhead, machine and total volume as function of gear ratio.*

*Table 3.3. Gear parameters used in the design example.*

| $\sigma_{H,lim}$ | $\sigma_{F,lim}$ | $SF$ | $\eta_{gs}$ | $b_c$ | $C_{gr}$ | $T_{cal}$ (Figure 2.4) |
|---|---|---|---|---|---|---|
| 1200 MPa | 300 MPa | 1.1 | 0.965 | 0.5$b$ | 1.2 | 222 Nm |

The gear inertia depends on the gearhead radius, therefore the solution with the highest inertia and the one with the lowest is plotted in Figure 3.19. As seen, for both cases the gear inertia is much lower than the inertia of the electric machine, the assumption of low gear inertia holds. For reference, the constant part of the load inertia, as seen from the machine side of the gearhead, is also shown in the figure (equation (2.4)).

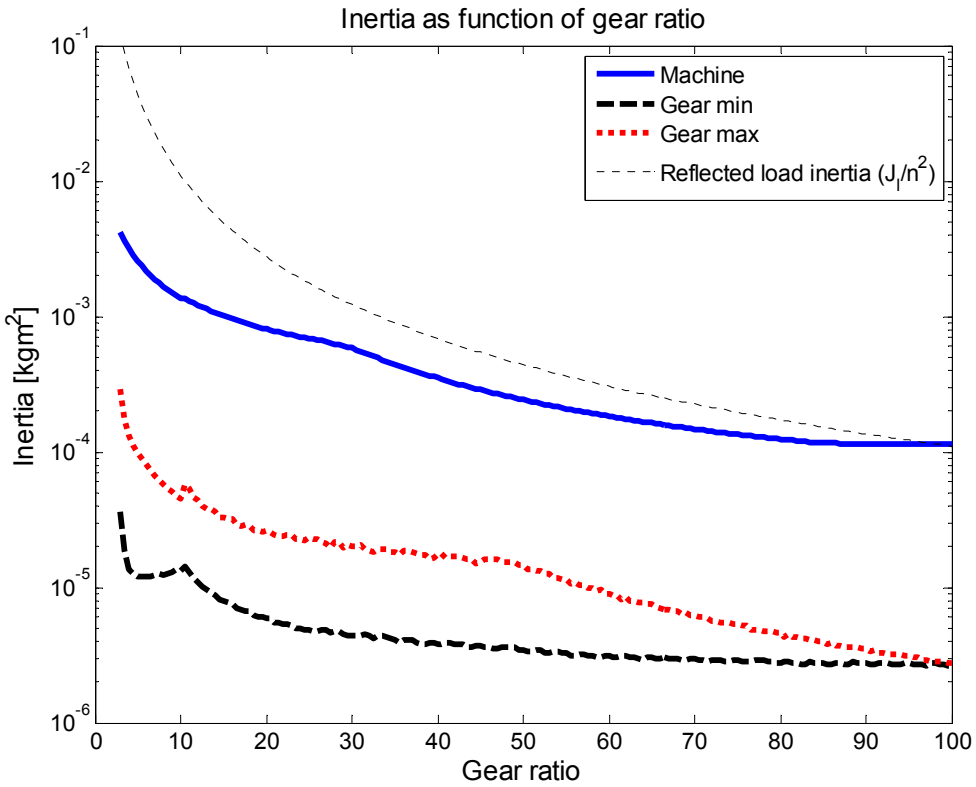


*Figure 3.19. Machine and gearhead inertia as function of gear ratio. The constant part of the load inertia, as seen from the machine side of the gear is also shown.*

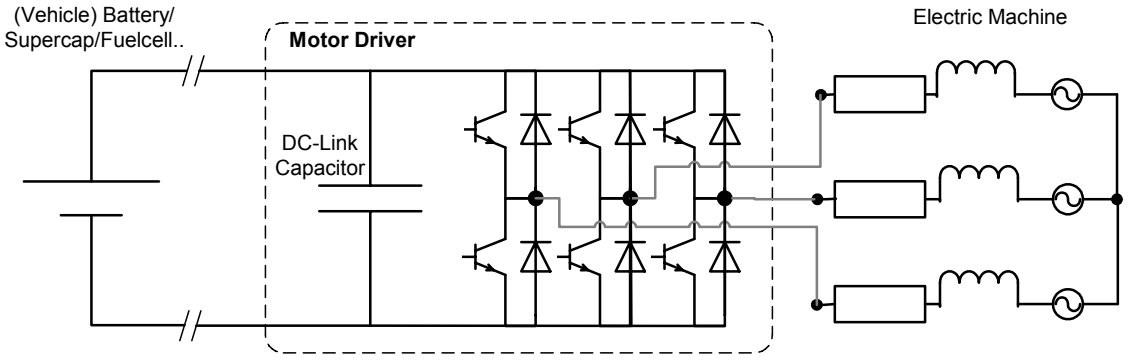


*Figure 3.20. Electric view of a three-phase converter (motor driver).*

## 3.5 MODELING OF THE MOTOR DRIVER

In contrast to the previous sections in this chapter, this section contains material that has not been published in the appended papers or elsewhere. The goal with this section is to derive models that may be used to predict the size and to some extent weight and cost of the drive unit, given a load profile. The input to this part of the methodology is, as before, the load profile, but here the load profile is translated to the motor currents required to follow the profile.

Three of the key components in a three phase drive unit are analyzed: the power transistors and diodes that constitute the PWM converter, the heatsink or heat exchanger required to keep the active components from overheating and finally the dc-link capacitor bank, that has to deliver the ripple currents required by the PWM-bridge (Figure 3.20 and Figure 3.21). These components are known to represent a major part of the cost, size and weight of a motor driver. Other important components in a drive unit include current sensors, microprocessor based logic, connectors and other parts that may be expensive but their size and cost are not directly dependent on the current and power rating.

In [38] the EMC-filter is recognized as a bulky part in an integrated servo system. It is however not analyzed here, and it is up to future research to investigate if it is a component important to include in the mechatronics design methodology. As seen in Figure 3.20, it is assumed that the motor driver is fed by a direct current electrical network, as for example in an automotive application. Applying this method for AC supplied systems might also require some additions related to the rectifier part of the converter.

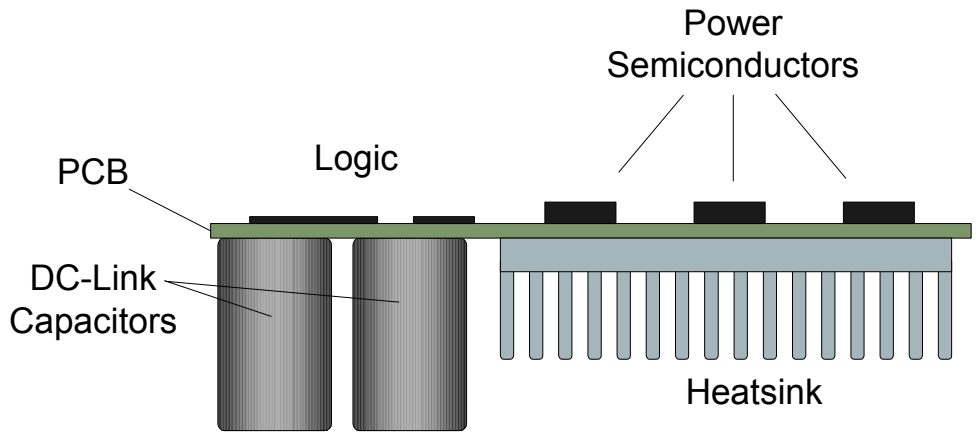


*Figure 3.21. Physical/mechanical view of the driver.*

The design and optimization of a switched converter is very complex in it self, the problem is multidisciplinary in its nature since it covers areas as electronics, electrochemistry, heat transfer and mechanical design. Hence, this part of the work is as all the other parts based on a simplified design approach. However, due to the complexity of switched converter design, the level of simplification is probably higher in this section than in the other parts of the thesis.

### 3.5.1 POWER SEMICONDUCTORS

The active parts in a motor driver are the power transistors and diodes that form the three-phase PWM converter (Figure 3.20). From a cost perspective it is unrealistic to design and manufacture application specific power semiconductor components. Therefore, the methods presented are based on the selection of the best combination of power semiconductors from a list of existing components.

The DC-bus supply voltage is assumed to be predefined, and not a design variable, a common situation when designing a servo system. The DC-bus voltage sets the required voltage rating of the semiconductor elements. Consequently, only components with the same or similar voltage rating are of interest, in the examples presented later on 600 V components are used.

It is the junction temperature in the semi conductors that limits the current and power rating of the motor driver. The junction temperature $\gamma_j$ is given by [48]

$$\gamma_j = \gamma_s + P_{l,s}\left(\theta_{jc} + \theta_{cs}\right) \tag{3.51}$$

where $\gamma_s$ is the temperature of the contact surface of the heatsink (cooler), $P_{l,s}$ the losses in the semiconductor element, $\theta_{jc}$ the junction to case thermal resistance of the component and $\theta_{cs}$ is the thermal resistance of the interface between component and heatsink (see also Figure 3.22).

The mean power loss in the power transistors, $P_{l,t}$ are given by

$$P_{l,t} = U_{CE(on)} I_{avg} + R_{on} I_{rms}^2 + W_{on-off} f_s \tag{3.52}$$

where $U_{CE(on)}$ is the collector to emitter constant voltage drop, which may be approximated to zero for components based on MOSFET technology but it can be significant for IGBT components. $R_{on}$ is the equivalent series resistance, $I_{avg}$ is the absolute average current and $I_{rms}$ is the rms current that flows through the component. $f_s$ is the switching frequency which is considered to be constant. $W_{on-off}$ is the switching energy loss for a switching period, which may be scaled from the value obtained from the component data sheet according to equation (3.53) [48].

$$W_{on-off} = \frac{U_{dc-link} I_{rms}}{U_{nom} I_{nom}} W_{on-off,nom} \tag{3.53}$$

Where index *nom* refers to the conditions presented in the data sheet of the transistor. The loss model for the free wheeling diodes (FWDs) is simpler, the losses, $P_{l,d}$ are given by

$$P_{l,d} = U_{on,d} I_{avg} \tag{3.54}$$

where $U_{on,d}$ is the forward voltage drop of the diode. A more complete loss model for the diodes would include resistive losses and so called recovery losses; but they are often small and therefore neglected here.

The phase rms-current is given by

$$I_{rms} = \frac{T_{m,rms}}{3K_e} \tag{3.55}$$

The absolute average phase current $I_{avg}$ is, assuming that it is sinus shaped, given by

$$I_{avg} = I_{avg,rms}\frac{2\sqrt{2}}{\pi} = \frac{2\sqrt{2}}{\pi 3K_e}\frac{1}{\tau}\int_0^{\tau}|T_m|dt \tag{3.56}$$

The equations above for the phase currents do however assume that all of the phase current passes through the same component. In reality the phase current may take one of four different paths through one phase leg of the converter. The amount of current that flows through the transistors compared to the FWDs depends on the power factor* and machine speed. Consequently, in order to determine an exact value of the losses a detailed study incorporating switching strategy, load power factor etc. has to be performed over a complete load cycle. Here a simplified approach is used to approximate the losses, $P_{l,tot}$

$$P_{l,tot} = 3\alpha P_{l,t} + 3(1-\alpha)P_{l,d} \tag{3.57}$$

where $\alpha$ represents a value between 0 and 1 and can be viewed as the mean duty cycle of the transistors over a load cycle. In this work it is set to 50% which means that the current, in average, is assumed to pass through the free-wheeling diodes half the time and through the transistors the other half. The temperature in the heatsink/component interface is then given by

$$\gamma_s = P_{l,tot}\theta_{sa} + \gamma_{ambient} \tag{3.58}$$

where $\gamma_{ambient}$ is the ambient temperature of the cooling medium (air temperature if passive air cooling), $\theta_{sa}$ is the thermal resistance of the heatsink to ambient. Even though the losses might be lower in the FWD, they are of the same magnitude as in the transistors. Therefore is it not so important to have an exact figure of the division of current between components ($\alpha$) when calculating the average power loss during a load cycle. However, in order to determine the maximum allowed temperature in the interface between component and heatsink, $\gamma_{s,max}$ a worst case scenario needs to be analyzed.

The thermal time constants of the semiconductor packages are assumed to be much shorter (milliseconds) than the thermal time constant of the heatsink. This leads to that the heatsink must be dimensioned such that it always is cool enough to avoid overheating of the semiconductors during the worst case scenario. The worst case that the converter must handle depends of course on the application, in a fan or pump application it might for example not be necessary to dimension

* The power factor (*PF*) is defined as the ratio of real average power to the product of rms voltage and rms current

$$PF = \frac{P}{U_{rms}I_{rms}}$$

the driver for locked rotor operation. In a general servo drive, locked rotor operation is difficult to avoid, usually there is always some (failure-) mode of operation that requires torque to be delivered at stand still. The condition with a locked rotor is critical, since the current then flows through one or two of the components in one leg of the converter, instead of all four. Here it is assumed that the worst case for the diodes is during a locked rotor condition, where the required max current flows through one of the diodes around 90% of the time. For the transistors the worst case is assumed to be max torque at full speed, which gives that the required max current flows through each of the transistors in a leg approximately 50% of the time. Reformulating equation (3.51) gives

$$\gamma_{s,\max} = \gamma_{j,\max} - P_{l,s,\max}(\theta_{jc} + \theta_{cs}) \tag{3.59}$$

where $P_{l,s,max}$ is the worst case power loss in a single component given by inserting the worst case currents in equations (3.52) and (3.54) respectively. The thermal resistance between junction and case $\theta_{jc}$ is given by the data sheets of the components. Generally a more expensive component has a lower $\theta_{jc}$ and vice versa. This implies that cheap semiconductors require larger cooling means than a more expensive selection, an interesting tradeoff not studied in detail here. The resistance between case and heatsink $\theta_{cs}$ depends on the component type, but also on how the component attaches to the heatsink, which will be discussed further in the following section. The maximum allowed heatsink temperature $\gamma_{s,max}$ has to be calculated for both the diode and transistor candidates and the lowest of the two obtained temperatures will be dimensioning for the heatsink.

By combining equations (3.57) and (3.59), the following expression for the maximum thermal resistance of the heatsink is obtained

$$\theta_{sa} \leq \frac{\gamma_{j,\max} - \gamma_{ambient} - P_{l,s,\max}(\theta_{jc} + \theta_{cs})}{P_{l,tot}} \tag{3.60}$$

### 3.5.2 HEATSINK

The main task of the heatsink is to reduce the surface temperature of the power electronic elements. There are a number of different types of heatsinks for power electronics. According to [49] they can be classified into (in order of increasing cost and decreasing thermal resistance)

- Passive heatsinks based on natural convection.
- Semi active heatsinks, using **existing** fans in the system.
- Active heatsinks with dedicated fans.
- Liquid cooled heatsinks
- Phase change recirculating systems, for example boiler/condenser systems.

The heatsink is one of the largest, heaviest and most expensive parts of a motor drive unit, and is therefore important to include in this type of system wide analysis. This thesis will for the sake of simplicity focus on natural convection cooled heatsinks, the most inexpensive and reliable solution. However, this approach is not always possible, for high power systems, a fan or water based cooling systems may either be required in order to reach the expected performance and/or be less expensive than huge natural convection heatsinks.

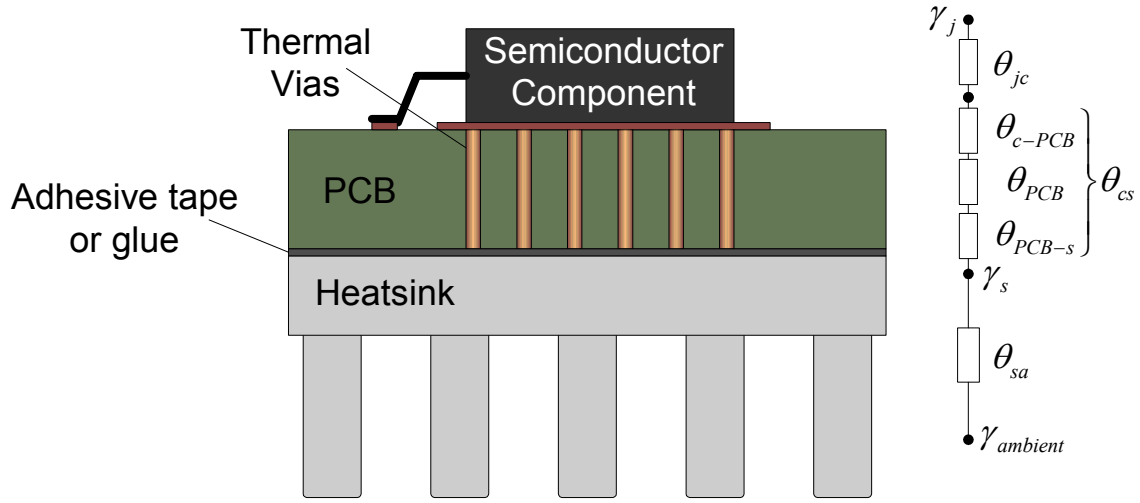


*Figure 3.22. PCB mounted heatsink with thermal vias (after Märtz [50]).*

The thermal resistance between heatsink and component $\theta_{cs}$ has a large influence on the required size of the heatsink. In order to minimize the thermal resistance the components should be mounted in direct contact with the heatsink, but that usually results in expensive solutions with relatively low power densities (much air in the drive unit) [50]. On the other hand, if the power electronic elements are mounted on a printed circuit board (PCB) with the heatsink glued to the PCB according to Figure 3.21 and Figure 3.22 there is a very good potential of lowering the cost of the motor driver while increasing its power density (higher integration) [50]. The drawback with this solution is that the PCB is a thermal insulator and not a conductor. This can be solved by using a technique with thermal vias, where a number of vias (holes) are placed under the semiconductor components and filled with copper or solder (Figure 3.22). According to [50] the thermal resistance of such a via is around 60 °K/W, using about 30 parallel vias per component results in a thermal resistance of the PCB of about 2 °K/W. The total thermal resistance between case and sink gets (assuming TO-220, TO-263 or equivalent packages)

$$\theta_{cs} = \theta_{c-PCB} + \theta_{PCB} + \theta_{PCB-s} \approx 0.5 + 2 + 0.5 \approx 3°\text{K/W} \tag{3.61}$$

This solution is only feasible for systems requiring relatively low power. For higher powers a thermal resistance of 3 is too high and the semiconductors have to be attached directly to the heatsink, yielding in this case a resistance of 0.5K/W. In the example presented later on, the approach with PCB-mounted components and heatsink is used, even though it results in a larger heatsink it is likely that the total system cost is lowered due the possibilities to reduce the manufacturing cost for high production volume products.

Inserting the thermal resistance from (3.61) in equation (3.60), results in the maximum allowed thermal resistance of the heatsink, $\theta_{sa}$. Here the problem with determining the optimal design of such a heatsink has been simplified into just estimating the required volume and weight of the heatsink. In [51] a diagram expressing the heatsink volume as function of thermal resistance is presented. Even though the use of such a diagram only gives a rough estimate of the heatsink volume, its simplicity makes it very attractive to use in this type of

work. In Figure 3.23, three of the curves presented by Soule [51] are shown, and as seen the required heatsink volume appears to, in a log-log diagram, be nearly linear to the thermal resistance. In order to verify Soules results, data on a number of commercially available aluminum heatsinks are shown in the graph. The solid line, represents a curve fitted to this data. As seen, the trend is the same as presented by Soule but it seems like he overestimates the volume a bit.

The equation for the solid fitted line, representing the volume $V_{hs}$ of natural convection heatsinks is

$$V_{hs} = \frac{5 \cdot 10^{-4}}{\theta_{sa}^{1.44}} \tag{3.62}$$

The weight of a heatsink $m_{hs}$ can be estimated to

$$m_{hs} = V_{hs} \rho_{hs} \tag{3.63}$$

where $\rho_{hs}$ is the mass density of the heatsink. Here it is obtained by dividing the weight with the volume of the commercially available heatsinks plotted as X's in Figure 3.23. This resulted in an average mass density of about 1000 kg/m$^3$.

$$\rho_{hs} \approx 1000 \text{kg/m}^3 \tag{3.64}$$

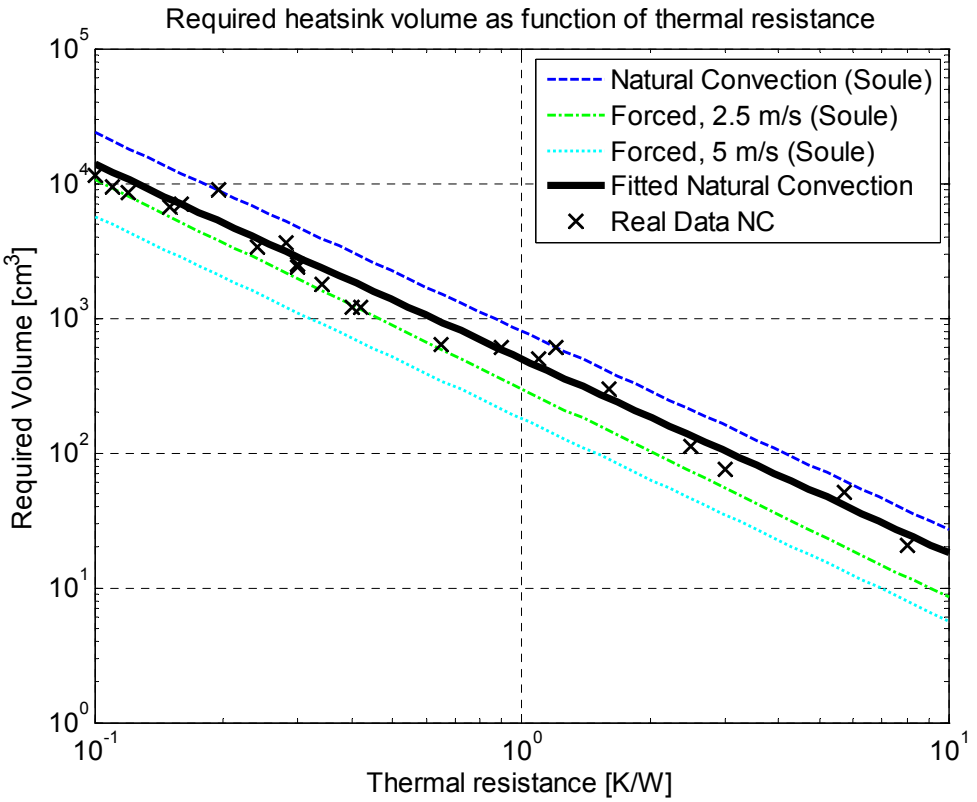


*Figure 3.23. Estimated heatsink volume as function of its thermal resistance.*

### 3.5.3 DC-LINK CAPACITOR

It is the DC-bus capacitors that account for the major fraction of the volume and cost of a converter, according to [52]. The authors have however not included the heatsink in their analysis. Nevertheless, it is important to include the dc-link capacitor in a mechatronics design and optimization methodology.

The DC-link capacitor needs to deal with the following problems ([52] and [53]):

- The ripple current due to converter switching
- Voltage fluctuation due to the source internal impedance
- Voltage transient due to stray inductance and device switching
- Over voltage due to regeneration

The capacitance needed to deal with the three first is generally not high, for those the major concern is the current handling capability of the capacitor. In [53] the authors state that regeneration do not require high capacitance if the battery is connected directly to the DC-bus (as in Figure 3.20). That may be true from a pure functional perspective, but concerning system efficiency it might be better to keep the regenerated energy within the dc-bus capacitor than charging a battery with it (eg. [54] and [55]). Capacitor sizing with respect to regeneration will however not be made here, it is assumed that the converter has in-built functionality to feed the regenerated current through a power resistor if an over voltage is detected at the dc-link.

Conventional converter design generally use electrolytic capacitors. Considering that it is the current and not the capacitance that is of interest in battery fed converters, other capacitor technologies with lower equivalent series resistance (ESR), as for example film capacitors might reduce the dc-link capacitor size (e.g. [52] and [53]). In this thesis the focus will however be on the conventional technology with electrolytic capacitors.

The converter input ripple current depends on the modulation index*, output current and load power factor. In [52] the input ripple current is derived to be about 45% of the converter output current at its maximum. In [53] a rule of thumb is presented stating that the dc-link ripple is up to 65% of the rated load current in an induction motor based traction drive, and possibly even higher in PM drives. To get the exact value of the ripple current, spectrum analysis of detailed converter simulations are required, which is not possible here. Therefore the dc-link ripple current is assumed to be 65 % of the machine rms current

$$I_{dc,ripple} = 0.65 I_{rms}$$

Even though it might be more realistic to design application specific capacitors than semiconductors, the approach is also here based on the selection of already existing components. The maximum allowed ripple current is often given directly in the capacitor data sheet, but it might be necessary to compensate for the frequency of the ripple current. The maximum ripple current is limited by the temperature of the capacitor; a high temperature means a shorter life expectancy.

* The modulation index is defined by the ratio of dc-link voltage and amplitude of the converter output voltage.

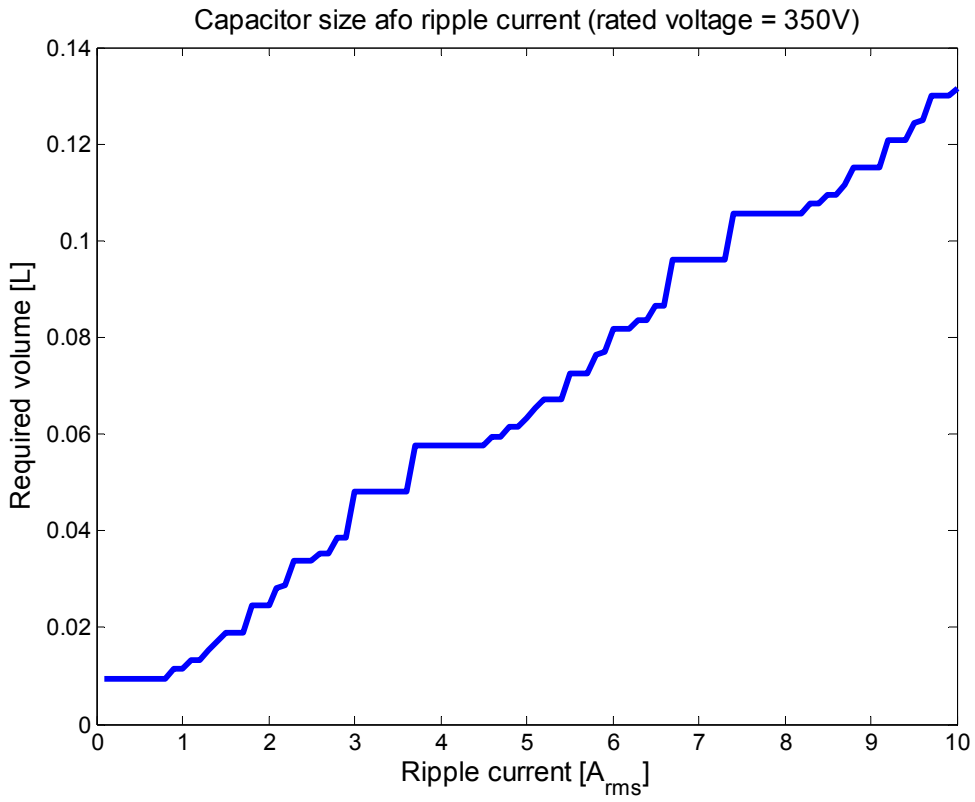


*Figure 3.24. Required capacitor volume as function of ripple current for 350V capacitors from ELNA [56].*

The temperature rise in the capacitor is mainly a result of the capacitor's ESR, which is frequency dependent. Generally the ESR gets lower with frequency which means that the required capacitor size decreases with switching frequency. However, above frequencies of about 2000 Hz, the ESR is rather constant with frequency ([52] and [53]). Since these types of applications use much higher frequencies than that, the ESR may be regarded as independent of switching frequency.

In Figure 3.24, the required capacitor volume as function of ripple current is presented. The capacitor data is taken from [56]. As seen, for a given voltage rating, the capacitor volume is almost linear with ripple current. This indicates that it would be possible to use a continuous linear model for the required capacitor size, instead of the discrete approach presented here.

The mass density of the capacitors is in this work assumed to be much smaller than the mass density of the other components, a model of the capacitor weight is therefore not presented here.

### 3.5.4 INTEGRATED DESIGN OF MACHINE, GEAR AND DRIVER

Now it is time to include the machine drive unit into the design example. As input to the sizing method the power transistor and diode data presented in Table 3.4 and Table 3.5 are used.

The first step is to determine the currents required to follow the example load profile (section 2.6). This is done by using equations (3.55) and (3.56) together with the equations derived in section 3.3.3. As before, the starting point is the

machine denoted PSA90/6-79B from Table 2.2. Applying equations (3.22), (3.27) and (3.35) on the derived machines from the previous section results in the currents presented in Figure 3.25. The maximum current is the maximum current required during the load profile, the rated peak current is the maximum allowed current (in this case 5 times the machines' rated current).

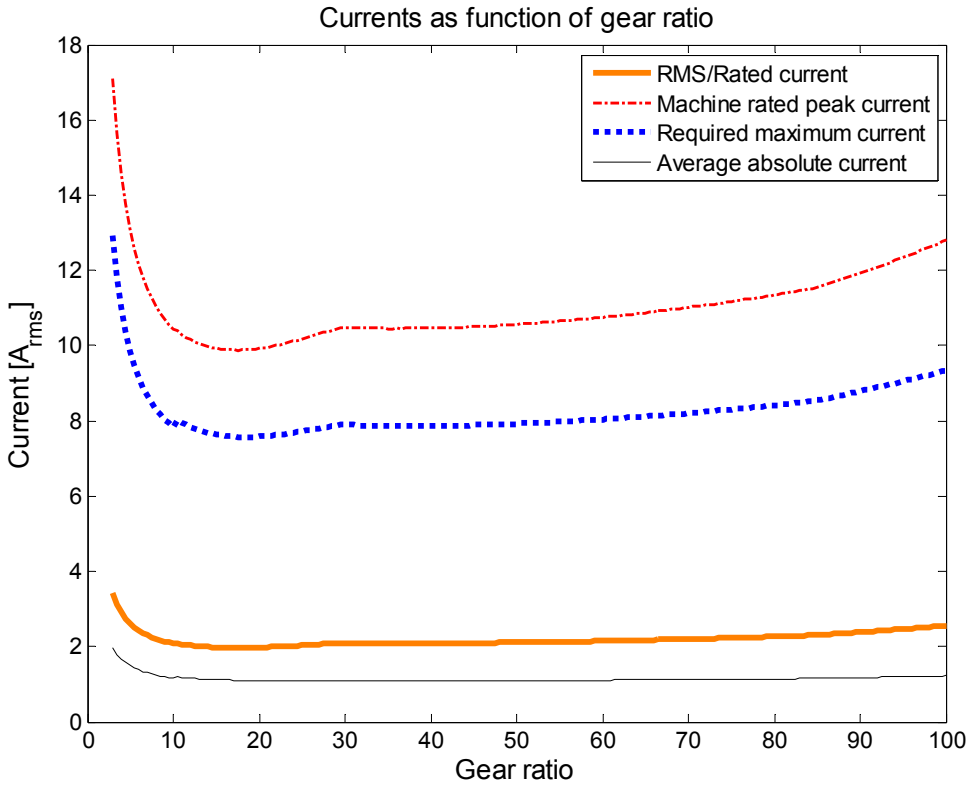


*Figure 3.25. Required current to follow the load profile as function of gear ratio.*

*Table 3.4. Data on the candidate IGBTs [57] (SI-units).*

| Component | | Max Voltage | $R_{ce}$ | $U_{ce(on)}$ | $W_{on-off}$ | $\gamma_{i,\,max}$ [°C] | $\theta_{jc}$ | Cost $ |
|---|---|---|---|---|---|---|---|---|
| **1** | IRSL4B60 | 600 | 0.33 | 1 | 0.17e-6 | 175 | 2.4 | 0.821 |
| **2** | IRSL6B60 | 600 | 0.19 | 1 | 0.14e-6 | 150 | 1.4 | 0.875 |
| **3** | IRSL8B60 | 600 | 0.11 | 1 | 0.15e-6 | 175 | 0.9 | 1.204 |

*Table 3.5. Data on the fast recovery free-wheeling diodes [57]and [58] (SI-units).*

| Component | | Max Voltage | $U_{on}$ | $\gamma_{i,\,max}$ [°C] | $\theta_{jc}$ | Cost $ |
|---|---|---|---|---|---|---|
| **1** | IRF 10 ETF | 600 | 1.5 | 150 | 1.5 | 1.169 |
| **2** | IRF 20 ETF | 600 | 1.5 | 150 | 0.9 | 1.725 |
| **3** | Infineon 45E60 | 600 | 1.5 | 175 | 0.8 | 2.0* |

*Table 3.6. Parameters related to the sizing of the machine drive unit.*

| $\gamma_{ambient}$ | $\theta_{cs}$ | $U_{dc\text{-}link}$ | $f_s$ |
|---|---|---|---|
| 25° C | 3°K/W | 300 V | 20 kHz |

* The cost of this component is made up by the author.

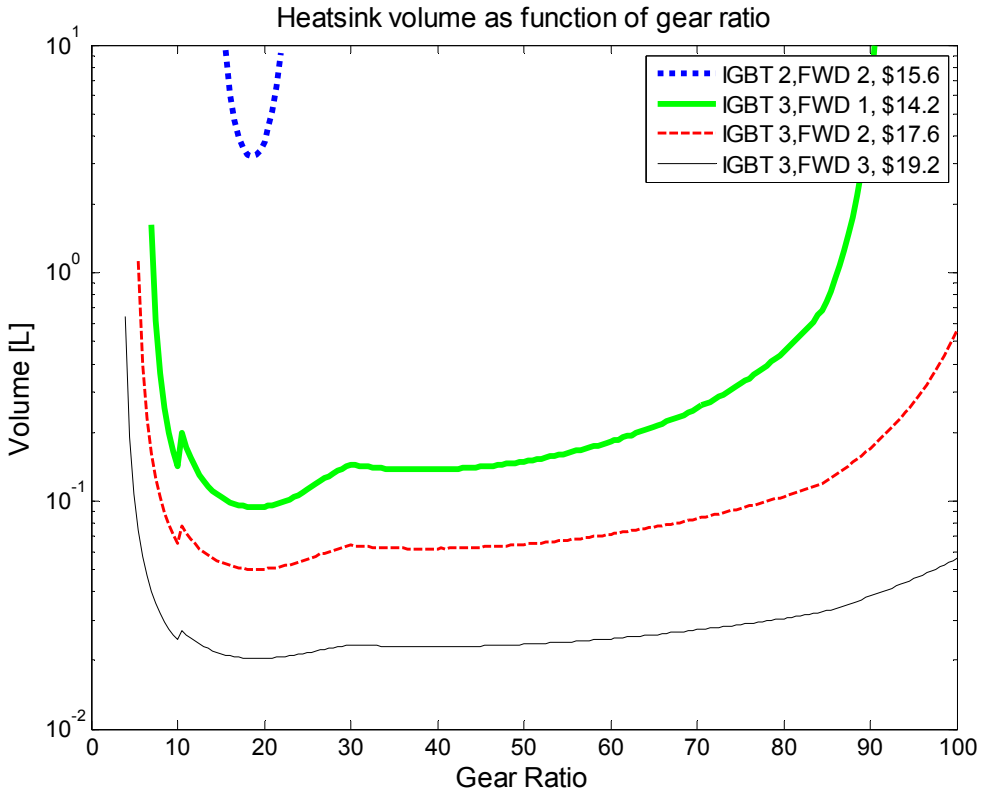


*Figure 3.26. Required heatsink volume as function of gear ratio for all viable semiconductor selections.*

In Figure 3.26 the required heatsink volume is plotted as function of gear ratio for all of the viable combinations of IGBTs and FWDs (Table 3.4 and Table 3.5). As seen in the figure, there is a delicate tradeoff between cost and size when designing motor drive units. The least expensive solution from the semiconductors point of view is the one requiring the largest heatsink and vice versa. Solutions requiring heatsink volumes of above 10 L or requiring active cooling have been marked as non viable and are not shown in the figure. How to weigh the heatsink size to the semiconductor cost will not be solved here, but it highlights the importance of including cost models into the methodology. In order to make a volume comparison between gear ratios, it is decided to select the same semiconductor combination for all gear ratios. Here the solution that corresponds to a total component cost (6 x IGBT_3 + 6 x FWD_1) of $14.2 is selected (Figure 3.26, Table 3.4 and Table 3.5).

The volume of the DC-link capacitor is directly given from the RMS-current, using the same electrolyte capacitors from ELNA [56], as used when generating Figure 3.24. The required capacitor volume is shown in Figure 3.27.

In Figure 3.28 the required heatsink volume for the selected semiconductor combination is shown together with the capacitor volume and machine and gear volume. As seen, the heatsink volume dominates the total volume for gear ratios over 85. As long as the gear ratio is kept between 20 and 70 the heatsink does not seem to affect the total system size very much (the curve is rather flat). The selected semiconductors can not be used for high and really low gear ratios, for those ratios it is necessary to select a more expensive combination from Figure 3.26

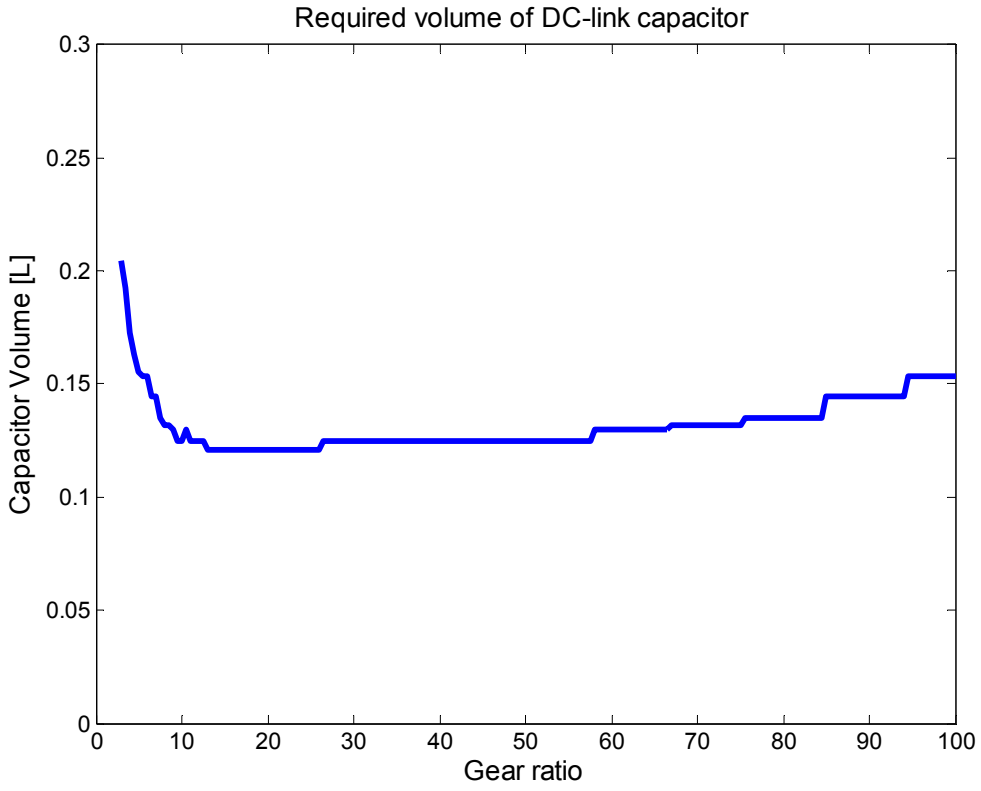


*Figure 3.27. Required dc-link capacitor volume as function of gear ratio.*

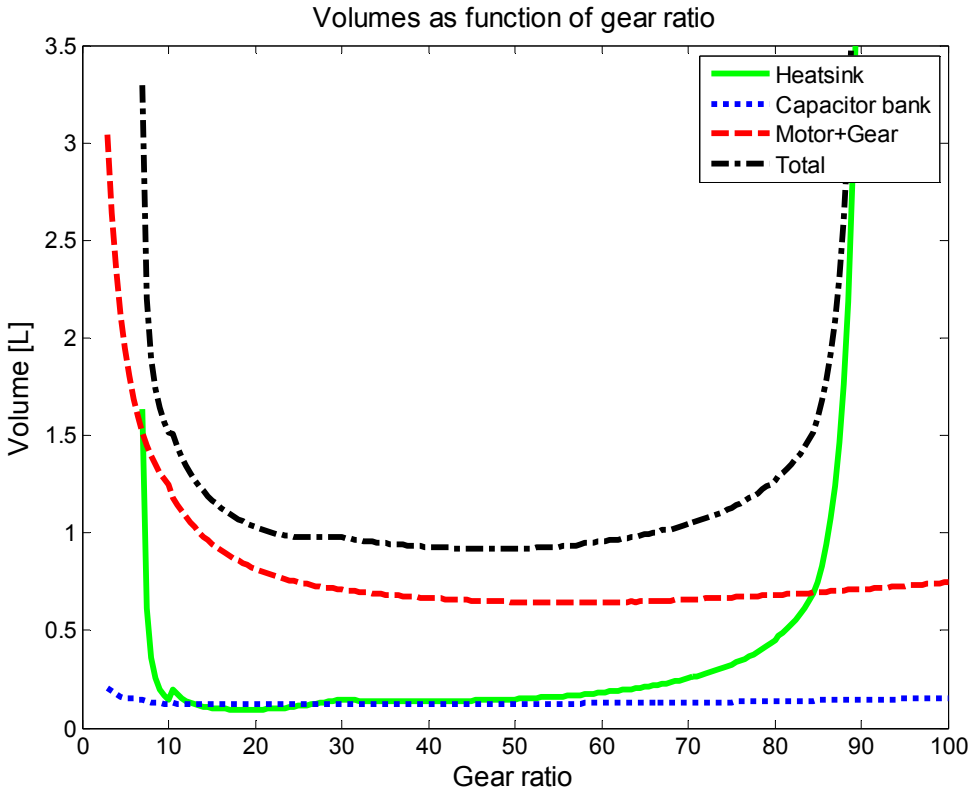


*Figure 3.28. Volume of the heatsink and dc-link capacitor in relation to the volume of the machine and gear.*

## 3.6 INTEGRATED DESIGN OF THE PHYSICAL SYSTEM

In the previous sections the physical components of a servo system have been dimensioned and optimized with respect to volume. It is shown that the optimal gear ratio depends on which components that are included in the analysis. In the design case, the gear ratio that minimizes the volume of the electric machine is 100 (Figure 3.9). Adding the required gearhead size reduces the optimal gear ratio to about 55. Finally adding the volume of the drive unit moves the optimum to approximately 45, but the curve is rather flat and the total volume is rather insensitive to gear ratios between 25 and 60.

Even though the total size of the system is analyzed, and the best gear ratio is selected with the whole system in mind, it is not certain that the true system optimum is obtained. The components have been dimensioned for the same load, but rather separate from each other. As mentioned before, the size of the electric machine depends on the gear efficiency and gear inertia. The gear inertia is concluded to be small in comparison to the machine, so it is disregarded. This simplifies the design method significantly. The gear efficiency is the only gear parameter, except for the gear ratio, that affects the machine size. However, the heatsink and capacitors in the motor drive unit was dimensioned for a set of size optimized machines. This approach may lead to a sub-optimum. If the machines are selected such that they minimize the required machine current instead, the size of the heatsink and capacitor decreases. In Figure 3.29, the total system volume is shown for the two cases. For the design example, it is slightly better from a system perspective to select machine with respect to current than size. This effect is mainly caused by the somewhat higher inertia of the size optimized machines, which in turn leads to higher acceleration torques and currents. In other words, the machines optimized with respect to current are long with small radii while the machine optimized with respect to size are shorter, with larger radii. This example highlights the need of optimizing all components together in order to find a better system design. It also addresses the issue discussed in section 2.4.2, regarding free design variables. From a systems perspective it is not certain that the true volume optimum is reached when only machines that exactly can drive the load are considered. It is possible that using an ‘oversized’ machine might reduce the total system volume. The introduced error by only considering machines that are exactly large enough to drive the load is however small (in some cases zero), and it is not justifiable to further complicate the methodology in order to solve this problem.

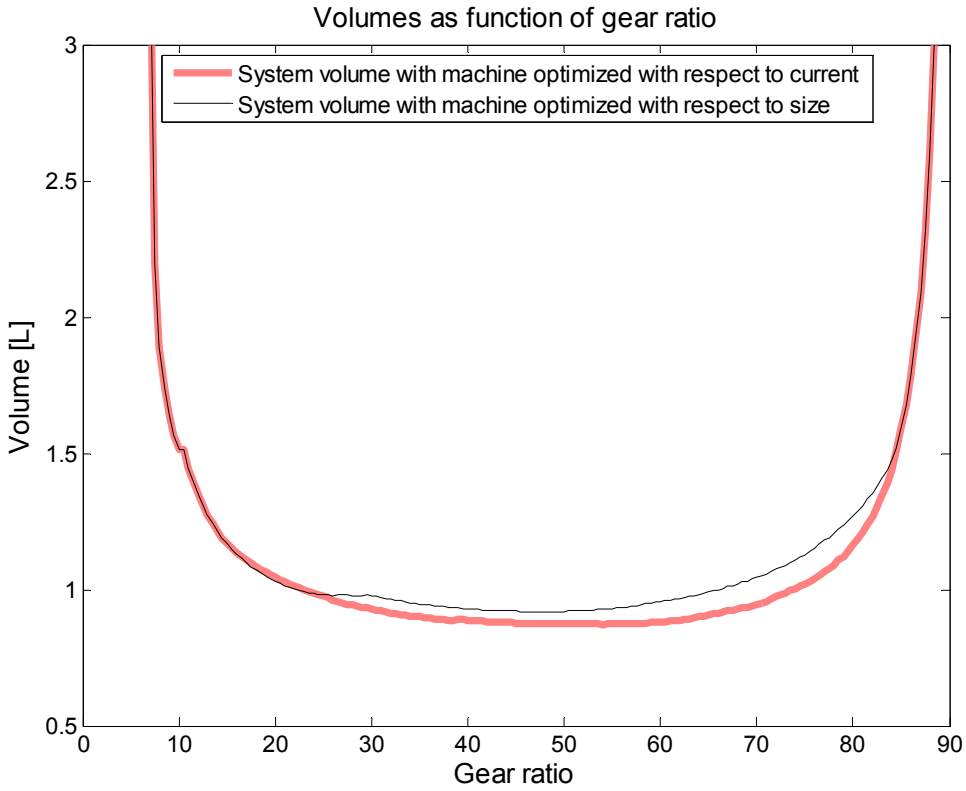


*Figure 3.29. Differences in system volume depending on if the machine is optimized with respect to size or current.*

Until now, only the volumes of the components have been analyzed as function of gear ratio. In addition, weight models have been presented. However, as mentioned in the previous chapters the long term aim is to include other optimization criteria such as energy efficiency into the methodology. One way of analyzing energy efficiency is to study the power losses in the servo system. The total losses are given by

$$P_{l,tot} = (1-\eta_g)\frac{1}{\tau}\int_0^{\tau}\left|T_l\dot{\varphi}_l\right|dt + 3R_pI^2 + P_{loss,driver} \tag{3.65}$$

Where $P_{loss,driver}$, is given by equation (3.57). Applying equation (3.65) on the example case gives the power loss presented in Figure 3.30. As seen, the losses are largest at low gear ratios, the lowest losses are in this case obtained at a gear ratio of approximately 35. Thus, from an efficiency point of view, a geared solution seems to be better than a direct drive configuration. In addition to the direct drive losses presented in Figure 3.30, comes the losses in the power electronics, which will make the difference even larger. One possible source to power loss is however not included in this analysis, the brake resistor. The regenerated energy during braking, cause a voltage rise in the dc-link, in order to avoid over voltages, the extra energy is often burned up in resistors. But in some cases the energy may be fed back to the source or stored in a local super capacitor.

The curves presented in Figure 3.30 highlight one of the most important shortcomings of the design methodology in its present form, the lack of speed dependent losses in the models. For both the gear and electric machine the speed dependent losses have been ignored, adding viscous friction and iron losses in the machine will increase the power loss at high gear ratios. As mentioned before, and as further discussed in chapter 6, it is a natural next step to implement speed-dependent losses into the methodology.

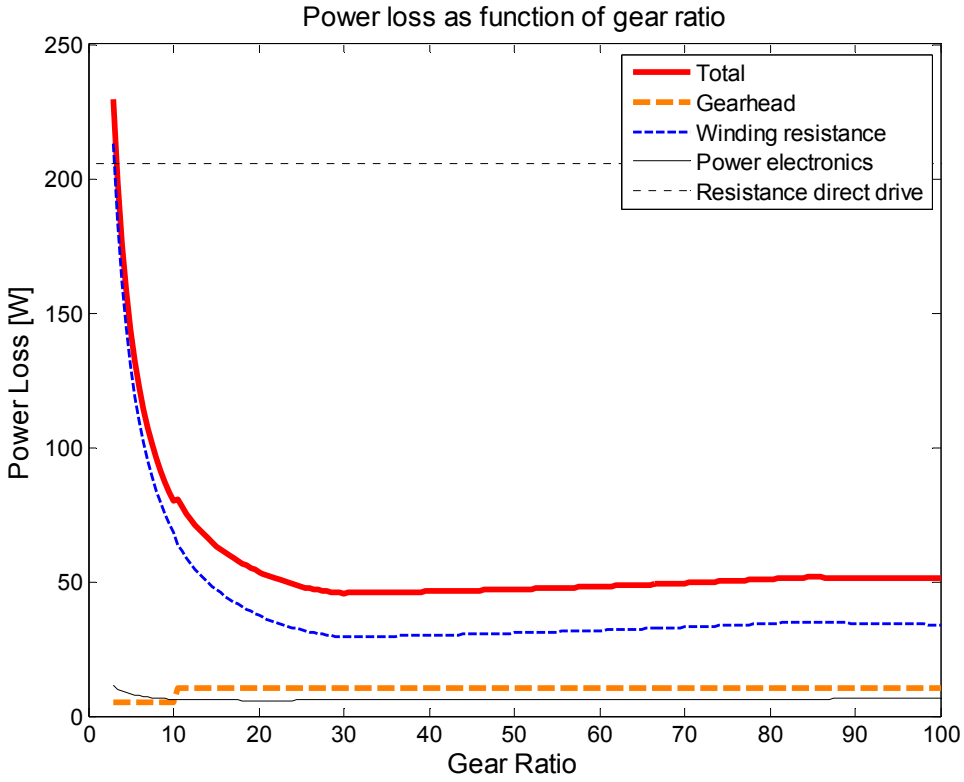


*Figure 3.30. Mean power loss as function of gear ratio.*

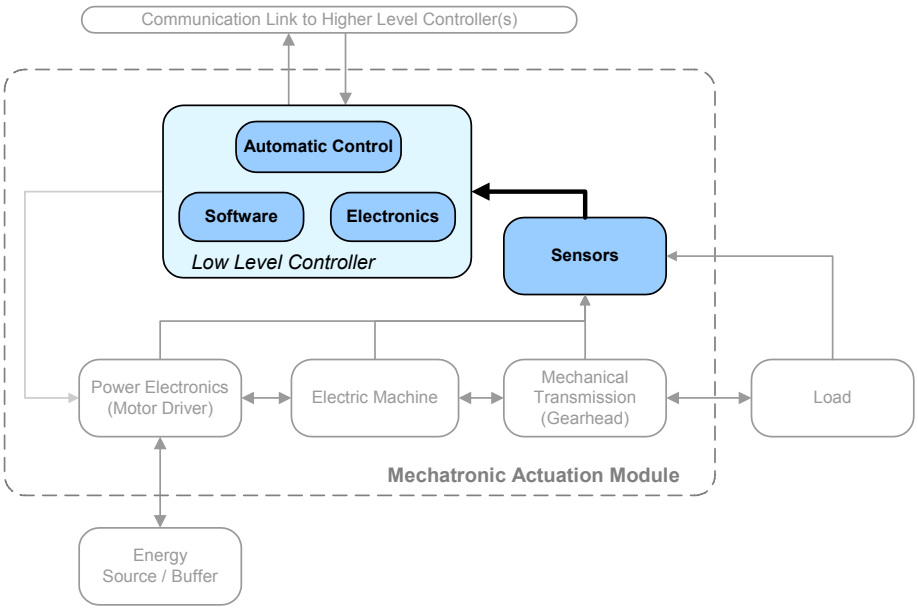


# 4 DYNAMICS AND CONTROL SYSTEM OPTIMIZATION

This chapter deals with the design and optimization of the control system of an actuation module. The control system is here defined to include the position sensor (encoder), the control algorithm and to some extent the electronic hardware which the algorithm is executing on. The focus is not on classic control design but rather on the integration of controller design with the design of the physical system. A large part of the chapter focuses on how the control performance is affected by the gear ratio and the majority of the content is based on paper D and paper E. First, a linear representation of the mechanism is analyzed with respect to bandwidth and stiffness. Then a more realistic, non-linear plant model is implemented and the resulting control performance is compared with the one obtained with the linear system model. Finally, the couplings between control performance and torque requirements are analyzed and discussed.

## 4.1 RELATED WORK

This section intends to give a short overview of the previously published work about dynamics of electromechanical servo systems. Dynamics analysis of servo mechanisms is a well established area in mechatronics (e.g. [59] and [60]). Nevertheless there are still some misunderstandings in the field. For example, the load to motor inertia ratio is a common measure of how easy a servo system is to control. A too high inertia ratio is known to result in stability problems. However, as concluded by Moscrop *et al*. [61], a change in inertia ratio has in it self no or very little effect on the systems performance. It is actually the system's stiffness that usually increases with a decrease in inertia ratio and hence the better controllability is achieved.

Most previous work in the area treats only linear systems, but the fact is that it often is the non-linear phenomena that stand for the strongest couplings between physical system design and the performance of the control system. The

importance with considering all fundamental performance limitations in control system design is highlighted in [62]. One example of a fundamental limitation is the current/torque saturation of the electric machine. Not considering torque saturation in the design of the controller results in performance that is unachievable in the real system. The effect of torque saturation on the control performance in servo systems is analyzed in [63]. Furthermore, the discrete nature of position encoders, digital to analogue converters (DA) and analog to digital converters (AD) causes quantization effects in the control system. In [64] a method to calculate the required resolution of DA and AD converters, to achieve the specified control performance is presented. The method removes the need to test a number of different resolutions. However, both these papers assume a fixed model of the physical system and can therefore not be directly applied in this research.

In this work a PID-controller has been selected as controller (see Figure 2.5). A choice based on the fact that PID-control is common in industry and that it is a simple control strategy. There is a lot of published material on PID design and optimization, a good review of the area is presented by Cominos and Munro in [65]. In this chapter the control system is optimized with a genetic optimization algorithm, a technique that is spreading for controller optimization; examples include [66] and [67].

## 4.2 DYNAMICS ANALYSIS OF THE MECHANISM

In the previous chapters all components in the servo system have been treated as stiff, a reasonable simplification when optimizing the size of the physical components. However, even though the shafts and gearhead are stiff, they are not infinitely stiff. The flexibility in these components affects the system's control performance, so from now on the shafts and gearhead are modeled as torsion springs.

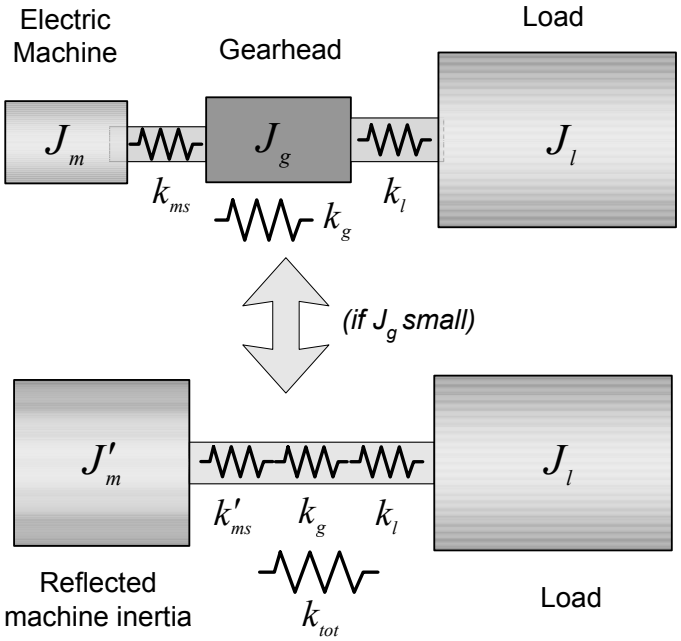


*Figure 4.1. The dynamics representation of the mechanism. The upper system is dynamically equivalent to the lower assuming low gearhead inertia.*

It is assumed that the electrical dynamics (e.g. inductance) of the electric machine and converter are much faster than the dynamics of the mechanical system. An assumption that generally is true for mechatronic servo systems. Therefore the system shown in Figure 4.1 is used as dynamic model of the physical system.

The original three-mass system shown in the upper part of Figure 4.1 may, assuming low gearhead inertia, be reduced to the two-mass model shown in the lower half of same figure. This assumption is generally true, and has already been shown to be valid for the design example used in the thesis (Figure 3.19). The gearhead stiffness $k_g$ is defined at the load side of the gearhead. It is therefore necessary to either transform the stiffnesses of the load and gearhead, $k_l$ and $k_g$ to the machine side, or to transform the stiffness of the machine shaft $k_{ms}$ to the load side. Here it is chosen to transform the machine parameters to the load side. Machine inertia as well as stiffness are transformed with a factor $n^2$ when viewed from the load side of the gearhead. Hence the reflected machine shaft stiffness and inertia are given by

$$k'_{ms} = k_{ms} n^2 \quad J'_m = J_m n^2 \tag{4.1}$$

The three flexible elements may be treated as one flexible element with the stiffness $k_{tot}$, which is given by

$$\frac{1}{k_{tot}} = \frac{1}{k'_{ms}} + \frac{1}{k_g} + \frac{1}{k_l} \Rightarrow k_{tot} = \frac{k'_{ms} k_g k_l}{k'_{ms} k_g + k_g k_l + k'_{ms} k_l} \tag{4.2}$$

Returning to the design example presented in section 2.6. The load shaft is assumed to have a diameter to fit with the direct drive machine, which gives a diameter of 72 mm. Assuming a shaft length of 200 mm and applying equation (3.16) gives

$$k_l = 7.9 \cdot 10^9 \frac{0.072^4}{0.20} \approx 1\text{MNm/rad} \tag{4.3}$$

Furthermore, as mentioned in the previous chapter, the gearhead stiffness is not modeled but taken from a planetary gearhead data sheet [68]. A gearhead with suitable torque rating has the following stiffness

$$k_g = 50\text{kNm/rad} \tag{4.4}$$

The machine shaft stiffness is given by equations (3.16) and (3.17). The individual stiffnesses of the three flexible elements ($k_{ms}$, $k_g$, $k_l$) and the total stiffness, $k_{tot}$ are plotted in Figure 4.2 below. As seen in the figure, the gearhead stiffness becomes dominant even at rather low gear ratios. This means that the machine shaft and especially the load shaft may be treated as infinitely stiff, at least for higher gear ratios. For the direct drive solution, only the load shaft stiffness is present, so it is obvious that a direct drive system will be much stiffer than a geared system. However, the gearhead and machine shaft have been dimensioned with respect to mechanical stresses (mechanical fatigue), and it is of course possible to select larger ‘over dimensioned’ components in order to increase their stiffness.

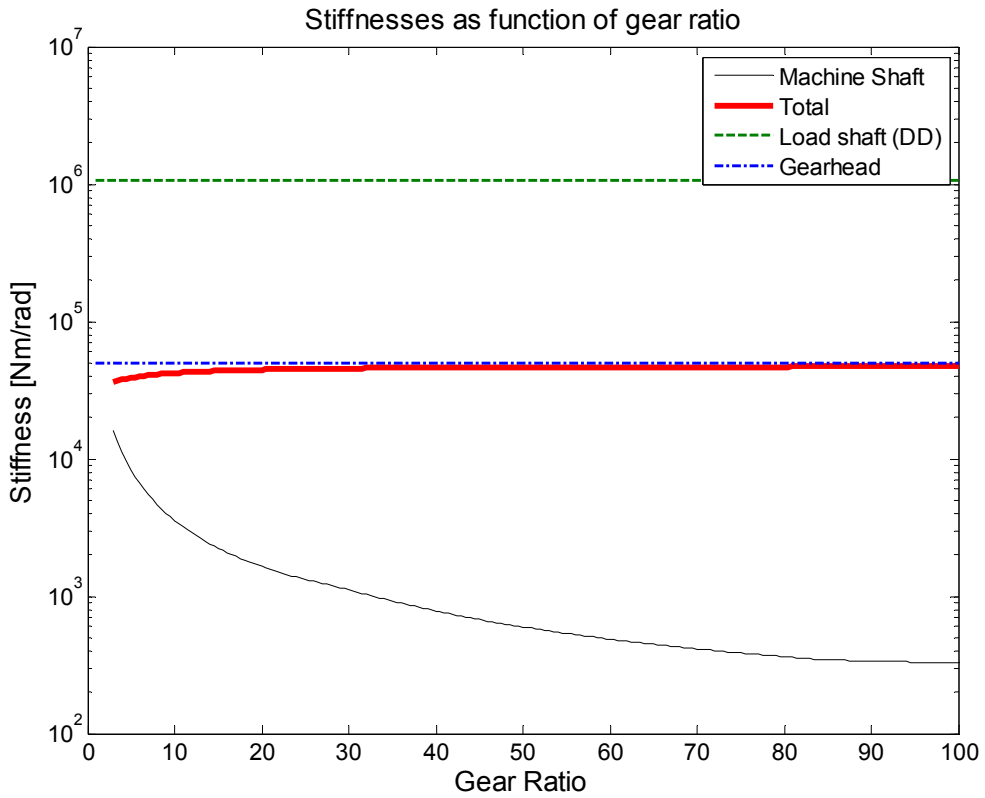


*Figure 4.2. Stiffnesses as function of gear ratio.*

It is assumed that the position sensor (encoder) is mounted on the machine shaft. This is standard in servo systems and has for example the advantage that the same sensor may be used for the control of the converter (e.g. commutation) as for the position/velocity controller. The transfer function from machine torque to machine angle, $G_{mm}$ is (neglecting friction)

$$G_{mm}(s) = \frac{(s^2 J_l + k_{tot})n^2}{s^2(s^2 n^2 J_m J_l + n^2 k_{tot} J_m + J_l k_{tot})} \tag{4.5}$$

where $s$ is the Laplace variable.

In paper D it is concluded that it is the anti-resonance frequency (zeroes in the pole zero map) that limits the bandwidth of the mechanism, assuming that the sensor is located at the machine side. Inserting the data of the direct drive solution in equation (4.5) and plotting the frequency response results in Figure 4.3. As seen in the figure, the negative peak of the anti-resonance occurs at a lower frequency than the resonance peak, which confirms that it is the anti-resonance that limits the bandwidth of the mechanism. The achievable bandwidth of the closed-loop system is in turn limited by the bandwidth of the mechanism. The anti-resonance frequency of the mechanism therefore gives an indication of the possible control performance. The anti resonance frequency, $\omega_{ar}$ is given by the zeroes of equation (4.5)

$$\omega_{ar} = \sqrt{\frac{k_{tot}}{J_l}} \tag{4.6}$$

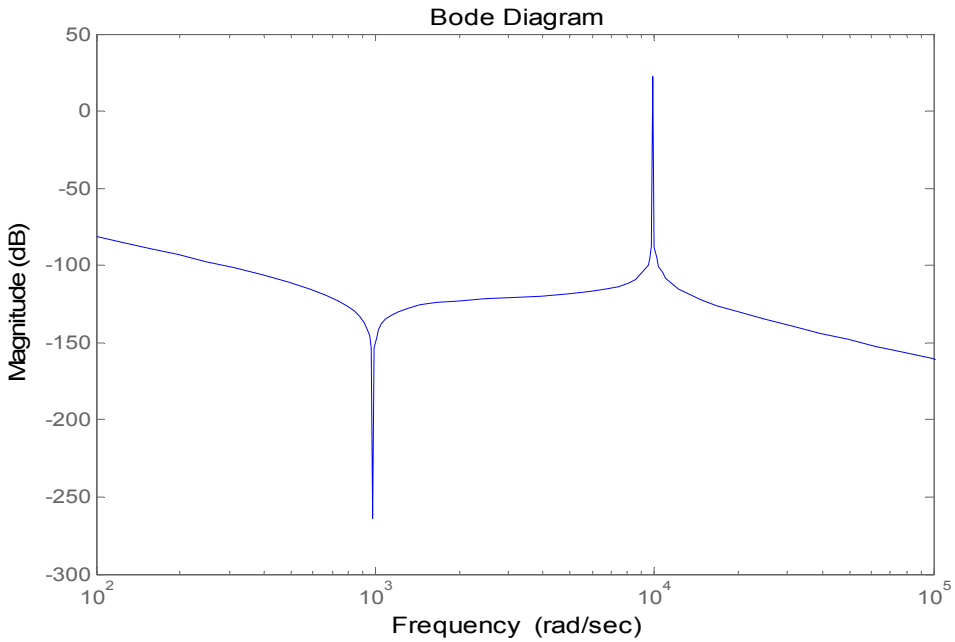


*Figure 4.3. Frequency response of the direct drive mechanism.*

The anti-resonance frequencies of the direct drive solution and of the geared configuration are plotted in Figure 4.4. The conclusions from this linear analysis are that a direct drive mechanism has significantly higher bandwidth than a geared solution and should therefore result in better control performance. Furthermore, the anti-resonance frequency of the mechanism increases with gear ratio, the increase is however small. Thus, the achievable control performance appears to be rather insensitive to gear ratio.

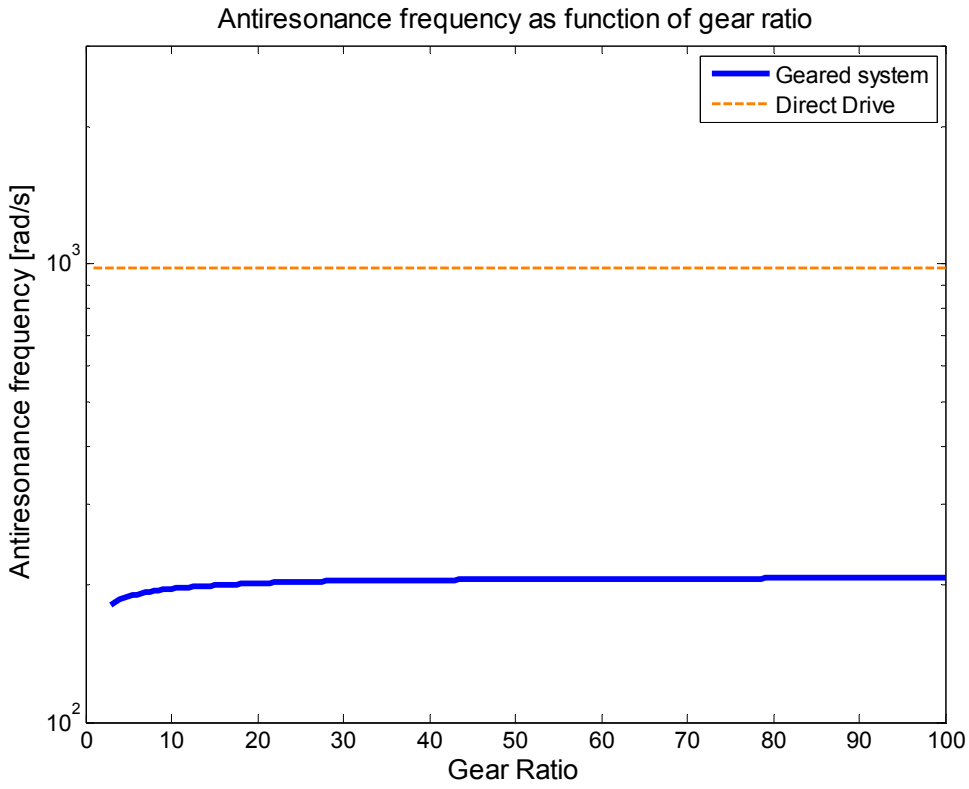


*Figure 4.4. Anti-resonance frequency as function of gear ratio.*

## 4.3 CONTROLLER OPTIMIZATION AND PERFORMANCE ANALYSIS

In this section the PID-controller is optimized, and the resulting control performance is evaluated as function of gear ratio. The idea is to compare the resulting performance with the anticipated performance from the bandwidth analysis of the mechanism (Figure 4.4). The linear representation of the entire closed-loop system is depicted in Figure 4.5. As already mentioned, the electrical parts of the machine and the driver are assumed to have much faster dynamics than the mechanical parts. They are therefore simply modeled as a low pass-filter with a cut-off frequency of 1000 Hz.

In order to analyze the control performance as function of gear ratio it is necessary to optimize the controller for each gear ratio. The controller optimization is made with a genetic optimization algorithm (see also section 2.4) and the optimization process is visualized in Figure 4.6. As seen, for each gear ratio the optimal parameters of the physical system (retrieved in the previous chapter) are loaded into the dynamic system model. Then the genetic algorithm optimizes the controller parameters ($P$, $I$, $D$) for that set of plant parameters. The optimal parameters are saved and the process is repeated for the next gear ratio. The integral square error (equation (2.3)) of the load position ($\varphi_l$) is used as objective function, $f_{obj}$

$$f_{obj} = \int_0^{\tau} \left( \varphi_l - \varphi_{ref} \right)^2 dt \tag{4.7}$$

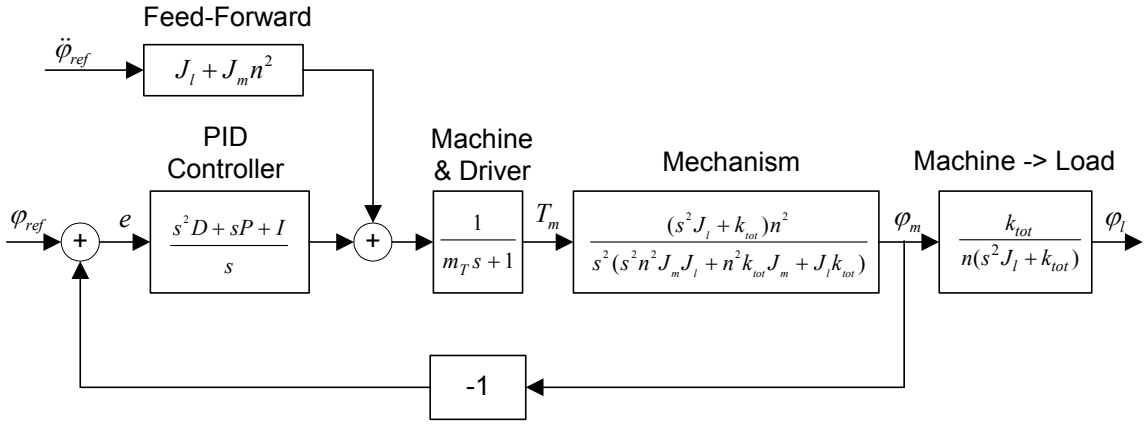


*Figure 4.5. Linear representation of the servo system.*

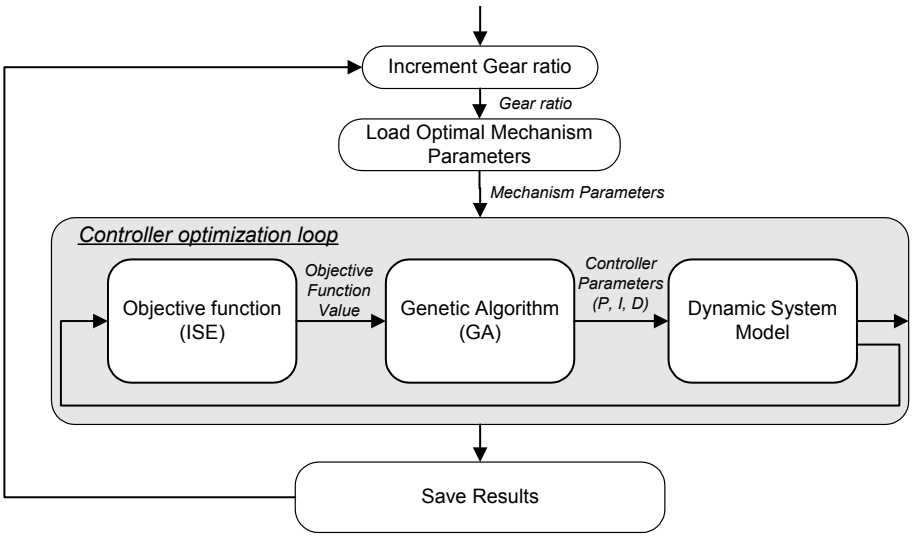


*Figure 4.6. Block diagram of the controller optimization process.*

### 4.3.1 LINEAR SYSTEM

The linear system described in Figure 4.5, does not exactly represent the load described in section 2.6, equation (2.4). The nominal load profile contains two non-linearities: the *load inertia* which is a function of load angle and the *coulomb friction torque* of 30 Nm. These two non-linearities and the *static load torque* of 15 Nm are added to the load side of the simulation model and are, from the controller's point of view, regarded as disturbances. Applying the controller optimization process described above to this linear representation of the servo system (non-linear load) results in Figure 4.7 below.

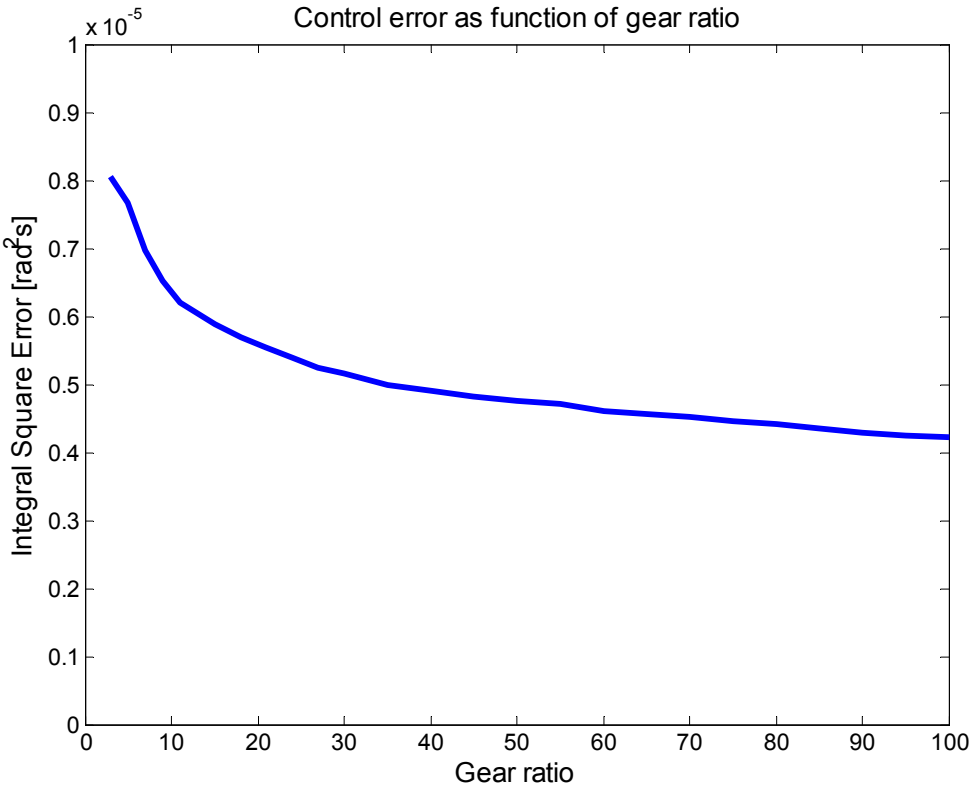


*Figure 4.7. Optimal performance (ISE) as function of gear ratio for the linear representation of the system.*

As seen in Figure 4.7 the control error reduces with gear ratio, as expected from the bandwidth analysis of the mechanism (Figure 4.4). However, these control errors are very small and the performance is close to perfect, so the difference in error between low and high ratios might be insignificant. The idea was to compare the obtained performance of the geared system with the direct drive configuration. However, the stiffness of the direct drive system is so high that it is difficult to simulate a fourth-order system. Hence, the direct drive system is modeled as a second order (infinitely stiff) system. This means that the optimization of the direct drive controller yields in ideal performance (control error = 0). The comparison gets more interesting in the next section where non-linearities in the machine, gearhead, sensor and controller are introduced.

### 4.3.2 EFFECTS OF THE NON-LINEAR PHENOMENA

In the section above the servo system is modeled as linear, a simplification often made for controller design. However, when considering the integration of controller design and the physical system design, the linearization might lead to that the most important couplings between the two domains are overlooked. Phenomena such as current saturation, backlash, sensor resolution and controller sampling frequency are directly related to the design and cost of the physical system but also directly related to the controller design and control performance.

The linear model of the servo system presented in the previous section is now replaced with a non-linear model that includes the most common non-linear phenomena present in electromechanical servo systems (Figure 4.8). As seen in the figure, the non-linearities are: current saturation in machine and driver, backlash and coulomb friction in the gearhead, quantization in the position sensor and in the current reference signal, and sampling and computational delay in the digitally implemented controller.

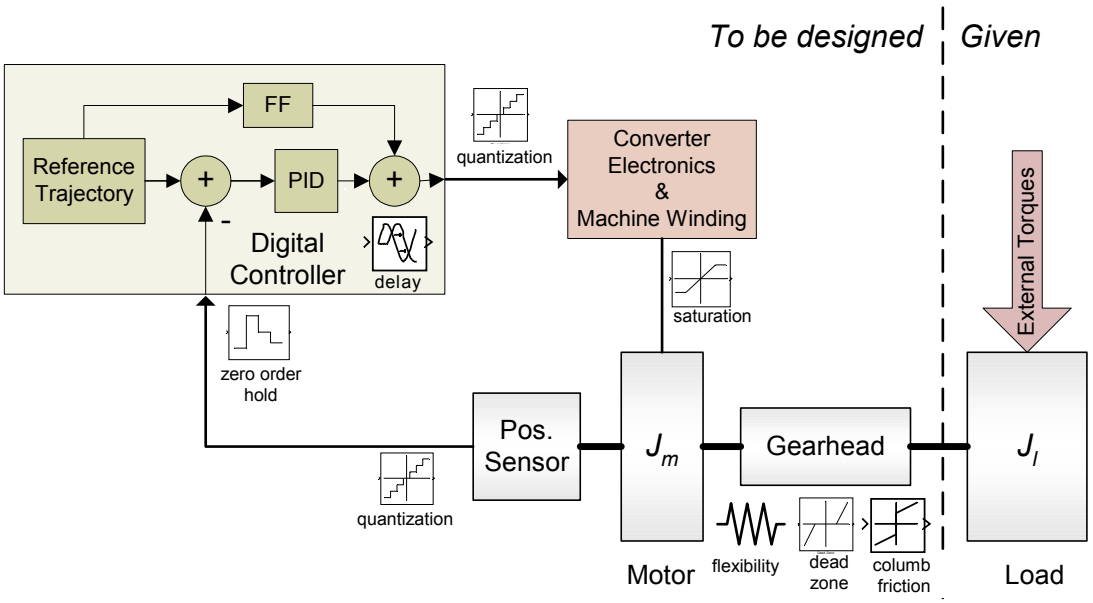


*Figure 4.8. Non-linear dynamic system model.*

For the example case used throughout the thesis it is assumed that the quantization effects in the current reference signal are small, hence they are disregarded. The computational delay in the controller is also disregarded. All of the other non-linearities are however implemented.

The coulomb friction in the gearhead is modeled as

$$T_{g,fr} = -\mu_g \left| T_l \right| \mathrm{sgn}\left( \dot{\varphi}_l \right) \tag{4.8}$$

Where $\mu_g$ is the friction coefficient, given by

$$\mu_g = 1 - \eta_g \tag{4.9}$$

The gearhead backlash, *BL* is taken from the same data sheet as the gear stiffness [68], and is (at the load side)

$$BL = \begin{cases} 2.9 \cdot 10^{-3} \,\mathrm{rad} & n < 10 \\ 4.3 \cdot 10^{-3} \,\mathrm{rad} & n \geq 10 \end{cases}$$

The controller sampling frequency is set to 2kHz and the current/torque saturation limit is set to the machine's peak torque, which is given by equation (3.13). The sensor resolution is to begin with set to 1000 pulses/rad. But later, results from both 100 pulses/rad and 10 pulses/rad are presented.

Applying the same optimization process (Figure 4.6) on the non-linear model as was used for the linear system representation, results in the graph presented in Figure 4.9. In this case the sensor resolution of 1000 pulses/radian was used. As seen, the optimal control error has increased significantly compared to the results obtained with the linear system. The discrete transition in gear backlash at a gear ratio of 10 is clearly visible in the figure.

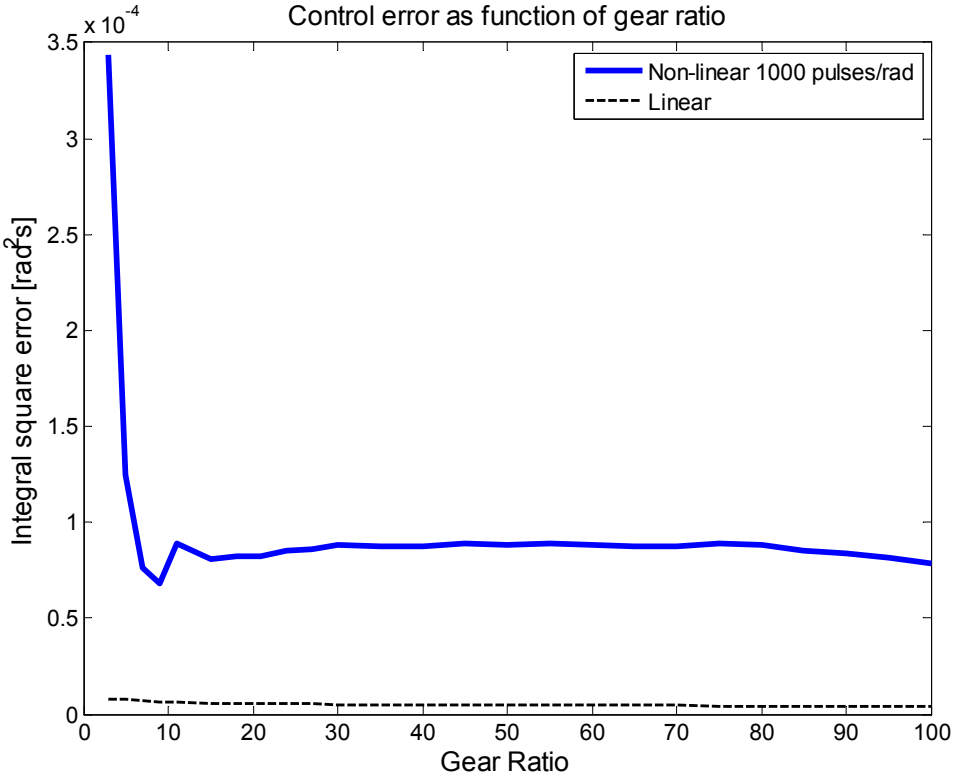


*Figure 4.9. Integral Square Error as function of gear ratio for the non-linear system model.*

The large difference in control performance seen in Figure 4.9 between the linear and non-linear system representations is alone enough to understand that it is important to include the non-linearities in the control system design and evaluation. But it is extra important in this type of system wide analysis since the non-linearities are tightly coupled to the size and cost of the physical parts of the system. For example, an increase in sampling frequency and sensor resolution is directly related to the electronic hardware cost, the same is true for a decrease in gear backlash.

### 4.3.3 REQUIRED MACHINE TORQUE

One very important limitation in the physical system has been disregarded in the analysis presented above, namely the continuous torque rating of the electric machine. The physical system has been designed to deliver the torque required to drive the nominal load profile, which assumes a completely stiff mechanism and an ideal control system. It is likely that the torque required in a real implementation of the system, containing non-linearities and flexibilities differ from the torques obtained from the nominal load profile. In Figure 4.10 the required torque, $T_{m,rms}$ to achieve the control performance presented in Figure 4.9 is presented. As seen, for low gear ratios the torques are higher than the rated continuous torque of the machines derived in the previous chapter. For high gear ratios the required torques are actually lower than the rated. The difference is however small, the required torque is within ±10% of the rated.

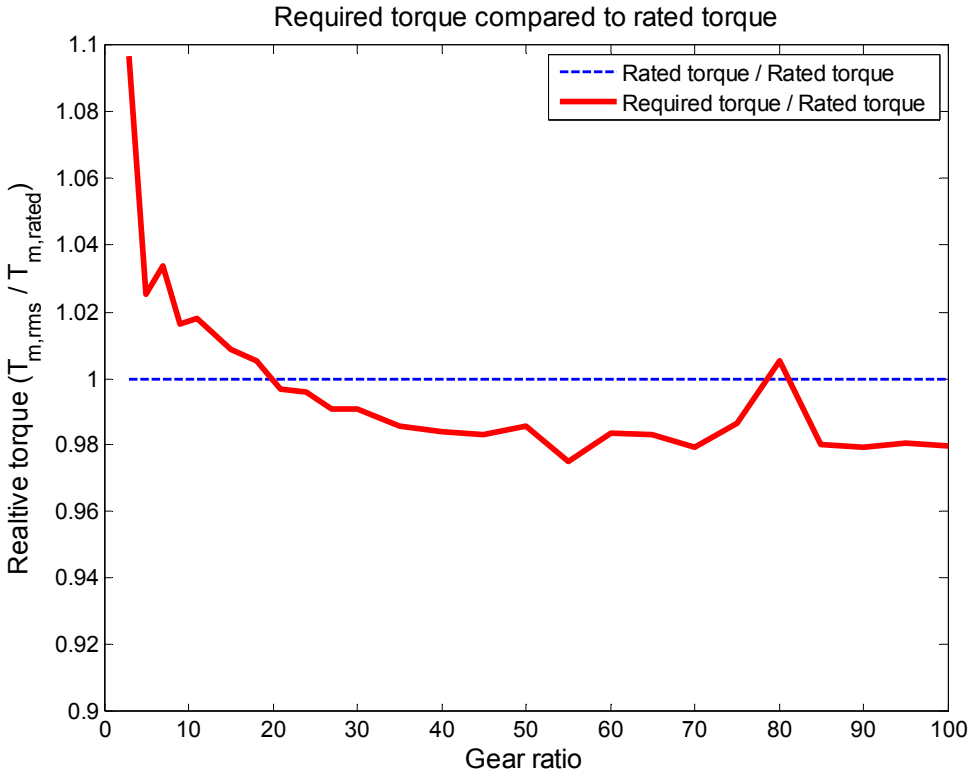


*Figure 4.10. Required torque to achieve the performance presented in Figure 4.9, compared to the rated machine torque.*

If a higher torque than the rated machine torque is required, it means that the obtained performance only is possible to achieve during a small number of consecutive repetitions, otherwise the machine driver will shut down to prevent overheating of itself and the machine. On the other hand, if the required torque is lower than the rated, the machine may have been oversized. The problem with exceeding the rated torque may be solved by changing the objective function of the optimization loop such that it incorporates the rms-torque, for example

$$f_{obj(T_{m,rms}>T_{m,rated})} = f_{obj}\left(\frac{T_{m,rms} - T_{m,rated} + 1}{T_{m,rated}}\right)^{10} \tag{4.10}$$

This objective function punishes all solutions that require higher torques than the physical parts of the system were designed for. It is only applied when the required torque is higher than the machine's rated torque, when it is lower, equation (4.7) is used as before.

## 4.4 PERFORMANCE EVALUATION

In this section it is investigated how the control performance depends of the gear ratio when all of the limiting physical phenomena discussed in the previous sections are included in the system model. Here the focus is on sensor resolution; the performance is investigated for three sensor resolutions. This is just an example; the same type of analysis should be made for other limiting phenomena such as backlash, sampling frequency and so on.

Applying the new objective function, equation (4.10), to the non-linear system results in the control performance presented in Figure 4.11. The performance in this figure is achieved without violating the rms-torque constraint. The performance of the geared system is compared to the performance of the direct drive system. As can be seen in the figure, the performance obtained with the direct drive system seems, assuming a high sensor resolution, much better than the best possible performance of a geared system. The main explanation for this difference in performance is the backlash and flexibility in the gearhead. It is however likely that the control error of the direct drive system is a bit underestimated since it is assumed to be infinitely stiff. Furthermore it is interesting to note that if the sensor resolution is lowered, the geared system outperforms the direct drive system (assuming a high enough gear ratio). For a sensor resolution of 1000 pulses/rad, the best performance is achieved at a gear ratio of 9. For the two lower resolutions, the best performance is achieved at a gear ratio of 100. At this gear ratio, a sensor resolution of 10 pulses/rad results in a control error similar to the one achieved with a 1000 pulses/rad sensor. To minimize sensor cost, it is obvious that a high gear ratio should be selected (assuming that the machine driver does not need a high sensor resolution).

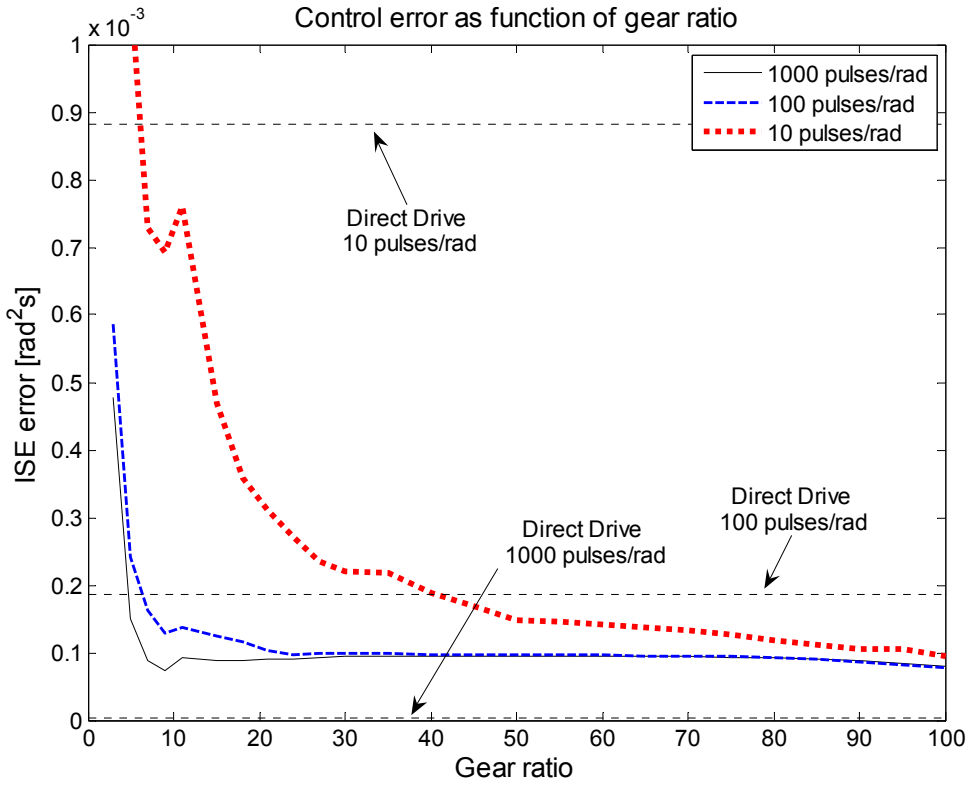


*Figure 4.11. Control performance as function of gear ratio for three different sensor resolutions.*

The approach throughout this thesis has been to find the smallest possible system solution that fulfills the requirements on control accuracy. As indicated above it might even be possible to lower the torque requirements from the torques obtained with the nominal load profile, and still be within the specification with respect to control error. In order to reach the system optimum it may therefore be necessary to iterate between physical system design and control system design, as indicated in Figure 2.2. However, this effect is, at least in the example case, small, and in many cases it is questionable if the input parameters to the methodology are so accurate that it is necessary to perform the iteration.

Nothing has so far been mentioned about system efficiency and its relation to control system design. It is obvious that if it is possible to lower the torque requirements by accepting a somewhat worse control performance it will increase the system efficiency and the other way around. But this is not investigated in detail here, but discussed further in section (5.2.3).

To sum up, it seems to be very important to include all limiting phenomena of the physical system in the design of the control system. It is the non-linearities that limit the control performance, and also to a large extent the cost and size of the system. Optimizing a system where the non-linearities are disregarded results in an unrealistic design solution. Furthermore, it is obvious that a system with a high gear ratio is easier to control than a low ratio system. A high gear ratio solution may use a less expensive sensor to achieve the same performance as a system with a lower gear ratio. One explanation for the improved performance at high gear ratios is the increase of torque margin with gear ratio. At higher gear ratios the rotor inertia corresponds to a larger part of the total machine torque

than at low. This in turn leads to that the relative extra torque available to handle a disturbance of some sort, is higher at high ratios than at low (assuming that the disturbance is on the load side of the gearing). The effect of torque margin on control performance is discussed further in paper D.

Finally it should be emphasized that this chapter investigates the possible control performance that is achievable with the physical system designs that are determined in the previous chapter. Those designs are optimized with respect to size, with a design method that is based on conventional design rules that mainly considers mechanical stresses and temperatures. This means that even though the performance is optimized, a particular design does not represent the true performance optimum on the system level. In order to maximize the control performance, properties such as stiffness and torque margin should be as high as possible; this is however in contradiction to the objective of minimizing the size of the physical system.

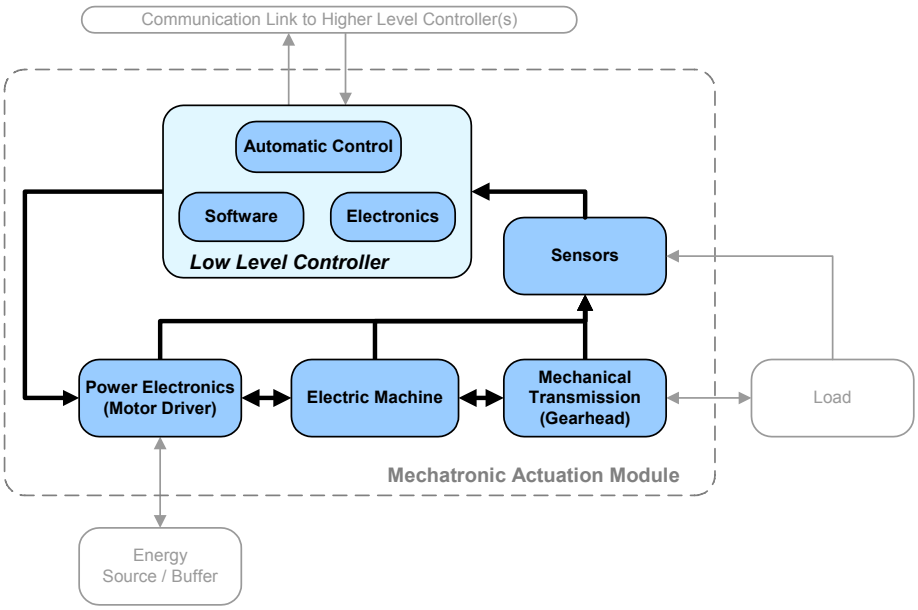


# 5 INTEGRATED SYSTEM DESIGN

In this chapter the implications on the system design, given four different design objectives are discussed. The objectives are *size, performance, efficiency* and *cost*. Also the relations between the main design variables are briefly analyzed. Finally a discussion about how to select the best gear ratio for the example system is presented.

| Influences → | Machine Size | Gear Size | Gear Ratio | Gear Backlash | Gear Stiffness | Driver Size | Driver Cost | Sensor Resolution | Controller Gains | | System Cost | System Efficiency | Control Performance | System Weight | System Size |
|---|---|---|---|---|---|---|---|---|---|---|---|---|---|---|---|
| Machine Size | | | | | | X | X | | **X** | | **X** | **X** | **X** | **X** | **X** |
| Gear Size | | | | X | **X** | | | | | | **X** | X | | **X** | **X** |
| Gear Ratio | **X** | **X** | | X | | **X** | **X** | **X** | **X** | | **X** | **X** | **X** | **X** | **X** |
| Gear Backlash | | | | | | | | | **X** | | **X** | | **X** | | |
| Gear Stiffness | | | | | | | | | **X** | | X | | **X** | X | X |
| Driver Size | | | | | | | **X** | | | | **X** | | | **X** | **X** |
| Driver Cost | | | | | | | | | | | **X** | **X** | | | |
| Sensor Resolution | X | | | | | X | | | **X** | | **X** | | **X** | | |
| Controller Gains | X | | | | | X | | | | | X | X | **X** | X | X |

Depends →

*Figure 5.1. Design structure matrix of the main design variables, and evaluation criteria (an X marks a relation; a bold **X** marks a strong direct relation).*

## 5.1 DESIGN VARIABLES

One way to illustrate the dependencies of the design variables is to use the Design Structure Matrix (DSM) [69]. In Figure 5.1, a DSM of the main design variables of a servo actuator is shown. As seen, the gear ratio is the variable that without competition has most dependencies. This, highlights why the contents of

this thesis have focused so much on the gear ratio. The gear ratio directly influences the size and efficiency of the gearhead, electric machine and the machine driver.

The evaluation criteria have been added to the right part of the DSM in Figure 5.1. As seen, the system cost depends directly or indirectly on all of the listed design variables. While the other criteria depend on many, but not all of the variables. This, confirms what already have been shown, that the design and optimization problem is very complicated. The next section discusses how the four evaluation criteria affect the methodology and the optimal design solution.

## 5.2 EVALUATION AND OPTIMIZATION CRITERIA

Here the effects on the system design are discussed when each of the four optimization criteria - size, performance, efficiency and cost are considered. Many of the conclusions drawn in this section are based on the results from the example system. It is therefore not sure that all conclusions are true for electromechanical servo systems in general.

### 5.2.1 WEIGHT AND SIZE

The main focus throughout this thesis has been to find the smallest possible system that fulfills the design requirements. Weight and size will therefore only be discussed briefly here. For the example load, the minimum system size occurs at a gear ratio between 30 and 65 (see Figure 3.29). This is however only true for the component types and design solution used in the thesis. Changing for example the material properties of the gearhead, or the semiconductor selection for the converter, may move the optimum. However, the shape of the size curves is rather general, at least for loads requiring high accelerations (inertial loads). As mentioned before, in order to retrieve the true system size optimum, it is necessary to iterate between physical system design and control system design. Something which has not been implemented in the methodology yet, since it is likely to only have a small effect on the resulting system design.

From a size perspective the optimal gear ratio in the example is 48, but as long as it is somewhere in the interval 30-65 the system size is close to optimal. Even though models of the components' weight are presented, the weight optimum has not been derived for the example system, but it will be located close to the size optimum.

### 5.2.2 PERFORMANCE

As discussed before, in order to optimize with respect to performance it is necessary to turn the design problem presented in this thesis upside down. Here the performance has been regarded as a requirement or design constraint. In order to find the optimal design with respect to performance it is needed to implement all design rules from chapter 3 as design constraints, and optimize the system according to the nested optimization approach. The usefulness of such a method can however be questioned, since optimizing with respect to performance only, will result in a large, heavy and expensive system.

Many of the system parameters affect the control performance, the most important ones include; the system stiffness, backlash, torque capability (torque margin), sensor resolution and the controller sampling frequency. In this work, many of these parameters have been selected with respect to other criteria (e.g. size) than control performance. The results show that high gear ratios generally are better from a control perspective than low. However, the discrete transition in backlash when adding an extra gear stage, might result in that the best performance is obtained at a gear ratio of 10 (highest possible with one gear stage). For the design example, a gear ratio of 10, results in the best performance given a high resolution sensor, decreasing the resolution gives that the highest possible gear ratio (100) minimizes the control error.

It is interesting that many of the major performance limiting phenomena, except for the machine torque saturation and the system stiffness, is more or less independent of the servo system size. Sensor resolution, controller sampling frequency and gear backlash are more related to the system's cost than its size.

From a performance perspective, the optimal gear ratio (given that the physical system is designed with respect to size) is 10 with a sensor resolution of 1000 pulses/rad, but 100 if any of the two lower sensor resolutions are used.

### 5.2.3 EFFICIENCY

Energy efficiency has only been discussed briefly in the previous chapters, mainly because the presented methodology focuses on size and weight optimization. The smallest possible system will not be the most energy efficient system. However, the two optima will not be very far from each other. Take the electric machine for example, it is designed with respect to heat, in this case all machines are designed such that they exactly can drive the given load. Thus, somewhat simplified one can say that a large machine generates more heat than a small. But the system efficiency would benefit from also considering machines 'oversized' with respect to torque.

In section 3.6, the power losses of the system were calculated with respect to the nominal load profile and the stiff system model. Now, it is possible to plot the power loss as function of gear ratio for the non-linear four mass model presented in the previous section. The two solid curves in Figure 5.2 represent the size optimized system, designed and analyzed with the presented methodology. The thick curve represents the case where the regenerated energy is utilized, while the thin one represents the case where all regenerated energy is burned up in a brake resistor. The first case is the one that also was calculated in section 3.6, and the agreement is very good with the simulated results presented here. In the second case, where all regenerated energy is converted to heat, the efficiency gets worse at gear ratios above approximately 10. The stored kinetic energy increases with gear ratio, since a high gear ratio means high rotor speeds. Hence, the heat developed in the brake resistor increases with gear ratio.

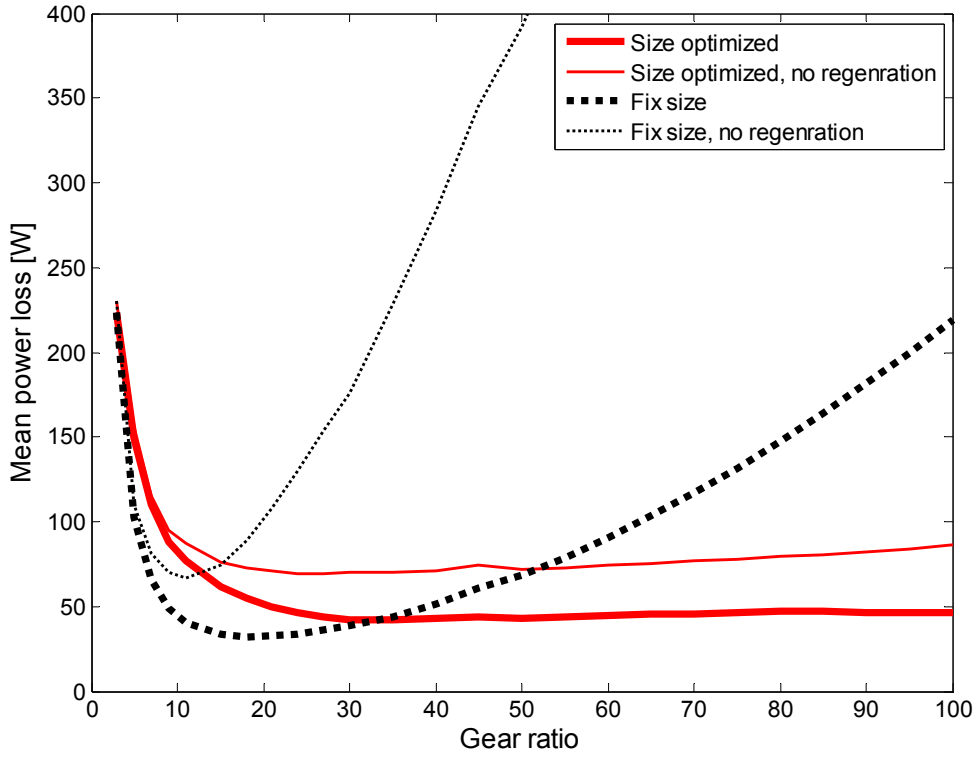


*Figure 5.2. Mean power loss as function of gear ratio. Four cases are presented: i) The size optimized system where the regenerated energy is stored somehow. ii) The size optimized system where the regenerated energy is burned up in brake resistors. iii) The system optimized for a gear ratio of three, but now used for all ratios. iv) Same as iii) but without regeneration.*

The two dotted curves, represent a case where the same electric machine and driver are used for all ratios. In this case the system originally designed for a gear ratio of three was used. The choice fell on that system since it has the torque capability to drive the load for all ratios. As seen, for low gear ratios the losses actually gets lower than for the size optimized system. This is a result of the large amount of copper in this machine, which results in lower resistive losses. However, when the gear ratio increases the torques required to accelerate the large rotor inertia of this 'oversized' machine results in large copper losses. This is even more obvious in the case where the regenerated electricity is converted to heat.

Thus, the smallest machine/system is not guaranteed to be the most energy efficient solution. However, for high gear ratios, the machine inertia plays a very important role for the efficiency. In high gear ratio systems, large parts (often up to 50%) of the power are used to accelerate the machine's rotor, which may reduce the efficiency drastically. This is especially true for systems where the regenerated energy can not be fed back to the source (e.g. diode rectifier systems). It is therefore very important to keep the inertia of the servo actuator as low as possible. The efficiency optimum for such a system will probably be very close to its size optimum. However, it is possible to design custom machines with more copper in the stator, but still the same low rotor inertia. Such a machine would result in better efficiency, but also in increased system cost.

It is also possible that a decrease in the required control performance can lead to lower torque requirements and hence a better efficiency. As discussed in section 4.3.3 and in paper E, there is a coupling between machine torque and the controller gains. It is therefore possible to optimize the controller with respect to system efficiency. The increase in efficiency would however in most cases probably be small. For future research it would be interesting to investigate the possibilities with load profile shaping to improve system efficiency.

As shown in Figure 3.30, it is the machine that is responsible for the main parts of the losses in the example system. The power electronics and gearhead only stands for a small part of the total losses. This is however not generally true, here a very efficient gear type is used. Low backlash gearings as harmonic drives are on the other hand known to be less efficient. Furthermore, as mentioned before, it is necessary to incorporate speed dependent losses in the methodology in order to get a more realistic analysis of the efficiency at high gear ratios.

Optimal gear ratio from an efficiency point of view is, in the example 20-50 (considering that the losses at high gear ratios probably are underestimated).

### 5.2.4 COST

The key to solve the cost optimization problem is to find cost models and weights of all the components. It is necessary to identify the properties that are expensive and those that are cheap. For example, the resolution of the position sensor is directly related to the cost, which also is the case for the size and weight of the components (material cost). The design of the motor driver represents an interesting tradeoff between size and cost, selecting a cheap set of semiconductors requires large cooling components and vice versa. This choice can only be made accurately if cost models of the heatsink where available. Similar types of trade-offs are necessary for all of the constituent components. As shown in Figure 5.3, even though the total volumes are almost the same, the sizes of the individual components differ greatly between a system with a gear ratio of 20 and one with a gear ratio of 65. It is therefore strongly recommended for future research to add cost-models of all components.

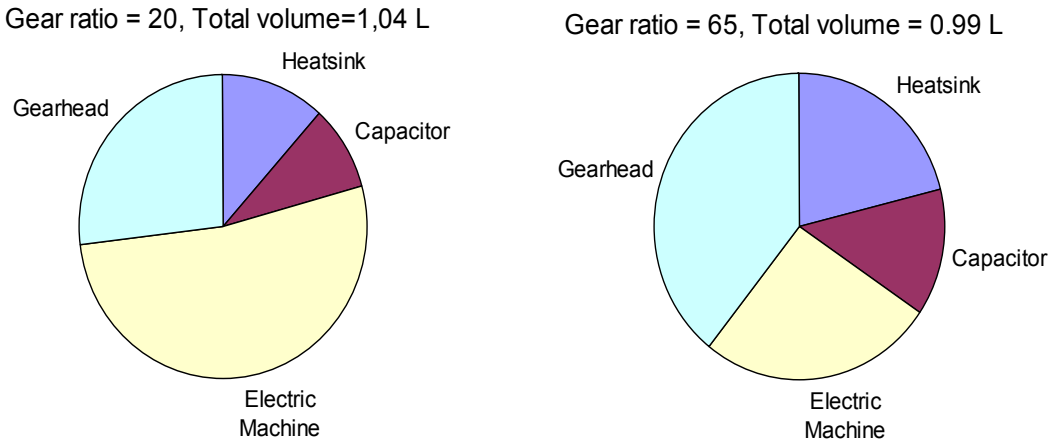


*Figure 5.3. Component relative volume for two different gear ratios, both representing a total system volume of about 1 L.*

In chapter 4 it was concluded that high gear ratios enable the use of sensors with lower resolutions, which is equal to less expensive sensors. The same is true for the sampling frequency and therefore the cost of the control electronics (paper E). So, it is likely that the gear ratios that are good from a weight and size perspective are good from a cost perspective too. Hence, the optimal gear ratio from a cost perspective would for the design example probably be somewhere in the interval 65-100.

## 5.3 SYSTEM DESIGN

Figure 5.4 illustrates the effects of the optimization criteria on the system properties associated with the four criteria. If the system is optimized with respect to cost, it obviously has a positive effect on the cost, but also on the size of the system (a compact system is cheaper than a large). But it will have negative effects on the performance and also to some extent on the system efficiency (e.g. copper is expensive).

| | System Cost | System Efficiency | Control Performance | System Size |
|---|---|---|---|---|
| Minimize Cost | ++ | - | -- | ++ |
| Maximize Efficiency | - | ++ | -- | - |
| Maximize Performance | -- | -- | ++ | -- |
| Minimize Size | + | - | - | ++ |

*Figure 5.4. Effects of the system properties if the system is optimized with respect to one of them.*

If the efficiency is maximized, it will likely have negative effects on all of the other criteria. Performance optimization will as discussed earlier be very negative to all other properties of the system.

When it comes to weight and size minimization it is beneficial for the system cost, partly because it obviously lowers the material cost, partly because the size optimum appears to occur at gear ratios where less expensive sensors and control electronics may be used. The efficiency will however not be the best if the system is optimized with respect to cost, but not so bad either (as shown in section 5.2.3). The same is true for performance, it will not be optimized, but it will not necessarily be bad either. As said, the gear ratio that minimizes size seems to be good also from a performance perspective.

The conclusion from this is that it is very difficult to develop a method that integrates all of these optimization criteria, since they are different in their nature. It is impossible to find a design solution that is optimal with respect to size, performance and efficiency at the same time. There is a significant risk that the implementation of one method that can optimize the system with respect to all of these criteria will be extremely computationally intensive. On the other hand it is

possible that the cost optimum is collocated with the size optimum. Hence, it would probably be quite straightforward to incorporate cost optimization into the methodology (but it might of course be difficult to come up with realistic cost models).

*Table 5.1. Best gear ratios for the design example with respect to the system properties.*

| Property | Gear ratio |
|---|---|
| Size/weight | 30-65 |
| Performance | 10, 80-100 |
| Efficiency | 20-50 |
| Cost | > 65 |

Returning to the design example, and how the gear ratio should be selected in this case. It has been shown that the system size is rather constant for gear ratios in the interval 30-65, hence secondary criteria may be used to select the exact gear ratio. Table 5.1 shows the best gear ratios with respect to the different criteria. Subjectively weighing all the criteria together yields in that the best gear ratio for the example system would be around 65. This gear ratio minimizes the system size, while it is also very good from a performance perspective. It enables the use of a low resolution position sensor and also less expensive control electronics, and it is good from an efficiency perspective.

# 6 DISCUSSION, CONCLUSIONS AND FUTURE WORK

The presented methodology should be viewed as a first attempt towards a holistic design methodology for mechatronic systems. It has in it present form many advantages but also many weaknesses. Some of the weaknesses are relatively easy to fix, others are more fundamental and therefore difficult to come around. But maybe the most important thing about the methodology is that it gives the system designers a feel for the dependencies between design variables and properties originating from different engineering disciplines. If the methodology also can find an approximate design optimum may perhaps be viewed as a bonus.

In this chapter the presented methodology is discussed and analyzed on several levels. First the major conclusions drawn from this work are presented. Both conclusions related to the methodology and conclusions related to how electromechanical servo systems should be designed are discussed. Then the identified weaknesses of the methodology in its current form are listed and discussed. The chapter is ended with a short section about the author's recommendations for future work.

## 6.1 CONCLUSIONS

There are many conclusions that can be drawn from the work presented in this thesis. First of all, there are several interesting technical conclusions about the design of mechatronic servo systems. However, maybe the most interesting conclusions in this context are the ones about the methodology itself. This section is therefore divided into two sub-sections, the first for the more technical conclusions and the second for the conclusions about the integrated design methodology.

### 6.1.1 CONCLUSIONS RELATED TO THE DESIGN OF MECHATRONIC SERVO SYSTEMS

Many of these conclusions are based on the design example used in the thesis. It may therefore be questionable how general some of these conclusions are. But, all conclusions stated here are valid for all designs cases that the methodology has been tested on throughout this research project.

When it comes to gearheads, it is proven in paper B that planetary gears are more compact and have significantly less inertia than conventional spur-pinion configurations. This is not new, but the author has not seen any previously published analytical comparison between the two gear types. Furthermore, a method for gear stage optimization has been derived. It is shown that it is, from a size perspective, favorable that the gear stage closest to the load has a lower gear ratio than the stages closer to the electric machine. Furthermore, the gearhead inertia is often neglected when modeling mechatronic servo system. The results of the design methodology validate that simplification. It is here shown that the machine inertia generally is the dominating inertia, assuming of course that the components are sized in a proper way.

Given that the position sensor is placed at the motor shaft, which is standard in servo system, it is known that the anti resonance-frequency of the mechanism limits its bandwidth. The anti-resonance frequency is directly dependent on the combined stiffness of the machine shaft and the gearhead. It is here shown that it generally is the gearhead that dominates the total stiffness (i.e. it has the lowest stiffness). This is especially true at high gear ratios.

It is shown that high gear ratios generally result in better control performance than low. Therefore, high gear ratios enable the use of low-cost sensors and control electronics without ending up with bad control performance. This also, in combination with the smaller system size, indicates that the system cost is lower at high gear ratios than low.

The gear ratio is identified to be a very important parameter when it comes to the optimization of electromechanical servo systems. The choice of gear ratio significantly influences the system size, performance, cost and efficiency. It is therefore important that the gear ratio is chosen with respect to a systems perspective before the domain specific design phase starts.

### 6.1.2 CONCLUSIONS RELATED TO THE DESIGN METHODOLOGY

The presented design methodology includes models of the electric machine, gearhead, motor driver and control system. Traditional methods for gear ratio selection do not consider the physical properties of the gearhead. Here it is shown that the gearhead stands for a significant part of the size of the servo actuator; at high gear ratios it may even represent a major part of the servo's size and weight (Figure 3.18). It is therefore important to include physical gear models in order to find the optimal system design.

The motor driver may stand for a major part of the system cost and for a significant part of the system's size and weight. The size and weight of the driver depends however more on the internal design of the drive unit, than on the gearhead and machine design. Nevertheless, the size of the drive unit is directly related to the required machine currents and not to the machine size. It may therefore be beneficial from a holistic design perspective to select the machine with respect to current instead of volume. See for example Figure 5.3, where the volume of the drive unit is much smaller for the case with a gear ratio of 20, than for a gear ratio of 65, even though the required machine volume decreases significantly with gear ratio. It is therefore important to consider the design of the machine driver in a complete design methodology for mechatronics.

The first part of the methodology, considering the physical parts of the system, is very powerful in itself. If the control requirements are low, it may be unnecessary to include the dynamic and control system parts of the methodology into the analysis. On the other hand, if the control requirements are high, the second part of the methodology is important. As shown, a good choice of gear ratio may reduce the requirements on sensor resolution, and therefore lower the system cost (this is also shown to be true for controller sampling frequency in paper E). Furthermore, it is concluded that flexibilities, backlash and controller gains influence both the control performance and the system's torque requirements. This in turn means that in order to reach the true system optimum it is necessary to iterate between physical system design and control system design.

The non-linear performance limiting phenomena, such as machine current saturation, sensor resolution, gear backlash etcetera have been shown to be very important to include in this type of cross-domain analysis. It is often the non-linearities that stand for the most important couplings between the design of the physical system and the design of the control system. Using a linear system representation, results in performance predictions unachievable by the real system.

Even though very simple component models have been implemented, the methodology is complicated. It will become even more complicated if it is extended to cover other component types and physical phenomena. In order to get the industry to adopt this type of design method it might be necessary to implement it in a design tool with a relatively easy-to-use graphical user interface. The part of the methodology that considers the dimensioning of the physical parts, would become a very powerful design tool if it is combined with a mechatronic simulation tool such as Dymola or 20-Sim. The presented method could then be used to derive values of the parameters required for the simulation model. And the user could, for example, immediately get an estimation of the actuator size required to achieve the simulated performance.

The first part of the methodology does not require much computing power. Given a load cycle as input, it takes less than a second on a P4 1.8 MHz PC to perform all calculations required for the design and optimization of the physical system. The genetic optimization loop for the control system optimization is much more computationally intensive. This is especially true if the control performance is optimized for several gear ratios as shown in section 4. This will probably become a problem if the methodology is extended to deal with performance and efficiency optimization too.

## 6.2 SHORTCOMINGS AND THOUGHTS ABOUT THE METHODOLOGY

### 6.2.1 SHORTCOMINGS AND POSSIBLE IMPROVEMENTS

Throughout the thesis a large number of assumptions and simplifications have been introduced. In general, these simplifications have been made to keep the complexity of an already complicated method down. However, the simplifications are, in a few cases, so large that they might affect the results of the design and optimization significantly. Here, the simplifications that the author feels might bee too large and therefore lead to incorrect results are listed and discussed. Furthermore, possible additions to the methodology are discussed.

Maybe the largest simplification within this work is that all speed dependent losses are neglected. In both the electric machine and in the gearhead there exist speed dependent losses. In the machine, the iron losses (eddy-currents and hysteresis) depend strongly on the machine speed. In addition, there exist viscous friction and windage losses, which also is true for the gearhead. These losses may, depending on application be more or less significant. But the problem gets obvious when the optimum always tend to be located at a rather high gear ratio. It is possible that if models of these losses were included into the methodology, it would, at least in some cases, affect the optimum significantly. There are however drawbacks with including the speed dependent losses. The main one is

the increased complexity that in turn will increase the computational needs of the methodology. It is also difficult to estimate the parameters of the loss models at the conceptual design stage and there is a risk that the models will be very inaccurate.

In this work it has been assumed that the load profile is given as input. If the methodology is expanded to include the shaping of the load profile it would probably be beneficial for the final system design. Shaping the profile such that it reduces the mechanical stresses on the gearhead and also the motor rms-torque could in many cases have great impact on the final system performance, efficiency, size and cost. However, in many cases it is impossible for the system designers to do anything about the profile, but in for example industrial automation systems it is often possible. Furthermore, a method or guideline that helps the system designers to identify the worst part of long complex load cycles would be useful.

The scaling approach used for the dimensioning and optimization of the electric machine gives, as shown in section 3.3, rather accurate results. Here the scaling constants have been derived from one single machine. The results may however be improved if data of a number of existing machines are available, then the scaling constant can be derived from the machine that is closest to the machine being designed. Furthermore, a model of the machine's peak torque rating needs to be derived; in this work it has been assumed to be linear with the machine's rated torque.

The methodology only considers the active parts of the physical components. For the electric machine, only the rotor length is considered, extra space for end windings and bearings are not accounted for. Regarding the gearhead, only the size and weight of the actual gearwheels are considered, casings, shafts and bearings are disregarded. Similar for the motor driver, space for casings, sensors, control electronics, PCB etcetera are not accounted for. In total these parts are likely to represent a minor part of the total size and weight, especially if the system is physically integrated. However, it is important to have these parts in mind when analyzing the results from the design and optimization methodology.

Throughout this work it has been assumed that all design variables can obtain any value in between the design constraints. However, many of the design variables are in reality constrained to discrete points. Examples include the number of gear teeth, number of turns in the machine winding, gear width (constrained to standardized widths of bearings) and standard in gear modulus. Also this is important to keep in mind when using the methodology.

### 6.2.2 GENERAL THOUGHTS ABOUT INTEGRATED DESIGN

Even though this design methodology may be used to find the component properties that minimize the sum of the components' volume, it is not a complete method for integrated design. In order to reach full support for component integration, the volumetric utilization of the assembly needs to be analyzed. Even though the total 'active' volume is minimized with the methodology, it might still be much space in the assembly that is occupied by air. This problem is maybe most obvious in the design of the machine driver, where the different components generally come in different shapes and it is difficult to reach a high

volumetric utilization. But the problem exists for the machine and gear integration too. To solve this problem it is necessary to develop more geometrically detailed component models, such that each component can be optimized to fit together with the other components. This may however be a too complex problem to solve during the conceptual design phase, and should probably be addressed after a conceptual design has been selected for further development.

The issue addressed above also raises another shortcoming of the design method. In order to design and optimize a highly integrated actuation module, it is required to analyze how the components affect each other. The most obvious property that needs much attention is the heat transfer between components. In the presented design method, each component is dimensioned as if not being in direct contact with the other components. The tight physical integration of machine and gearhead may for example be of benefit for the machine, since the gear probably is cooler than the machine. On the other hand, the machine may be heated by the power electronics, which reduces the possible output power. A thorough analysis of the heat transfer in an actuation module is necessary, this is however also too complex to perform at the early design stage that this method aims at, and needs to be performed after preliminary geometrical dimensions have been decided.

The presented design methodology focuses on size and weight optimization of mechatronic actuation modules. The plan when this project started was to derive a method that also was capable of system wide optimization of cost and energy efficiency. It has however been shown to be hard to design such a general method. The optimization problem gets much more complicated if efficiency and especially also if performance where added to the list of optimization criteria. It may also be questioned if such a methodology is useful, since there is a risk that the design optimum generally will be unrealistic when it comes to size and cost. It is however up to future research to investigate the possibilities with system wide optimization of performance and efficiency. Cost optimization would however be more straightforward to include in the methodology.

Another important question is if it really is valuable to put any effort in finding the true system optimum based on conceptual design models and inexact requirements. Design models will never be perfect; they still are just models of the reality. Especially the models used on this relatively high level of abstraction and with uncertain parameter values. Since the error in the input data and in the design models are relatively large, it will probably be inefficient to spend much time and computational power in solving the exact mathematical system optimum. Finding a point relatively close to the optimum would therefore be enough. Hence, the proposed iterations (Figure 2.2) between physical system design and control system can in most cases be omitted. The following section will continue the discussion about modeling and simulation.

### 6.2.3 THOUGHTS ABOUT THE MODEL BASED APPROACH

All of the results presented in this thesis are based on mathematical component models and simulations. Furthermore, the used component-models have a relatively high level of abstraction to keep the total complexity as low as possible. It is then relevant to ask the question if the results and conclusions from this research are correct and useful also in reality and not only in the world of modeling and simulation.

For example, for performance analysis a relatively simple non-linear friction model is used with estimated parameter values, see equation (4.8). These values are often hard to identify even if you have access to the real system, in this case the system does not exist and it is therefore difficult to know if they are even remotely correct. Furthermore, people write entire PhD-theses about friction models, and it is well known that the simple model used here not is a very good representation of reality. Then you can ask if the simulation results get closer to reality when friction is included, or if the friction model is so far from reality that it would be better to neglect friction in the system model. This type of reasoning can be made for many of the components and phenomena analyzed in this thesis. Many of the parameters used in the dynamic simulations are derived with the static component models. It is thus possible that small errors in input can affect the results from the dynamic simulations greatly. These problems are however general in model based design and not unique for this research project, but it is wise not to trust the exact figures in the results too much but rather look at the relative effects and trends. And even tough the results not are exactly correct, it is obviously better to analyze and optimize the system this way than not doing it at all. It is also possible to obtain more correct results after a few iterations of the design cycle, having prototypes or previous versions of the systems that may be used for parameter identification.

Another aspect regarding models and simulations is the question of linearization. Dynamic systems are often linearized when modeled, such that the classic analysis methods for dynamic systems can be applied (e.g. bode, Nyquist, pole-zero maps etc.), but that also introduces a modeling error. In this thesis (paper D and E) it is shown that the non-linear elements represent some of the strongest couplings between physical system design and controller design. For example motor current saturation, sensor quantization and controller sampling frequency are strongly related to system size, cost and control performance, neglecting to include those in the system model makes it impossible to find the system wide optimum. Keeping them in the model, on the other hand, makes it very hard to analyze the results, since none of the conventional linear analysis methods are applicable. From an academic perspective you can ask your self which is most correct, to analyze a linear system which does not show the effects being investigated, or to accept the results from the non-linear model without the possibility of extensive analytic analysis. The author has chosen the second approach since the first is difficult to use if the strong couplings between mechanism and controller design are to be investigated.

## 6.3 RECOMMENDATIONS FOR FUTURE WORK

In the previous sections several shortcomings of the present implementation of the methodology have been recognized. Here is a short list of what the author feels that future research in the area should focus on.

- *Speed dependent losses.* Future research should focus on investigating the effect of speed dependent losses on the design optimum. If the effects turn out to be significant, the most important types of speed dependent losses should be included into the methodology.
- *Design tool*. A natural next step would be to implement the complete methodology into a software based design tool. Stand-alone or as a plug-in to an existing design tool is up to future research to investigate.
- *Cost models*. In order to make the trade-offs between sizes and cost of the system's components it is necessary to develop cost models for each component. This also enables system wide optimization of the system cost.
- *Models of other component types*. Models of low-backlash gears, ball screws etcetera would be really useful to compare different design concepts to each other.
- *The load profile*. A method for the design of the speed (position) profile of the load would be beneficial to include into the methodology.
- *Methods for control system design.* Other complementary methods for the design and analysis of the control system would be valuable to include.
- *Modeling.* Mathematical models of the gear stiffness, backlash, machine peak torque rating, machine top speed, etcetera, would probably improve the accuracy of the methodology.

# REFERENCES


[1] Li Q. Zhang W. J., Chen L., "Design for Control – A Concurrent Engineering Approach for Mechatronic Systems Design", *IEEE Transactions on Mechatronics*, Vol. 6, no 2, pp 161-169, 2001.

[2] van Amerongen J., Breedveld P., "Modelling of physical systems for the design and control of mechatronic systems", *Annual Reviews in Control*, vol 27, pp 87-117, 2003.

[3] Rothfuss R., Lasa M., Heinkel H. M., Tirigari P., "Systems Engineering in the Design of Mechatronic Systems", *International Journal of Vehicle Design*, Vol. 28, no 1/2/3, pp 18-36, 2002.

[4] Schöner, H. P., "Automotive Mechatronics", *Control Engineering Practice*, Vol. 12, pp 1343-1351, 2004.

[5] Thramboulidis K., "Model-Integrated Mechatronics – Toward a New Paradigm in the Development of Manufacturing Systems", *IEEE Transactions on Industrial Informatics*, Vol. 1, No1, February 2005.

[6] VDI 2206, "Entwicklungsmetodik für mechatronische Systeme", Entwurf, *Beuth Verlag*, Berlin 2003.

[7] Gausemeier J., Moehringer S., "New Guideline VDI2206 – A Flexible Procedure Model for the Design of Mechatronic Systems", *ICED 03* International Conference on Engineering Design, Stockholm, August 2003.

[8] Valasek M., Breedveld P., Sika Z., Vampola T., "Software Design tools for Mechatronic Vehicles; Design Through Modelling and Simulation", *Vehicle System Dynamics*, Supplement, vol 33, pp. 214-230, 1999.

[9] Dynasim, www.dynasim.se/, accessed 2006-12-29.

[10] 20sim, www.20sim.com/, accessed 2006-12-29.

[11] AMEsim, www.amesim.com/, accessed 2006-12-29.

[12] Mathworks, www.mathworks.com, accessed 2007-01-10.

[13] van Amerongen J., Coelingh E., de Vries T. J. A., "Computer support for mechatronic control system design", *Robotics and Autonomous Systems*, vol 30, pp. 249-260, 2000.

[14] El-Khoury J., "A Model Management and Integration Platform for Mechatronics Product Development", Doctoral Thesis, KTH, Machine Design, TRITA-MMK 2006:03, ISSN 1400-1179, ISBN 91-7178-268-0, Stockholm 2006.

[15] Veitl A., Gordon T., van de Sand A., *et al.*., "Methodologies for Coupling Simulation Models and Codes in Mechatronic System Analysis and Design", *Vehicle System Dynamics*, Supplement, vol. 33 pp. 231-243, 1999.

[16] GAtoolbox, www.geatbx.com, accessed 2007-01-10.

[17] DeCicco J., Fung F., "Global Warming on the Road- The Climate Impact of America's Automobiles", Report by Environmental Defense, www.environmentaldefense.org, 2006, accessed 2006-12-06.

[18] "Sales of Hybrids in the US Up 24% in December; Up 22% in 2006", http://www.greencarcongress.com/, 2007-01-04, accessed 2007-01-08.

[19] "Hybrids for Commerce", *Automotive Engineering International*, SAE International, November 2006.

[20] "Nissan Plans to Put Electric Vehicle on Market in 3 Years", http://www.greencarcongress.com/, 2006-11-25, accessed 2006-12-06.

[21] "Report: Mitsubishi to Sell Electric Vehicle in US", http://www.greencarcongress.com/, 2006-10-09, accessed 2006-12-06.

[22] "Making cars more fuel efficient", Report by the European Conference of Ministers of Transport (ECMT) and the International Energy Agency (IEA) ISBN 92-821-0343-9 – No. 54039, 2005.

[23] Shen J., Masrur A., Garg V. K., Monroe J., "Automotive Electric Power and Energy Management – A Systems Approach", *Global Automotive Manufacturing and Technology*, April, 2003.

[24] Hendricks T., O'Keefe M., "Heavy Vehicle Auxiliary Load Electrification for the Essential Power System Program: Benefits, Tradeoffs, and Remaining Challenges", *SAE Paper* 2002-01-3135, 2002.

[25] Emadi A., Williamson S. S. , Khaligh A., "Power Electronics Intensive Solutions for Advanced Electric, Hybrid Electric, and Fuel Cell Vehicular Power Systems", *IEEE Transactions on Power Electronics*, Vol. 21, No. 3, pp. 567- 577, May 2006.

[26] Kassakian, J. G., "Automotive Electrical Systems- The Power Electronics Market of the Future", *IEEE Applied Power Electronics Conference and Exposition*, APEC 2000. Vol. 1, pp. 3-9, 2000.

[27] Roos F. "Theoretical Evaluation of Electric Power Steering in Heavy Vehicles", Technical Report, TRITA-MMK 2005:29, ISSN 1400-1179, ISRN/KTH/MMK/R-05/29-SE, 2005.

[28] Jonasson M., Roos F., "Design and Evaluation of an Active Electromechanical Wheel Suspension System", submitted for publication in Mechatronics, June, 2007.

[29] Fathy H. K., Reyer J. A., Papalambros P. Y. and Ulsoy A. G., "On the Coupling between the Plant and Controller Optimization Problems", *Proceedings of the American Control Conference*, v 3, pp. 1864-1869, 2001.

[30] Reyer J. A., Papalambros P. Y., "Combined Optimal Design and Control With Application to an Electric DC Motor", *Journal of Mechanical Design*, vol 124, pp. 183-191, June 2002.

[31] Kim M.S., Chung S.C., "Integrated design methodology of ball-screw driven servomechanisms with discrete controllers. Part I Modeling and performance analysis" *Mechatronics*, Vol 16, pp. 491-502, 2006.

[32] Kim M.S., Chung S.C., "Integrated design methodology of ball-screw driven servomechanisms with discrete controllers. Part II: Formulation and synthesis of the integrated design" *Mechatronics*, Vol 16, pp. 503-512, 2006.

[33] Kwok S. T., Lee C. K., "Optimal Velocity Profile Design in Incremental Servo Motor Systems Based on a Digital Signal Processor", 16th *Annual Conference of IEEE Industrial Electronics Society*, 1990.

[34] http://www.alxion.com, Direct Drive Motors, accessed 2007-03-28.

[35] Roos F., Johansson H., Wikander J., "Optimal Selection of Motor and Gearhead in Mechatronic Applications", *Mechatronics*, vol. 16, no 1, pp. 63-72, 2006.

[36] Danaher motion API-Elmo, "Servo motors, motor data sheet" API-Elmo 2003.

[37] Cetinkunt S., "Optimal design issues in high-speed high precision motion servo systems", *Mechatronics*, vol 1. no. 2 pp. 187-201, 1991.

[38] Harris N. C., Jahns T. M., Huang S., "Design of an Integrated Motor/controller Drive for an Automotive Water Pump Application", *IAS Annual Meeting* (IEEE Industry Applications Society), vol. 3, pp. 2028-2035, 2002.

[39] Pash K. A., Seering W. P., "On the drive Systems for High Performance Machines", *ASME Journal of Mechanisms, Transmissions and Automation in Design*, vol. 106, no. 1, pp 102-108, 1984.

[40] Van de Straete H. J., De Schutter J., Belmans R., "An Efficient Procedure for Checking Performance Limits in Servo Drive Selection and Optimization", *IEEE/ASME Transactions on Mechatronics*, Vol. 4, No. 4, pp 378-386, 1999.

[41] Van de Straete H. J., Degezelle P., De Schutter J., Belmans R., "Servo Motor Selection Criterion for Mechatronic Applications", *IEEE/ASME Transactions on Mechatronics*, Vol. 3, No. 1, pp 43-49,1998.

[42] Ottoson R, Siekkinen A., "Optimization of motor and gearbox in nut-runner systems", Master of Science Thesis, Department of Machine Design KTH, MMK2007:13 MDA 297, 2007.

[43] Slemmon G. R., Liu X., "Modeling and Design Optimization of Permanent Magnet Motors", *Electric Machines and Power Systems*, Vol. 20, pp. 71-92, 1992.

[44] Benson H., "University Physics", John Wiley & Sons inc., ISBN 0-471-51785-2, 1991.

[45] Bayside precision gearheads "Using gearheads in motion control – Precision planetary vs Harmonic/Cycloidal drives" available at http://www.baysidemotion.com, accessed 2007-02-19.

[46] Svensk Standard SS 1863, "Kugg och snäckväxlar – Cylindriska kugghjul med raka kuggar – Geometriska data., Spur gears- geometrical data", Utgåva 4, SIS- Swedish Institute of Standards, 1978.

[47] Svensk Standard SS 1871, "Kugg och snäckväxlar – Cylindriska kugghjul med raka eller sneda kuggar – Beräkning av bärförmåga. Spur and helical gears – Calculation of load capacity." Utgåva 3, SIS- Swedish Institute of Standards, 1978.

[48] Ottersten R., "Hybrid Vehicle Drives – System components – Power electronics", Course Material at the Department of Electric Power Engineering, Chalmers University of Techonolgy, 2004.

[49] Lee, S., "Optimum Design and Selection of Heat Sinks", *IEEE Transactions on components, packaging and manufacturing technology*, Vol 18, no. 4, December 1995.

[50] Märtz M., "Thermal management in high-density power converters", in Proceedings of the *IEEE International Conference on Industrial Technology*, 2003.

[51] Soule C. A., "Give Priority to heat sinks to reduce design time", *IEEE Spectrum*, February 1998, pp 61-66.

[52] Grinberg R., Palmer P. R., "Advanced DC Link Capacitor Technology Application for a Stiff Voltage Source Inverter", in proceedings of *IEEE Vehicle Power and Propulsion Conference*, 2005.

[53] Lai J-S, Kouns H, "A Low-Inductance DC Bus Capacitor for High Power Traction Motor Drive Inverters", *IAS Annual Meeting* (IEEE Industry Applications Society), vol. 2, pp. 955-962 , 2002.

[54] Al-Mosawi Y., "Energy Regeneration and Super Capcitors in Mechatronic Systems", Master of Science Thesis, Department of Machine Design KTH, MMK2005:46 MDA 256, 2005.

[55] Sundberg N., "Efficiency Improvements with Super Capacitors in Mechatronic Systems", Master of Science Thesis, Department of Machine Design KTH, MMK2007:02 MDA 284, 2007.

[56] Elna, "Large Capacitance aluminum electrolytic capacitors L3J" Component Data sheet.

[57] International Rectifier, www.irf.com , accessed 2007-04-02.

[58] Infineon, www.infineon.com , accessed 2007-04-02.

[59] Coelingh H. J., "Design Support for Motion Control Systems – a Mechatronics Approach", *Doctoral Thesis University of Twente*, 2000.

[60] Miu, D. K., "Mechatronics- Electromechanics and Contromechanics", *Springer-Verlag*. ISBN 0-201-09528-9, 1992.

[61] Moscrop, J., Cook C., Moll P., "Control of Servo Systems in the Presence of Motor-Load Inertia Mismatch", in *IEEE IECON'01,* vol 3, pp 351-356, Denver, USA 2001.

[62] El Rifai, O.M., Youcef-Toumi, K., "Trade-offs and perforamce limitations in mechatronic systems: a case study", *Annual Reviews in Control*, Vol. 28, pp.181-192, 2004.

[63] Goldfarb, M., Sirithanapipat T., "The effect of actuator saturation on the performance of PD-controlled servo systems", *Mechatronics*, vol 9., pp. 497-511, 1999.

[64] Ohkubo K., Yagishita Y., Katayama, "An Analysis of Quantization Errors in Digital Control Systems and its Application to a Hard Disk Drive" Proceedings of the *IEEE International Conference on Industrial Technology,* 1996.

[65] Cominos P., Munro N., "PID controllers: recent tuning methods and design to specification", *IEE. Proceedings Control Theory and Applications*, Vol. 149, No. 1, 2002.

[66] Da Silva W., Acarnley P., Finch J., "Application of Genetic Algorithms to the Online Tuning of Electric Drive Speed Controllers", *IEEE Transactions On Industrial Electronics*, Vol. 47, No. 1, 2000.

[67] Alfaro-Cid E., McGooking E. W., Murray-Smith D.J., "GA-Optimised PID and pole placement real and simulated performance when controlling the dynamics of a suuply ship", *IEE Proceedings – Control Theory and Applications*, Vol. 153, No2. March 2006.

[68] ZF Machineantriebe GmbH, "ZF-Servoplan Produktinformationen", *Product CD-ROM* (2004).

[69] Browning T. R., "Applying the Design Structure Matrix to System Decomposition and Integration Problems: A Review and new Directions", *IEEE Transactions on Engineering Management*, Vol 48, No 3, pp292-306, 2001.

# NOMENCLATURE

The nomenclature used in the appended papers may in few cases differ from the nomenclature listed below. Thus, see primarily the nomenclature section in the particular paper.

| | |
|---|---|
| $\alpha$ | Power share IGBT/FWD [1] |
| $\gamma_j$ | Semiconductor junction temp. [°K] |
| $\gamma_s$ | Heatsink temperature [°K] |
| $\gamma_{ambient}$ | Ambient temperature [°K] |
| $\delta$ | (air) Gap width [m] |
| $\varepsilon_r$ | Normalized machine radius [1] |
| $\varepsilon_N$ | Normalized number of turns [1] |
| $\varepsilon_l$ | Normalized machine length [1] |
| $\eta_g$ | Gear total efficiency [1] |
| $\eta_{gs}$ | Gear stage efficiency [1] |
| $\theta_{jc}$ | Junction to case thermal resistance [°K/W] |
| $\theta_{cs}$ | Case to heatsink thermal resistance [°K/W] |
| $\theta_{sa}$ | Heatsink to air, thermal resistance [°K/W] |
| $\mu_0$ | Magnetic permeability of air [H/m] |
| $\mu_g$ | Gear friction coefficient [1] |
| $v$ | Poisson's number [1] |
| $\rho_m$ | Average machine mass density [kg/m$^3$] |
| $\rho_g$ | Mass density of the gears [kg/m$^3$] |
| $\rho_{hs}$ | Average heatsink mass density [kg/m$^3$] |
| $P$ | Resistivity [Ωm] |
| $\sigma_{\tau,,max}$ | Max shear stress [Pa] |
| $\sigma_{H,,max}$ | Maximum allowed flank press. [Pa] |
| $\tau$ | Cycle time of the load profile [s] |
| $\varphi_l$ | Load angle [rad] |
| $\varphi_m$ | Machine angle [rad] |
| $\Phi$ | Magnetic flux [Wb] |
| $\omega_{ar}$ | Anti-resonance frequency [rad/s] |
| $\omega_m$ | Machine speed [rad/s] |
| $\omega_{m,peak}$ | Machine rated peak speed [rad/s] |
| $A_{slot}$ | Slot cross sectional area [m$^2$] |
| $A_w$ | Cross sectional area of winding wire [m$^2$] |
| $b$ | Gear width [m] |
| $b_c$ | Carrier width [m] |
| $B_{ag}$ | Magnetic flux density(airgap) [T] |
| $BL$ | Gear backlash [rad] |
| $C$ | Arbitrary constant |
| $C_\omega$ | Machine rated speed [rad/s] |
| $C_{gr}$ | Relation between outer and inner ring gear radius [1] |
| $C_K$ | Machine electric scaling constant [Vs/m$^2$] |
| $C_L$ | Machine inductance scaling constant [H/m] |
| $C_m$ | Machine torque scaling constant [N/m$^{1.5}$] |
| $C_{mj}$ | Machine inertia scaling constant [kg/m$^3$] |
| $C_{ms}$ | Motor shaft scaling constant |
| $C_{pt}$ | Machine peak torque scaling constant [1] |
| $C_R$ | Machine resistance scaling constant [Ωm] |
| $d_{ms}$ | Diameter of motor shaft [m] |
| $D$ | Controller derivative gain [1] |
| $E$ | Module of elasticity [Pa] |
| $f_{obj}$ | Objective function |
| $f_s$ | Switching frequency [Hz] |
| $G_{mm}$ | Torque to angle transfer function |
| $I$ | Controller integral gain [1] |
| $I$ | Root-mean square phase current [A] |
| $I_{avg}$ | Average phase current [A] |
| $I_{dc\text{-}ripple}$ | DC-link rms ripple current [A] |
| $I_{rms}$ | Root-mean-square current [A] |
| $J$ | Complex number (sqrt(-1)) |
| $J_0$ | Other inertia [kgm$^2$] |
| $J_g$ | Gearhead inertia [kgm$^2$] |
| $J_{gs}$ | Gear stage inertia [kgm$^2$] |
| $J_l$ | Load inertia [kgm$^2$] |
| $J_m$ | Machine inertia [kgm$^2$] |
| $k_g$ | Gearhead stiffness [Nm/rad] |
| $k_l$ | Load shaft stiffness [Nm/rad] |
| $k_{ms}$ | Motor shaft stiffness [Nm/rad] |
| $k_{tot}$ | Total actuator stiffness [Nm/rad] |
| $K_e$ | Machine voltage constant [Vs/rad] |
| $K_t$ | Machine torque constant [Nm/A] |

| | |
|---|---|
| $l_m$ | Machine active length [m] |
| $l_{ms}$ | Length of motor shaft [m] |
| $l_r$ | Machine rotor length = $l_m$ [m] |
| $l_w$ | Length of phase winding [m] |
| $L_p$ | Phase inductance [H] |
| $m_{gs}$ | Gear stage weight [kg] |
| $m_{hs}$ | Heatsink weight [kg] |
| $m_m$ | Machine weight [kg] |
| $n$ | Total gear ratio [1] |
| $n_s$ | Stage gear ratio [1] |
| $N_p$ | Number of winding turns per phase [1] |
| $p$ | Number of poles [1] |
| $P$ | Power [W] |
| $P$ | Controller proportional gain [1] |
| $P_{l,s}$ | Semiconductor power loss [W] |
| $P_{l,t}$ | Power loss in the transistors [W] |
| $P_{l,d}$ | Power loss in the diodes [W] |
| $r(t)$ | Controller reference signal |
| $r_g$ | Gear outer radius [m] |
| $r_{gr}$ | Gear reference radius [m] |
| $r_m$ | Machine stator radius [m] |
| $r_r$ | Machine rotor radius [m] |
| $R_{on}$ | Transistor equivalent series resistance [Ω] |
| $R_p$ | Phase resistance [Ω] |
| $s$ | Laplace variable |
| $SF$ | Safety Factor [1] |
| $t$ | Time [s] |
| $T_{eq}$ | Gearhead equivalent continuous torque [Nm] |
| $T_g$ | Gearhead torque [Nm] |
| $T_{gs}$ | Gear stage torque [Nm] |
| $T_{g,fr}$ | Gear friction torque [Nm] |
| $T_l$ | Load torque [Nm] |
| $T_m$ | Machine Torque [Nm] |
| $T_{m,max}$ | Required machine max torque [Nm] |
| $T_{m,peak}$ | Machine rated peak torque [Nm] |
| $T_{m,rms}$ | Required machine rms torque [Nm] |
| $T_{m,rated}$ | Machine rated continuous torque [Nm] |
| $U_{CE(on)}$ | Cathode to emitter constant voltage drop [V] |
| $U_{dc\text{-}link}$ | DC-link (supply) voltage [V] |
| $U_{emf}$ | Induced voltage [V] |
| $U_{on,d}$ | Diode forward voltage drop [V] |
| $U_p$ | Machine phase voltage [V] |
| $U_{pp}$ | Machine phase to phase voltage [V] |
| $V_g$ | Gearhead volume [$m^3$] |
| $V_{hs}$ | Heatsink volume [$m^3$] |
| $W_{on\text{-}off}$ | Switching energy loss [J] |
| $y(t)$ | Controlled output signal |